Effects of different climate generation methods on the hygrothermal performance of a wood-frame wall under current and projected future climates

Henry Lu

A thesis in the Department of

Building, Civil and Environmental Engineering

Presented in partial fulfillment of the requirements for the degree of

Master of Applied Science (Building Engineering) at

Concordia University

Montreal, Quebec, Canada

December 2021

Concordia University

School of Graduate Studies

This is to certify that the thesis prepared

By: **Henry Lu**

Entitled: **Effects of different climate generation methods on the hygrothermal performance of a wood-frame wall under current and projected future climates**

Submitted in partial fulfillment of the requirements for the degree of: **Master of Applied Science (Building Engineering)**

complies with the regulations of the University and meets the accepted standard with respect to originality and quality.

Signed by the final Examining Committee:

_____ Chair
Dr. Ted Stathopoulos

_____ Examiner
Dr. Bruno Lee

_____ Thesis co-Supervisor
Dr. Abhishek Gaur

_____ Thesis co-Supervisor
Dr. Hua Ge

Approved by: _____
Dr. Mazdak Nik-Bakht, Graduate Program Director
Department of Building, Civil, and Environmental Engineering

_____
Dr. Mourad Debbabi, Dean
Gina Cody School of Engineering and Computer Science

Date: _____

Abstract

Effects of different climate generation methods on the hygrothermal performance of a wood-frame wall under current and projected future climates

Henry Lu

Climate change will subject the built environment in Canada to unprecedented climatic conditions in the future, which may result in adverse effects on the durability of buildings. Therefore, it is vital to be able to accurately describe future climatic conditions and how buildings will perform under them. Hygrothermal simulation models are important tools for building practitioners to assess the moisture performance of wall assemblies. Hygrothermal simulations require a wide range of climate variables such as cloud cover, wind speed, wind direction, solar radiation, rainfall, snow cover, temperature, and humidity in high temporal frequency. Typically, recorded historical data was used for hygrothermal simulations, but they do not account for changes in climate excepted due to future global warming. Consequently, many climate data generation techniques have been developed to prepare climate data incorporating future projected climate change, which can be used to assess hygrothermal performance of buildings under current and future projected climates. The objective of this work is to evaluate the differences in the various future climate data generation methods and determine their impacts on the hygrothermal performance of a wood-frame wall assembly in the current and future projected climate. The analysis is performed on 6 cities, representing different climates across Canada and future projected climate data is prepared using morphing downscaling method, and two multivariate and a univariate bias correction method. Results indicate that morphed and bias corrected climate data perform better than RCM when compared to the observations. While this is generally true for the hygrothermal performance as well, the bias corrected data often fail to replicate the same degree of mould growth in the simulations with observational data. An analysis of the climate change scenario indicated that all the studied locations will experience warmer and wetter climatic conditions. For instance, the WDR deposited on the OSB in Montreal is expected to increase by at least 14%, resulting in increased MC and mould growth on the OSB. According to morphed climate data, the average MC in the OSB could increase by 54% while mould index exceeds 3.

Acknowledgements

I would like to thank my supervisors Dr.Hua Ge and Dr. Abhishek Gaur, without whom this would not have been possible. The advice they gave helped a lot during my graduate study and I sincerely appreciate their time and effort during this time.

I would also like to thank my parents for their unconditional support through my studies and everything they've done for me.

Special thanks to Chetan Aggarwal for his guidance in some of this work.

Contents

List of Figures

List of Tables

1.0 Introduction

1.1 Background

The changes in climate along with the growing understanding of its consequences result in an ever-evolving area of research. These changes in climate can have adverse effects on the built environment, leading to an increasing interest in jointly studying climate change and building science. For example, [1] projects an increase in future wind-driven rain loads for many areas across Canada, which may lead to higher moisture damage risks. To better prepare for the rapidly changing climate conditions, the building practitioners will have to incorporate understanding of climate change and their impacts on the built environment to ensure sufficient durability throughout a building's service life.

Understanding the transport of heat, air, and moisture (HAM) through the building envelope is essential for building practitioners to evaluate the building envelope performance and its effect on the indoor environment. Moisture deposited on the envelope may lead to issues such as mould growth [2] or wood decay [3]. Consequently, it is extremely important to be able to accurately simulate HAM through the building envelope. One or multi-dimensional hygrothermal models are commonly used to simulate the complex interactions between HAM and can consider the wall assembly in detail. The development of transient building simulation tools has advanced greatly in recent years with popular programs such as WUFI, DELPHIN, and hygIRC.

Traditionally, climate data used to simulate and design the energy performance of building systems in Canada came from the Canadian Weather Energy and Engineering Datasets

(CWEEDS) and Canadian Weather Year for Energy Calculation (CWEC), produced by Environment and Climate Change Canada (ECCC). These files are provided for hundreds of locations across Canada which have at least 10 years of historical hourly and daily observational data. This set of data produced by ECCC can also be used in the hygrothermal context, given with a few additional variables. The use of appropriate weather data is paramount to accurately evaluate the hygrothermal and energy performance of buildings. For example, [4] showed that the resolution of the supplied wind-driven rain data can cause a loss of detail in the resulting hygrothermal simulations or lead to large errors depending on the situation.

While these products are extremely useful datasets in studying current climate conditions, they do not account for any variability or projected trends in the future climate. For example, [5] found that using historical CWEEDS data from 1998-2014 to study the heating and cooling loads produced results that reduce the representativeness of weather data in building energy simulations over time as the climate changes. This will be a problem as climate change progresses, since these weather files are not frequently updated, and can only account for historical weather patterns.

Early ventures to generate future weather data files for use in the building context, such as the “Morphing” method developed by [6], involves relatively simple linear combinations of additive or multiplicative factors depending on the climate variable. This method morphs existing weather files into climate change weather data by applying a statistical downscaling method, which uses mathematical equations to transform current weather observations by changes found in climate model outputs. [7] has shown the practical approaches of morphing weather data for climate change adaptation through building simulations. The use of the

morphing method has become prevalent in the context of climate change and its implications for buildings [8]. However, some research has pointed out issues in implementing this method. For instance, [9] challenges imposing the current climate variability onto future projected changes and suggests that using high-resolution climate model data to be sufficient to study climate change impacts on the built environment. Alternatively, [10] points out that the morphing method does not account for intervariable dependencies among the climate variables.

Given the limitations associated with the Morphing method, recent studies have focused on generating reliable historical and future projected climate data for use in building simulations. For example, [11] demonstrated a method to synthesize representative future weather data out of regional climate models based on temperature, with result showing that the synthetic weather data is able to replicate hygrothermal conditions similar to the original Regional Climate Model (RCM) data. However, this does not address the bias that studies have shown that are present in climate models, which can be seen when comparing climate model data to historical observations [12, 13].

Consequently, advanced bias correction methods have been developed to help mitigate the effects of the model bias in climate research analyses. Although countless studies have compared the effectiveness of various bias correction methods and climate datasets in terms of climatic conditions [14, 15, 16], efforts to extend that work to the building performance context has been limited. [17] introduces a bias correction approach to generating climate data suitable for hygrothermal and whole building simulations. With the results indicating a reduction in the bias associated with the modelled climate data.

Effectively simulating the hygrothermal performance of building envelopes is an important and crucial component in the design process. There are many ways to generate historical and future climate data suitable for building simulations. However, research on the effectiveness of these approaches is limited to individual methods. An analysis comparing different data generation methods in the hygrothermal context would be useful to better inform the selection of data processing techniques and facilitate more accurate climate impact assessments for the current and future climate.

1.2 Objectives

The goal of this research is to investigate the effects different climate data generation methods have on the hygrothermal performance of wall assemblies in various cities representing different climates across Canada. The performance is evaluated through 1-D hygrothermal simulations using DELPHIN spanning multiple decades, with the following questions in mind:

I. Do different climate data generation methods of raw climate model data lead to different hygrothermal responses of a building envelope when compared to historical observations? How significant are these differences? And which method would lead to more accurate prediction of hygrothermal responses?

II. How does pre-processing of historical and future climate model data affect the projected changes in hygrothermal response of the simulated wall assembly?

1.3 Outline

This thesis includes five chapters. The first chapter provides an introduction for the thesis, and a summary of the main objectives. Chapter two contains a literature review of common approaches used in hygrothermal building modelling, existing climate data generation methods, and the effects of future projected climate change on building performance. Chapter three outlines the steps used in pre-processing the climate data in this work and provides a description of how the hygrothermal simulations are performed. Chapter four presents the results of the analysis, and lastly, chapter five summarizes the work done and provides a conclusion.

2.0 Literature Review

This chapter provides a review of the utility of hygrothermal modelling and its applications in assessing building envelope design, followed by a review of the impacts of climate change in the context of building hygrothermal performance. Lastly, various methods currently used to generate climate data suitable for building hygrothermal and energy simulations will be discussed.

2.1 Hygrothermal Modelling

2.1.1 Overview of HAM Modelling

The presence of moisture in wall assemblies is well known to induce damage in buildings, leading to a necessity among engineers to accurately quantify the potential risks involved. Consequently, numerical HAM models have been developed to simulate the hygrothermal response of wall assemblies. These simulations can be used to study the changes in temperature and moisture content within the building assembly to evaluate its hygrothermal performance. There is significant variation in the many hygrothermal models, which depend on their mathematical complexity. [18] showed that the complexity depends on the extent to which the model considers parameters such as: type of flow (transient/steady state), moisture transfer, quality of information, and specificity of data (weather/material properties). The state of hygrothermal modelling has developed even more since [19] detailed the physics of HAM transfer and compiled a comprehensive list of models.

In general, hygrothermal simulation tools require three inputs: the material properties, geometry, and boundary conditions. The material properties dictate how it interacts with other

components, which include properties such as: thermal conductivity, vapor permeability and diffusivity, specific heat capacity, density, sorption isotherm, suction pressure, liquid diffusivity, specific moisture capacity, and porosity. The boundary conditions describe model selections, parameters, time limits and assigned climate conditions. Finally, the configuration of the assembly itself is just as important, as this is what defines the space where the simulation is to take place.

Hygrothermal simulations allow researchers to identify building envelope systems based on the desired performance criteria such as affordability, durability, air tightness, thermal performance, or energy efficiency. Compared to traditional lab tests, hygrothermal modelling is a quicker and reasonably accurate alternative. Studying the reliability of specific models has produced numerous reports. For example, [20] examined the drying and moisture content of OSB through experimental and simulated data using hygIRC and found relatively good agreement between the results. Similarly, [21] compared three hygrothermal models 1D-HAM, MATCH, and WUFI-2D to lab measurements of three wall types composed of different insulation materials and different air and vapour barriers. Despite some differences between the simulations and lab tests, the analysis showed that all three programs yielded comparable results to the measurements. Additionally, [22] showed that different hygrothermal models can accurately represent HAM behavior at different degrees of complexity.

The objective of combined HAM modelling is to predict changes in moisture content and temperature in the building assembly as a result of the imposed initial, boundary, or ambient conditions. Subsequently, more specific aspects of the building's performance can be quantified

by the hygrothermal performance of the wall assembly related to durability, energy, indoor air quality, and comfort.

2.1.2 Moisture Performance

[23] proposed a methodology to evaluate the moisture performance of masonry wall in Canada by analyzing the HAM calculations obtained through hygrothermal simulations by hygIRC and presents a case study focusing on a brick veneer wall assembly with a steel stud back-up. The performance was characterized by three hygrothermal indicators, which include the relative humidity/temperature index (RHT), freeze-thaw index (FTI), and moisture mass index (MMI), which were used to predict the potential for moisture damage. Ideally, walls should be allowed to dry whenever the moisture load ends, consequently, the MMI tests for the continuous increase of moisture mass in the wall assembly component considered.

Similarly, the FTI is used to predict the moisture damage related to repeated freeze-thaw cycles in the wall assembly. A larger FTI means more potential for freeze-thaw damage and is defined as the number of cycles when temperatures oscillate between the freezing and thawing point for components of the wall assembly that are almost at their saturation level. A study by [24] proposed a similar indicator used to evaluate the risk of freeze-thaw damage called the freeze-thaw damage risk index (FTDR Index). This index considers the largest difference between the degree of saturation of ice content in each freeze-thaw cycle, which is defined as the process where ice in a porous medium form and then completely disappears. Subsequently, [25] used the FTDR Index to assess the potential changes in the risk of freeze-thaw damage in internally insulated masonry walls. Through calculating the FTDR Index at

historical and projected climate change periods, the risk of free-thaw damage is expected to decrease due to an increase in air temperature in this case study.

The RHT Index is used to predict the potential moisture damage under consistent and long-term high moisture levels and warm temperatures, which can be the source of swelling and expansion, corrosion, efflorescence/subflorescence, or biochemical damages. The RHT index is calculated simply by multiplying the temperature and moisture potential. However, the potential is calculated differently considering the material and moisture damage involved. For instance, biochemical damage may require higher temperature and lower relative humidity depending on the species. [26] studied the hygrothermal response of an exterior wall assembly through the RHT index. The study showed that the hygrothermal response in the wall assembly can be assessed using the RHT Index, where higher values illustrate an increased severity of the hygrothermal response. They concluded that the RHT Index can be a useful tool for building practitioners to assess the potential risks of moisture damage in exterior walls since it can be used as a long-term indicator.

The moisture content of porous material like wood-based materials can also be used as a performance indicator of a wall assembly [27,28]. For instance, [29] characterized the impact of moisture content and temperature on the hygrothermal properties of wood-based products. Specifically, in this study, they tested the thermal conductivity and the diffusion of water vapour from a steady-state test of oriented strand board (OSB), wood-fiber insulation board, and solid wood at different moisture contents. It was found that as the moisture content increases, the thermal conductivity increases with it linearly. The vapour diffusion resistance of

the three products were similar where solid wood and OSB were observed to be more impermeable to water vapour than wood fiber insulation.

2.1.3 Biodegradation

A study conducted by [30] examined the increasing risk of mould growth in buildings which can hinder the well being of its occupants. They found that a combination of humidity, temperature, and time are the major deciding factors that determine the potential for mould growth, whereas the type of material plays a lesser role if not negligible. Not all materials are as susceptible to mould growth as others, for each material, there is a critical moisture level after which growth occurs. [31] compared mould growth in laboratory tests and several realistic environments to characterize the critical moisture content. Consequently, when the actual conditions of humidity and temperature exceed the expected critical moisture level, mould growth in the realistic tests occurred as expected. Therefore, they concluded that despite simplified conditions in a lab, the results can be used to indicate mould growth within a building construction.

In the past, many methods have been developed to characterize mould growth in the wood-based materials as [32] pointed out. However, the mathematical model developed by [2] has become the most prevalent in building science and is often used to evaluate mould growth risk in buildings. This model describes mould growth on wooden materials, where a critical RH is calculated at which point growth occurs, which depends on the ambient temperature and relative humidity. The different levels of severity summarized by the mould index is presented in Table 8.

[33] applies this mould growth model and compared the measured mould growth risk at a real building to that of the simulated risk through the WUFI program. An analysis was performed for a single year, where temperature and relative humidity data used in the hygrothermal simulations were measured at the site of the building. The results showed that it is possible to predict real mould growth risk in wood-based wall assemblies following the aforementioned mould growth risk model. Work done by [34] further expends this model to include mould growth on surfaces of other building materials such as gypsum board, spruce plywood, porous wood fiberboard, and cement screed on concrete.

2.2 Climate Change

2.2.1 Climate Predictions

Global and regional climate model simulations are commonly used to study the impacts of climate change [35, 36]. Historical temperature records show that in the last 70 years, the annual average temperature in Canada has increased by 1.7°C, while the annual average precipitation increased by more than 30% [37]. Several future emissions scenarios were studied which limit radiative forcing from 2.6W/m^2 to 8.5W/m^2, termed representative concentration pathways (RCP) [38]. RCP8.5 is widely accepted as the business-as-usual case. Under this high emissions scenario, the annual average temperature across Canada is projected to increase by 6.3°C by the end of the century. Consequently, buildings across Canada will be exposed to unprecedented weather from extreme rain events, flooding, wildfires, and heat spells. To avoid the premature failure of buildings due to climate change, the influences of these changes need to be considered by building practitioners.

2.2.2 Impacts of Climate Change on Building Performance

One area research has focused on, with respect to the impacts of climate change on building performance, is in studying the changes in heating and cooling demand of buildings [39, 40, 41]. For example, [42] examined changes in office energy usage across five different climates in China, severe cold, cold, moderate, warm, and hot, under two emissions scenarios. Even under the low forcing scenario, the estimated cooling demand increase was 18.5% in the severe cold climate, 20.4% in the cold climate, 11.4% in the moderate climate, 24.2% in the warm climate and 14.1% in the hot climate. On the other hand, the reduction in heating ranges from a low of 13.8% in the warm climate to a high of 55.7% in the moderate climate. Similarly, [43] investigated the impacts of climate change on the heating and cooling energy demand in residential buildings across five climates in Australia, varying from cold to hot humid. They found that climate change will have significant impacts on the energy requirements which may range from -26% to 101% by 2050, with the increase in cooling demand significantly outweighing the decrease in heating. The residential houses in a more temperate climate such as Sydney was found to be more sensitive to climate change and could potentially impose the greatest pressure on local energy grid.

A study by [44] proposes a method to estimate the potential changes in energy use due to climate change by using historical measurements. After applying their methodology to a case study house in Montreal, they concluded that the energy used for heating would decrease by 11%-13.1% in 2040-2069. [45] assessed the potential changes in energy usage associated with uncertainties in the future climate of 153 existing residential buildings in Stockholm over a period spanning from 1961 to 2100. The analysis considered four major uncertainties in the

projected climate concerning global climate models, regional climate models, emissions scenario, and initial conditions in the climate models. The energy performance was evaluated by studying the indoor temperature, and heating and cooling energy demand with reference to three cooling strategies: natural, natural and mechanical (hybrid mode) and only mechanical. Their results showed that heating demand will decrease by 30% at the end of the study period, compared to 2011 levels. Additionally, the heating demand varies by up to 30% between different climate scenarios. Differences between climate scenarios result in large variations in the cooling demand of up to 500%, but despite the large differences, the results do not lead to a significant increase of cooling demand since it is quite low in the current climate conditions.

Research on the indoor temperature and thermal comfort naturally follows from studying the impacts of climate change on heating and cooling energy usage. Many studies have evaluated the potential effects of climate change on the indoor thermal environment [46, 47, 48, 49, 50]. For example, [51] used projected climate change data to examine the effects of the most extreme climate change scenario on the future indoor? temperature change, in an effort to study the potential energy consumption during summertime overheating, and thermal comfort in residential buildings located in England. A number of passive adaptation measures were investigated in relation to their ability to reduce the negative impacts on comfort and energy consumption due to climate change. For the four different style homes that were studied, they found that the ability for users to control the shading in the home yielded the best results. Other effective measures they found include increasing the surface albedo of the building façade and increasing the thermal mass of the building itself. However, it was concluded that none of the passive measures included in this study could completely mitigate

the risk of overheating in English homes, especially by 2080 in the climate change scenario that was studied.

Similarly, [52] studied the thermal comfort and heating and cooling energy demand across 15 cities and 7 climate zones in the U.S., based on 3 different emissions scenarios. Combining typical meteorological year datasets with the morphing method and projections from a global climate model, weather data was downscaled to hourly data suitable for use in building energy simulations. By the 2080's, annual temperature in the 15 cities will increase by 2.3-7°C compared to the 1960's. Consequently, the majority of the cities will see a net increase in energy used for cooling by that time.

Another area of research studies the impact of climate change on the durability of buildings. For instance, [53, 54, 55, 56] examined the expected durability of the built environment under a changing climate. [57] assessed the impact of future climates on the durability of typical residential wall assemblies retrofitted to the PassiveHaus standard over the current and projected future climate in Montreal. The durability of the assembly was characterized by analyzing the frost damage risk to bricks and the biodegradation of plywood sheathing through hygrothermal simulations using WUFI. Additionally, the moisture content, RHT, and mould growth index were used as performance indicators to evaluate biodegradation in the plywood sheathing. They concluded that by upgrading the typical wall assembly to the PassiveHaus standard, the frost damage risk would increase in the near future. The decay risk of the plywood sheathing would decrease while mould growth risk following the RHT criteria would increase due to climate change.

Climate indices can provide a concise summary of building performance [58], which can be easily extrapolated to include projected climate data to study the potential consequences of climate change in a broad manner [59]. [60] studied the potential decay of wood structures under projected climate change conditions in Norway. The potential decay in wood structures was calculated based on Scheffer's climate index during a historical 30-year period from 1961-1990, which allows different guidelines on protective measures to be applied depending on the distribution of the climate index. The results showed that climate change will lead to a higher risk of decay in wood frame structures.

[61] investigated the potential effects climate change has on the wind-driven rain loads in Sweden, and the impacts on the hygrothermal performance on rain screens walls of common construction. The response of the façade was assessed under historical and future climates with uncertainties in the GCM, emissions scenario, and spatial resolution of the climate model in mind. The results showed that uncertainties in the climate can produce significant variations in the prediction of hygrothermal performance on the studied assembly. Overall, the risk of moisture related damage due to an increase in future moisture load will also increase the risk of moisture related damage in building facades. Similarly, [62] investigated the impact of climate change on the hygrothermal performance and mould growth risk in ventilated attics. The historical and projected climate were obtained through a regional climate model, which also considered three future emissions scenarios. The results imply an increase in mould growth risk due to climate change as moisture problems increase in the future. Considering the different emissions scenarios that was examined, the different narratives do not affect the risk of mould growth in the attic due to the mitigating factors of other variables.

The increase in carbon dioxide in the atmosphere in conjunction with changes in temperature and relative humidity as a consequence of climate change can also cause a decrease in the durability of concrete by process of carbonation [63, 64, 65]. Correspondingly, [66] investigated the impacts of increased carbonation and chlorination of concrete buildings due to climate change. With results that suggest that existing concrete structures will exceed the recommends levels of carbonation and chlorination well within their design life, which could result in potentially expensive repairs.

2.3 Climate Data Generation

Weather data is an integral component to study the built environment through building simulations. As suggested by [67], ideally, weather files should be able to represent typical and extreme conditions. Additionally, it should be available in an appropriate temporal and spatial resolution to be able to accurately characterize the local conditions. And to study climate change, it should also illustrate future possible changes in climate. Consequently, many studies have focused on developing methods to generate reliable historical and future projected climate data for use in hygrothermal and energy simulations.

2.3.1 Morphing

One such approach, called the “Morphing” method, was developed by [6] with this exact purpose in mind. The morphing method is a statistical downscaling method which uses mathematical equations to transform current weather observations by changes found in climate model outputs. It has subsequently become widely used in this context [68, 69, 70, 71, 72]. This method combines the current observed weather data with the average projected

changes in climate calculated by climate models, resulting in a set of data that accounts for changes in climate while retaining the characteristics of observed weather data. Therefore, morphing can be viewed as a downscaling method, bringing coarse resolution climate model data to a finer spatial and temporal resolution, suitable for use in hygrothermal simulations.

[73] applied the morphing method on global climate model outputs to generate hourly weather files for future climatic conditions in Vancouver for three time periods under the RCP8.5 emissions scenario; the purpose of which was to support climate resilient building design. Weather variables such as: dry-bulb temperature, relative humidity, solar radiation, cloud cover, wind speed, and atmospheric pressure, necessary for energy simulations through EnergyPlus was adjusted. Simulations of the various time periods implies that climate change following RCP8.5 will have significant effects on the building energy performance and demand in Vancouver due to an increase in cooling and decrease in heating requirements. Similarly, [74] performed an analysis morphing existing EnergyPlus weather data with general circulation model predictions of a moderate future climate change scenario. The study showed that morphing the present-day weather data is an appropriate way to generate weather data to account for future climate change. However, in order to thoroughly assess the building performance, it is necessary to include several climate change scenarios. Additionally, some of the limitations of the morphing method were also discussed. It has been shown that weather files morphed with GCM predictions are likely to underestimate the effects of climate change when compared to those made with RCM predictions, all else being equal such as emissions scenario and timeframe. This effect is more pronounced for more distant timeframes. Consequently, morphing should be performed on RCM outputs whenever possible.

[75] morphed weather files for building energy simulations to evaluate the lifetime energy consumption of prototype buildings. The study was performed on three US cities, each with different climates, to exhaustively study the regional effects on long term energy usage in the changing climate. In general, they found that overall energy demand will increase due to increased cooling demand. Additionally, it was suggested that due to the large variability in their results arising from the different locations and climate projections, it is critical to understand that results obtained through a similar methodology should not be applied too broadly as specific modelling is needed in each case. The morphing method was used to analyze the hygrothermal performance of internal wall insulation under current and future climates in [76]. Historical weather station data was morphed by calculations with global climate model to perform hygrothermal simulations with DELPHIN. They found that because of climate change, the buildings in London will experience higher exposure to WDR in both intensity and duration. Hygrothermal simulations showed that in the three different internal wall insulation systems tested, the increased moisture loads will lead to significant gains in interstitial relative humidity. That combined with higher average temperatures throughout the year will yield more conditions favourable to mould growth.

2.3.2 Typical Meteorological Year

Another approach to prepare climate data is to subset the data into a typical meteorological year first introduced by [77] which involves a statistical analysis of the study period to select one typical meteorological month for each month of the year. This method has subsequently been used in the building energy performance field in an effort to reduce the

number of simulations required to accurately describe the effects of a typical climate on the building [78, 79, 80].

This method has been further expanded on by [11], to synthesize typical and extreme datasets out of regional climate models. Due to the numerous uncertainties in climate modelling, there are many variables to consider for those studying the impacts of climate change. Consequently, to reduce the number of potential simulations required to study climate change in the building context, this method was developed to simplify these assessments. This method relies on a similar process to the typical meteorological years, producing one typical (typical downscaled year) and two extreme (extreme cold year and extreme warm year) weather datasets out of one or more regional climate models based on the dry-bulb temperature, with the goal of decreasing the amount of data without losing the details and quality of the original future climate projections. [11] applied this methodology of typical and extreme weather datasets to the hygrothermal simulation of a wood-frame wall. The conclusion in this study affirms the validity of using this synthesized weather data method in the context of hygrothermal simulations. The findings showed that this method helps to minimize the number and duration of the required simulations in studying climate change, while also keeping the quality of the data on a similar level to the original RCM.

2.3.3 Bias Correction

Despite the advances in climate modelling, accurately representing the climate system is still a major challenge for climate modelers as simulations are often biased compared to historical observations [81, 82]. This means their summary statistics such as the mean, variance, and extremes may differ from historical observational records. These deficiencies in the model

result in large uncertainties in the output which could affect the reliability of subsequent climate impact assessments.

Many bias correction (BC) methods have been developed to correct for the statistical discrepancies in climate model simulations. The earliest proposed BC methods started by adjusting the univariate distribution of climate variables, which accounted for features such as the mean [83], variance [84], or quantiles [85]. Univariate BC methods are only designed to correct climate variables independently of each other. In reality, climate variables are highly dependent, which can lead to inappropriate intervariable dependencies in the multivariate setting. Failure to account for intervariable dependence can result in bias corrected outputs which violate physical laws and dimmish the reliability of impact studies [86]. Consequently, the intervariable dependence of corrected data need to be carefully considered before using in climate impact assessments.

As a result, multivariate bias correction methods (MBC) have been developed to adjust the univariate distribution as well as the intervariable dependence of climate model outputs. Many MBC methods have been developed; however, they can be grouped into three main categories [87]. The marginal/dependence approach consists of methods that adjust the univariate distribution and the dependence separately. The all-in-one category includes MBC methods that correct the 1-dimensional features and multivariate dependencies simultaneously. Lastly, the successive conditional MBC methods perform corrections successively, based on the condition of variables that have already been corrected. This category has two major limitations. The order of the variable affects the quality of the

correction, and the correction becomes decreasingly robust as the amount of available data reduces at each step.

Bias correction processes have been widely used in climatology to study climate and climate change. However, the use of bias correction in climate impact studies are limited, especially in the field of building science. [88] proposes using a bias correction approach to generate climate data to undertake hygrothermal and whole building simulations. In this case study, hourly regional climate model data suitable for building simulations were generated during historical and future projected periods for 11 major cities in Canada, which includes variables such as solar radiation, cloud cover, wind speed, wind direction, humidity, rainfall, temperature, and snow depth. The results demonstrated that the implemented methodology reduces the bias associated with the regional climate model, suggesting that the generated climate data is appropriate for building simulations. Subsequently, several studies have used this approach to generate weather data to understand the effects of climate change in the building context [89, 90].

For example, [91] applied the bias corrected climate data to study the variability in climate and its impacts on the hygrothermal performance of wood-stud and retrofitted historical masonry. They showed that by using a large ensemble of climate model data, which represents various plausible paths of climate change, the hygrothermal simulations yield robust results suitable for climate impact assessment. Whereas the use of a single member of the ensemble results in a loss of details related to the internal variability of the climate model. Similarly, [92] examined the effects of climate change on the moisture performance of tall wood building envelopes in 5 cities across Canada. The study involves performing 1-D

hygrothermal simulations through DELPHIN using a complete ensemble of regional climate model data for a historical and projected climate change period. Using the mould growth index as a performance indicator, results showed that at every location the mould growth risk will increase due to a rise in rainfall, but the degree to which varies from city to city.

2.4 Summary

Hygrothermal modelling has been an extremely useful tool for building practitioners to examine the performance of the wall assembly using several criteria such as: thermal performance, moisture performance, and biodegradation. However, until relatively recently, the focus of such studies has been on the hygrothermal performance of wall assemblies in the current climate. As climate change progresses, more and more focus has been shifted to assess the impacts of climate change in the built environment. To accommodate the increasing necessity of accurate climate change projections, a number of climate data generation methods have been developed to produce climate data suitable for use in studying the impacts on hygrothermal performance such as the morphing method. A novel idea borrowed from climate science involves the bias correction of raw climate model data to produce weather files applicable in hygrothermal simulations. Consequently, the research presented here is motivated by the need to understand the differences in the various data generation methods and how they may affect results in future projected climates in the context of hygrothermal performance of a wall assembly.

3.0 Methodology

The general methodology used to generate climate data through bias correction or morphing used in hygrothermal simulations for this work is summarized in Figure 1. The set of observational climate data spanning a baseline period from 1998-2017 is used in conjunction with raw CanRCM4 data to calculate bias correction factors, which are used to bias correct raw CanRCM4 data in the baseline (historical) and future time periods. Subsequently, bias corrected data is used as inputs in DELPHIN. Morphed data follows a slightly different path before used as input in DELPHIN simulations. First, morphing factors are derived from the baseline and future periods, which are then applied to observational data, resulting in morphed climate data for that particular future time period, which are then inputted into DELPHIN. More details on the processes used to bias correct and morph climate data is presented in the following sections.

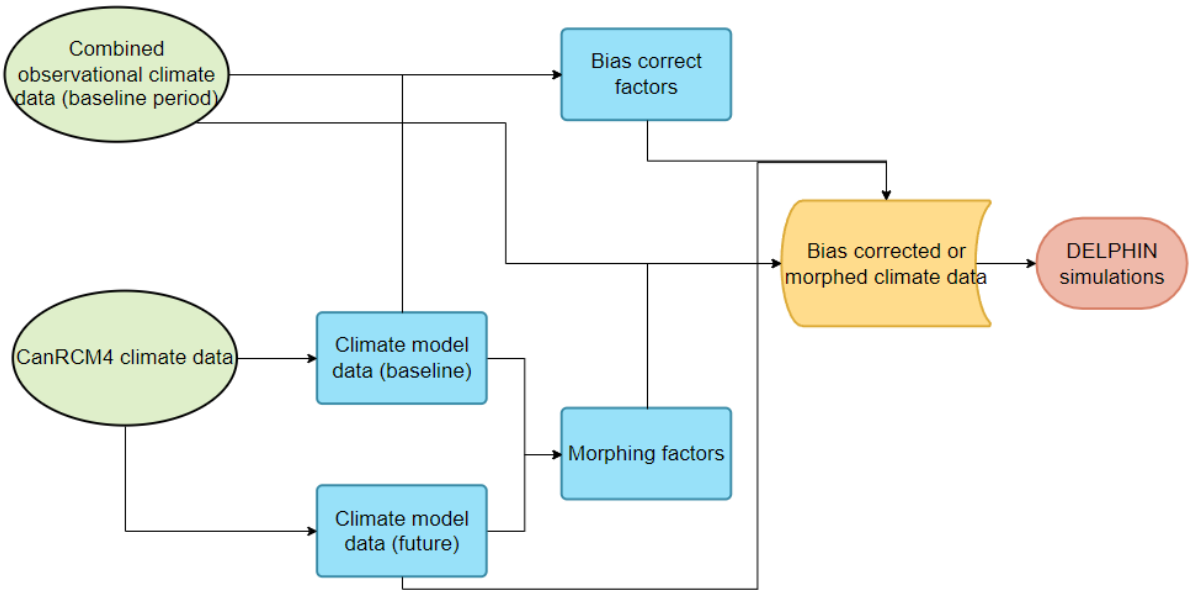

Figure 1. Summary of methodology used to generate climate data for hygrothermal simulations

3.1 Selected Locations

6 cities were selected for this work including: Vancouver, Calgary, Ottawa, Montreal, Kuujjuaq, and St. John's. Their geographical locations are illustrated in Figure 2 while some of their climate design data such as heating degree-days, moisture index, and annual rainfall are listed in Table 1 as reported in the National Building Code of Canada [93]. The selected locations represent a diverse range of climates in Canada, from the mild but wet climate of Vancouver, to the cold and dry of Kuujjuaq.

Figure 2. Location of cities selected for analysis

Table 1. Locations selected for analysis

City	Prov	ID	Lat	Lon	UTC	HDD	MI	Rainfall (mm)
Ottawa	ON	6106001	45.32	-75.67	-5	4500	0.84	750
Montreal	QC	7025251	45.47	-73.74	-5	4200	0.93	830
St.John's	NL	8403505	47.62	-52.75	-4	4800	1.41	1200
Calgary	AB	3031092	51.11	-114.02	-7	5000	0.37	325
Vancouver	BC	1108395	49.19	-123.18	-8	3100	1.93	1850
Kuujjuaq	QC	7113535	58.09	-68.42	-5	8550	0.80	280

3.2 Data

3.2.1 Climate Model Data

Historical and projected climate data was taken from the Canadian Regional Climate Model version 4 (CanRCM4). The data is a product of dynamically downscaling the results of a Global Climate Model (GCM), Canadian Earth System Model version 2 (CanESM2), from a spatial resolution of approximately 2.8° to 0.44° [94, 95]. CanRCM4 was initialized from 5 randomly selected historical members of the CanESM2 model, and selecting 10 sets of cloud physics parameterizations, resulting in a total of 50 realizations of simulated climate data. Out of these 50 realizations, 15 were archived in hourly time-steps. Since this work is only focused on evaluating the impact of climate data generation methods, and not on assessing uncertainty in future climate projections from multiple climate realizations, a single realization was chosen among the 15 realizations.

The historical simulations cover a time period from 1950-2004, and the projected time period follows the RCP8.5 future emissions scenario, which is generally accepted as the business-as-usual case [96, 97, 98]. This work uses a global warming threshold approach to

assess the impact of warming for selected Canadian cities. This technique allows climate change to be studied in terms of global warming thresholds independent from specific GCM's or RCP's, which can address some uncertainties associated with climate change impact assessments [99]. The projected future changes in climate are calculated between a historical time period starting from 1991-2021, and a future time period coincident with 3.5°C of global warming. The future period was determined by calculating the average global temperature simulated by CanESM2 over a 31-year window. In this case, a period ranging from 2064-2094 was identified as associated with 3.5°C of global warming.

Since CanRCM4 is a gridded product, to get the model data at a particular location, the closest grid to the weather station where the observational data was measured is identified based on the given longitude and latitude. Subsequently, the necessary variables are extracted from this grid. The selected locations include Ottawa, Montreal, St. John's, Calgary, Vancouver, and Kuujjuaq, and details of their weather stations are listed in Table 1. Three BC methods are used to correct hourly climate data simulated by CanRCM4, with reference to six locations representing several different climates across Canada. The multivariate set of climate data includes the total cloud cover, relative humidity, station pressure, global horizontal irradiance, dry bulb temperature, wind speed, wind direction, rainfall, and snow depth.

3.2.2 Climate Observations

Hourly observational data, from ECCC's CWEEDS product was obtained which includes variables such as: global horizontal solar irradiance, relative humidity, air temperature, station pressure, 10m wind speed and wind direction, and snow depth. Since CWEEDS record does not contain detailed rainfall or cloud cover data, these variables were taken from hourly

observations from ECCC, where missing values were filled by using a quantile mapped version of hourly Climate Forecast System Reanalysis datasets [100]. Data for Ottawa, Montreal, St. John's, Calgary, and Vancouver have historical data spanning from 1998-2017, while Kuujjuaq only has data starting from 2005 and ending in 2017. The variables and their units are listed in Table 2.

Table 2. Climate variables and their units considered for bias correction and morphing

Climate Variable	Units
Global Horizontal Irradiance	kJ/m^2
Rainfall	mm
Relative Humidity	%
Wind Speed	m/s
Wind Direction	Degrees clockwise from North
Total Cloud Cover	%
Temperature	°C
Atmospheric Pressure	Pa
Snow Depth	cm

3.3 Bias Correction

3.3.1 Quantile Delta Mapping (QDM)

The Quantile Delta Mapping method is a univariate BC method which was developed by [101]. This method preserves the absolute quantiles for interval variables like temperature or relative changes in ratio variables like precipitation. An interval scale is one where there is order and the difference between two values is meaningful. And a ratio variable, has all the properties of an interval variable, and also has a clear definition of 0.0. When the variable equals 0.0, there is none of that variable. QDM is similar to other univariate methods such as quantile delta change [102] and quantile perturbation [103] which also preserve the relative

changes. However, QDM preserves relative changes in all quantiles of a distribution. The QDM algorithm is performed in two steps. First, the future model outputs are detrended by quantile and bias corrected to observations by quantile mapping, then the projected relative changes in quantiles are superimposed on the bias corrected model outputs. A more detailed description of the QDM algorithm is presented:

1) The empirical cumulative distribution is calculated for the reference (observational) and climate model series.
2) The relative change in quantiles between the reference dataset and the climate model data is calculated for the reference time period.
3) Quantiles of the climate model data during the reference period is then bias corrected by applying the relative changes calculated in step 2.
4) The bias correction of future projected climate model data results from applying the relative changes found between quantiles in the historical and future time periods of climate modelled data. To preserve absolute changes rather than relative changes, this step can be applied additively as opposed to multiplicatively.

3.3.2 Multivariate Bias Correction with N-dimensional probability density function transform (MBCn)

The Multivariate Bias Correction with N-dimensional probability density function transform was developed by [104] and falls under the marginal/dependence category. MBCn allows the transfer of statistical features of one reference multivariate distribution to another. The univariate distributions of climate variables are first corrected with a univariate BC method. Any method could have been chosen for this purpose, however, QDM was chosen for the task.

After the univariate distributions are corrected, the intervariable dependence is iteratively adjusted. At each step, the climate variables are partially decorrelated by random rotations of the matrices, after which QDM corrections are applied before recorrelation, where the inverse rotation takes place. This step is repeated until the multivariate distributions between the reference and climate simulations converge during the calibration period. By doing so, MBCn allows changes in the dependence structure to follow model changes. Consequently, the procedure to undertake MBCn can be explained in 3 steps:

1) The marginal distribution (distribution of each individual climate variable) is univariately corrected using QDM.
2) The multivariate dependence structure (the dependence of one climate variable to another) is adjusted by iteratively performing a random orthogonal rotation to the matrix of all the climate variables in consideration.

   Correction factors calculated in step 1 are then applied to the rotated marginal distributions before the matrix is rotated back to its original structure.

   This step is repeated until the multivariate distribution of the corrected simulations matches those of the reference dataset (observations).
3) The quantiles of each variable obtained in step 2 is replaced with those obtained during step 1, which will prevent the deterioration of the climate model trend due to the correction of the multivariate dependence structure in step 2. That is to say that each column obtained in step 2 are re-ordered according to the ordinal ranks of the corresponding column found in step 1. Where the ordinal rank is the value given a certain position in a sequence of numbers where no positions are equal.

3.3.3 Rank Resampling for Distributions and Dependences (R2D2)

The Rank Resampling for Distributions and Dependences method was developed by [105] and belongs to the marginal/dependence category. R2D2 relies on a reordering technique called the Schaake Shuffle, which was introduced to post process temperature and precipitation forecasts from numerical weather prediction models [106]. The shuffling ensures that the rank structure of the sample dataset corresponds to the rank structure of a reference dataset thus allowing the multivariate dependence structure to be reconstructed. Since the R2D2 method belongs to the marginal/dependence category, it first performs a univariate correction to adjust the distribution of each climate variable. Like the previous marginal/dependence method MBCn, QDM is chosen for this task. Following the univariate correction, a reference dimension/variable can be selected for which the rank structure remains unchanged, thus introducing stochasticity in the bias correction. Then the intervariable correlation of the reference dataset is reconstructed with the constraint of preserving the structure of the reference dimension. The R2D2 procedure can be summarized into 5 steps:

1) The marginal distribution (distribution of each individual climate variable) is univariately corrected using QDM.
2) One “reference dimension” (physical variable) is selected for the shuffling, where the time sequence of the ranks of the 1-D bias corrected data is kept intact. Where rank is defined as the maximal number of linearly independent columns of the matrix of climate variables. This provides a multivariate structure to the data resulting from step 1.

3) For each time step in the corrected data from step 1, R2D2 searches for a time step in the reference period where the rank of the reference dimension is the same as.
4) The time series of the “non-reference dimensions” are shuffled so that the rank structure of the reference dataset is reproduced in the 1-D bias corrected climate data resulting from step 1.
5) Steps 2-4 are repeated until each dimension (climate variable) has been used as the reference dimension.

3.3.4 Bias Correction Methodology

The steps presented in this section to perform bias correction only apply to the QDM, MBCn, and R2D2 methods. BC methods can be applied to climate simulations in several different ways. The most common approach is to correct for the intervariable properties grid by grid, while ignoring the spatial correlation of neighboring grid cells. Alternatively, BC can be used to correct for spatial dependence, where all the grids of a particular climate variable is corrected independently of other variables [107, 108]. Otherwise, the spatial and intervariable correlation could also be corrected simultaneously, where all grids and variables are jointly corrected. However, in this work, only individual grids of the climate model are of interest, and therefore no spatial corrections were performed.

The aforementioned BC methods are used to correct climate model simulations produced by CanRCM4 over the three time periods of interest, 1991-2021 (historical), 1998-2017 (observational), and 2064-2094 (projected). The reference dataset used to train the BC models is the result of historical measurements at six locations across Canada, with the earliest measurements starting from 1998 and ending in 2017 with a caveat for the Kuujjuaq station,

where the measurements start from 2005. From this set of data, a subset of 10-years (2008-2017) was taken as the reference data to train the model. Consequently, bias correction of raw climate model data was performed in 10-year blocks.

To preserve seasonal trends, each month is often bias corrected separately from each other. There are two approaches that can be taken in this context. First, the most common setup is to separate each month such that data for January is only corrected with respect to January, February with February, and so on. The second setup involves a moving window of three months such that corrections for January are performed on December, January, and February, then corrections for February includes January, February, and March (Cannon, Sobie, & Murdock, 2015). This is done to alleviate some of the sampling variability which is more prevalent when corrections are done in smaller one-month blocks. Additionally, common practice is to apply a threshold of 1mm to the simulated precipitation before correction, and values lower than 1mm are replaced by 0mm after BC is completed.

3.4 Morphing

The Morphing method was introduced by [6] to produce weather data suitable for use in hygrothermal building simulations that would account for future changes in climate. Ideally, the Morphing procedure would yield a time series of weather data that encapsulates the average projected changes in climate in future conditions, while preserving the climate patterns from observations. A shift (1) or stretch (2) factor is calculated by evaluating the difference between the future and present monthly mean in the model data on a month-to-month basis, and the factor is then applied to the observational climate data. Depending on the variable,

either a shift (3), stretch (4), or a combination of both factors (5) is applied to the observational data.

$$\Delta x_m = \langle x_{future} \rangle_m - \langle x_{present} \rangle_m \quad (1)$$

Where:

- $\langle x_{future} \rangle_m$ is the monthly mean of future modelled data
- $\langle x_{present} \rangle_m$ is the monthly mean of present modelled data

$$a_m = \frac{\langle x_{future} \rangle_m}{\langle x_{present} \rangle_m} \quad (2)$$

$$x = x_0 + \Delta x_m \quad (3)$$

Where:

- x is the future monthly weather variable
- x_0 is the monthly observed weather variable
- Δx_m is the shift factor, estimated absolute change in the monthly mean value of the variable for month (m)

$$x = a_m x_0 \quad (4)$$

Where:

- a_m is the stretch factor, predicted fractional change in the monthly mean value of the variable for month (m)

$$x = x_0 + \Delta x_m + a_m (x_0 - \langle x_0 \rangle_m) \quad (5)$$

Originally, [6] developed the Morphing method intended for use in correcting climate data in one-month blocks, such that the factors applied on January are only calculated using modelled data in January. But [73] has experimented with the Morphing method on a daily time scale rather than monthly. For this study, to be consistent with the bias correction methods, the 3-monthly mean is calculated such that factors applied on January include taking

the average over December, January, and February. This 3-month moving window is applied to each subsequent month, centered around the desired corrected month. The baseline observational data was chosen as the "present" data, during the 2008-2017 since data is available during this period at all locations. Correspondingly, factors are then calculated between 10-year segments of the projected (e.g. 2064-2074) and the baseline period (i.e. 2008-2017) in the raw RCM data. After which, the stretch or shift factor is applied to the present-day observational data, following the methods outlined in Table 3, to arrive at the Morphing corrected projected climate.

Table 3. Methodology to generate climate variables through morphing

Variable	Method
Total Cloud Cover	Stretch
Wind Speed	Stretch
Wind Direction	Shift
Global Horizontal Irradiance	Stretch
Rain	Stretch
Relative Humidity	Stretch
Temperature	Combination of Shift and Stretch
Atmospheric Pressure	Shift
Snow Depth	Stretch

3.5 Hygrothermal Simulation

1-D hygrothermal simulations were performed using DELPHIN v5.9. Considering 3 time periods, 6 locations, and 6 different climate datasets, a total of 96 simulations were performed; a summary of which is described in Table 4. The same brick veneer wall assembly was used for each location and wall orientation. The materials and thickness of the assembly are summarized in Table 5 and a cross section of the wall assembly is illustrated in Figure 3.

Similarly a list of initial/boundary conditions can be found in Table 6. Water penetration in the wall assembly was assumed to be 1% of the wind-driven rain deposited on the exterior of the OSB sheathing.

Table 4. Summary of all DELPHIN simulation scenarios

(O-Observational period 1998-2017, H-Historical 1991-2021, F-Future 2064-2094)

Location	Obs	RCM	MBCn	QDM	R2D2	Morph
Ottawa	O	O,H,F	O,H,F	O,H,F	O,H,F	O,H,F
Montreal	O	O,H,F	O,H,F	O,H,F	O,H,F	O,H,F
St.John's	O	O,H,F	O,H,F	O,H,F	O,H,F	O,H,F
Calgary	O	O,H,F	O,H,F	O,H,F	O,H,F	O,H,F
Vancouver	O	O,H,F	O,H,F	O,H,F	O,H,F	O,H,F
Kuujjuaq	O (2005-2017)	O,H,F	O,H,F	O,H,F	O,H,F	O,H,F

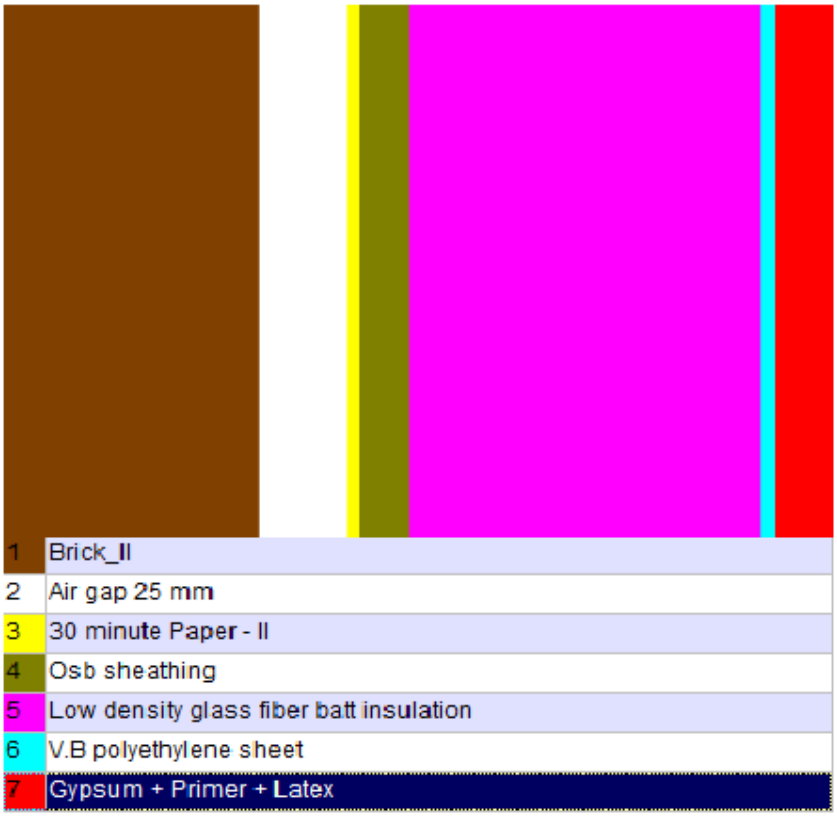

Figure 3. Cross section of brick veneer wall assembly

Table 5. Wall assembly materials and thickness

Materials	Thickness(mm)
Brick	90
Air gap	25
30-minute Paper	0.22
OSB SHEATHING	11
Low density glass fiber batt insulation	140
V.B. polyethylene sheet	0.15
Gypsum+Primer+Latex	12.7

Table 6. Hygrothermal simulation – initial and boundary conditions

Setting	Value
Air cavity ACH	10/h
Indoor RH	50%
Indoor temperature	21°C
Initial temperature	21°C
Initial RH	50%

The orientation of the wall assembly for each location was determined by calculating the total amount of WDR during the period for which observational data was available and choosing the orientation with the largest amount. The amount of WDR was calculated following the ASHRAE model [109], which is given by (6). The chosen orientation (i.e. max WDR) for each location is presented in Table 7.

$$R_{wdr} = F_E \times F_d \times F_L \times U_{10} \times \cos\theta \times \mathrm{R_h} \quad (6)$$

Where:

- F_E is the rain exposure factor
- F_D is the rain deposition factor
- F_L is an empirical constant (0.2)
- U_{10} is the hourly mean wind velocity at 10m
- θ is the angle between the normal of the wall and the wind direction
- $R_h$is the rain intensity on the horizontal surface

Table 7. Wall orientation used in hygrothermal simulations for considered locations

Location	Orientation (Clockwise from 0°N)
Ottawa	270°
Montreal	247.5°
St. John's	247.5°
Calgary	337.5°
Vancouver	112.5°
Kuujjuaq	292.5°

3.6 Analysis Performed

While the various climate data generation methods were performed on all climate variables that are necessary for hygrothermal simulations, the most influential variables for a given wall orientation are usually the horizontal rainfall, relative humidity, temperature, wind speed, wind direction, and solar radiation. In the case of the univariate processing methods, QDM and morphing, each variable is corrected independently of each other. Naturally, under the MBC methods, all variables are corrected together. Additionally, the DELPHIN simulated hygrothermal response to these different climate datasets are evaluated against simulations performed with the observed data. Subsequently, comparisons in moisture content, mould index, relative humidity, and temperature are made measured on exterior side of the OSB.

The mould growth model on wooden materials developed by [2] is used to evaluate the mould growth risk in this work, and as a basis to compare the accuracy of the various climate data generation methods. This model calculates the critical RH relative to the temperature shown in equation (7). The mould growth potential defined in (8) indicates favourable conditions for mould growth, which occurs when m is greater than 1. When conditions are favourable, the mould growth index is described by (9). When a component is exposed to

prolonged favourable mould conditions, the risk of mould growth will likely increase. However, under unfavourable conditions, mould growth will slow down, which can be characterize by (10). The mould index ranges from 0-6, where 0 represents no growth and 6 for heavy growth covering 100% of the surface. Further details on the levels of mould growth are summarized in Table 8.

$$RH_{crit} = \begin{cases} -0.00267T^3 + 0.161T^2 - 3.13T + 100, when\ T \leq 20 \\ 80\% \qquad\qquad\qquad\qquad\qquad\quad , when\ T > 20 \end{cases} \tag{7}$$

$$m = \frac{RH}{RH_{crit}} \tag{8}$$

$$\frac{dM}{dt} = \frac{k_1 k_2}{7e^{-0.68lnT - 13.9lnRH + 0.14W - 0.33SQ + 66.02}} \tag{9}$$

$$\frac{dM}{dt} = \begin{cases} -0.032, when\ \ t - t_1 \leq 6h \\ 0, when\ 6h \leq t - t_1 \leq 24h \\ -0.016, when\ t - t_1 > 24h \end{cases} \tag{10}$$

Table 8. Mould Index Scale [2]

Mould Index	**Growth Rate**
0	No growth
1	Some growth detected only with microscopy
2	Moderate growth detected with microscopy (coverage more than 10%)
3	Some growth detected visually
4	Visually detected coverage more than 10%
5	Visually detected coverage more than 50%
6	Visually detected coverage 100%

4.0 Results and Analysis

This section is divided into 6 sub-sections, which presents the climatic and hygrothermal results for each location. These sections are further subdivided into validation and climate change periods for analysis. In the validation sections, the ability of the presented BC methods to reproduce realistic climate conditions are assessed by comparing the results to the observational dataset during the 1998-2017 period (2005-2017 for Kuujjuaq). In the climate change sections, two 31-year time periods are compared in the context of global warming commensurate with an increase in global temperatures of 3.5°C. The differences in climate and its effect on the hygrothermal performance of the wall assembly is analyzed using the same parameters as in the validation section. The historical period ranges from 1991-2021, while the future projected period starts from 2064 and ending in 2094.

4.1 Ottawa

4.1.1 Baseline Validation Period

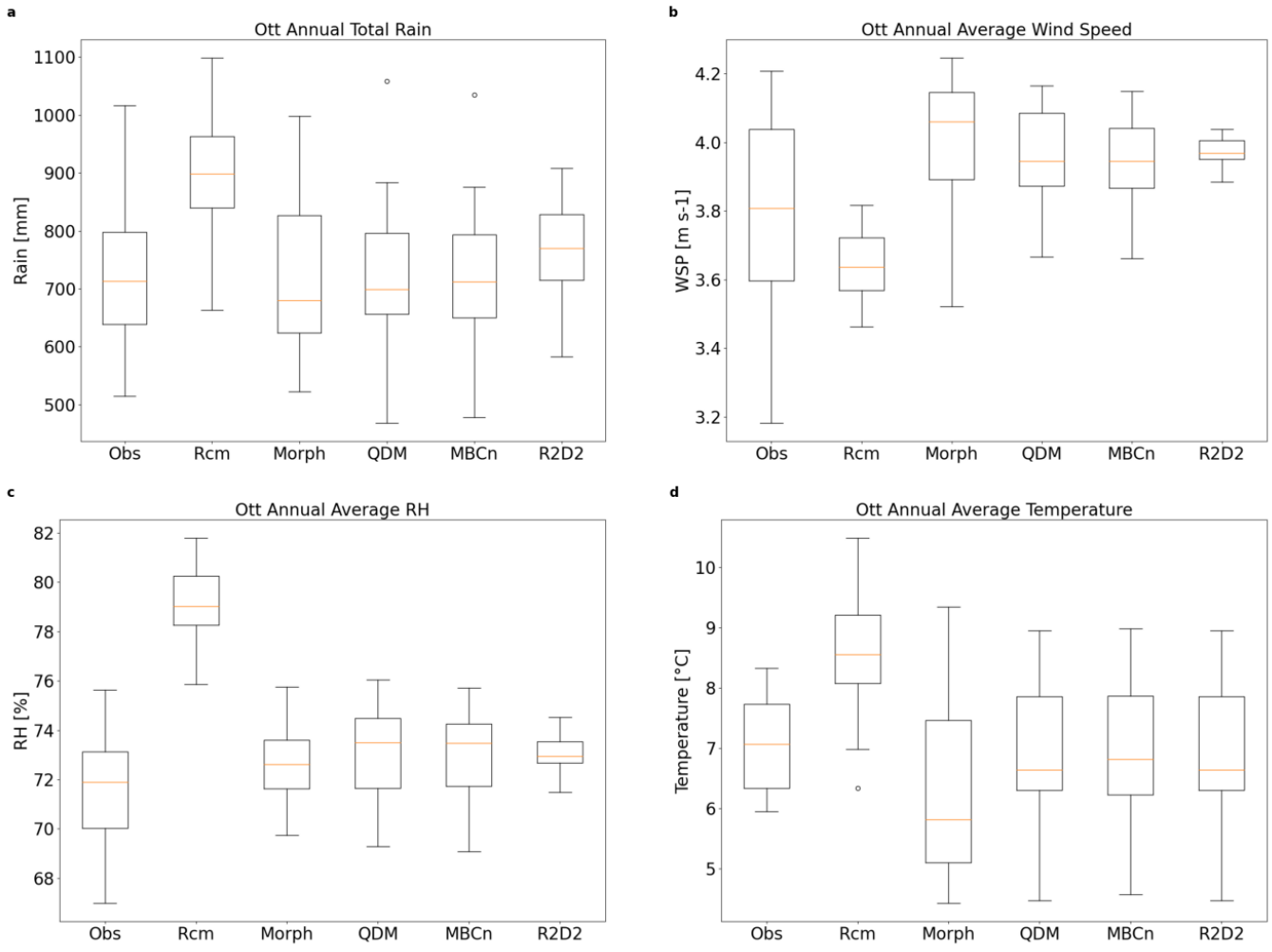

Figure 4. Ottawa annual total horizontal rainfall (a), and average wind speed (b), relative humidity (c), and temperature (d) during the observational period (1998-2017)

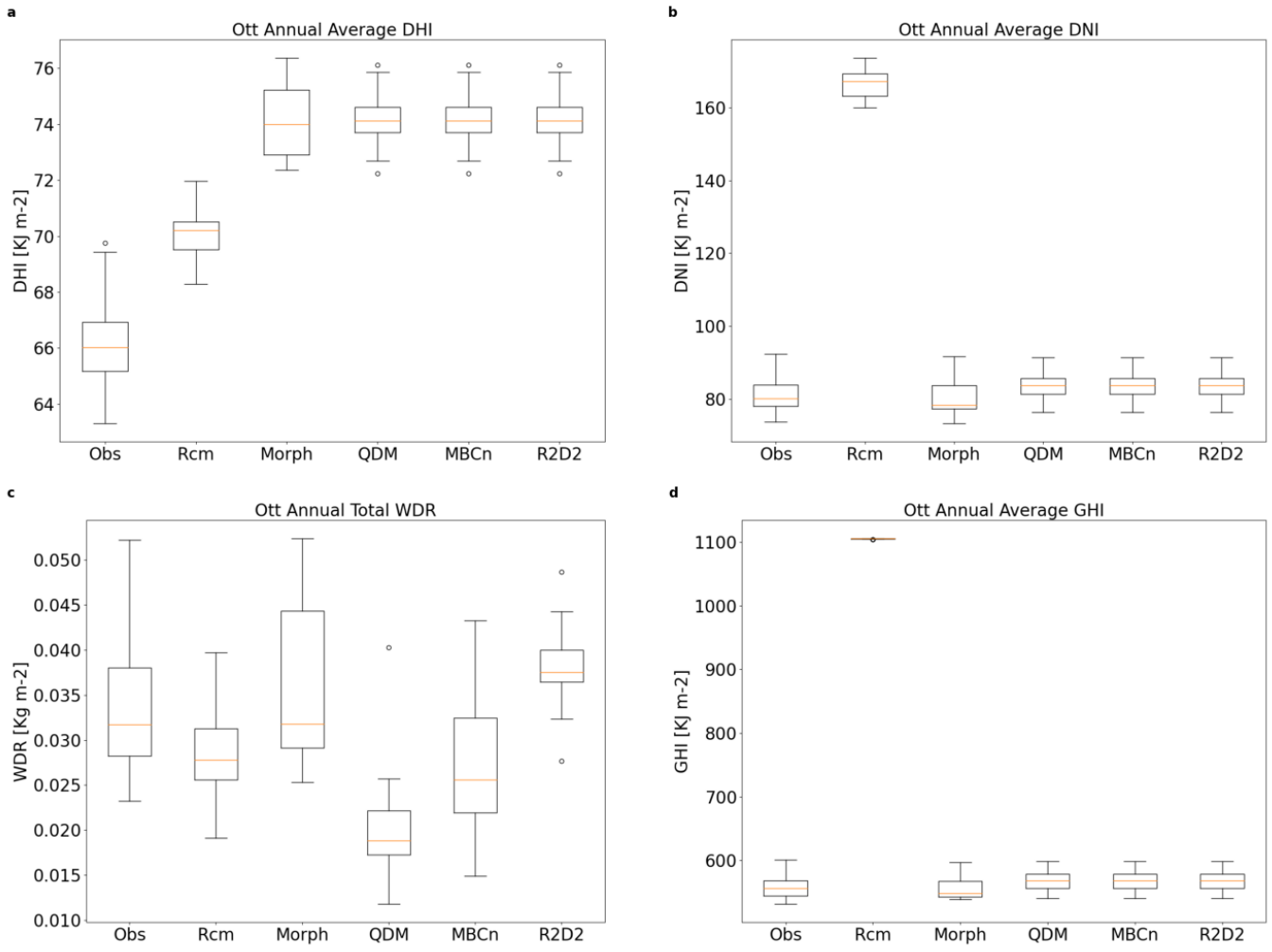

Figure 5. Ottawa annual average diffuse horizontal irradiance (a), direct normal irradiance (b), total wind-driven rain (c) on the wall assembly, and global horizontal irradiance (d) (1998-2017)

A boxplot of the annual total horizontal rainfall in Ottawa during the observational period (1998-2017) is shown in Figure 4a. The boxplot shows the minimum (Q1 – 1.5*IQR), the 25th percentile (Q1), the median, the 75th percentile (Q3), the maximum (Q3 + 1.5*IQR) and the outliers (circles), where IQR is the interquartile range. The figure indicates that during this period, the median annual total rainfall Ottawa received was 713.3mm, according to the

observations. On the other hand, the raw RCM data predicts a relatively higher median annual rainfall of 899mm. The morphing and BC methods show that they are able to correct the overprediction of rainfall from the RCM, with a median ranging from 680mm by the Morphing method, to 770mm by R2D2.

A similar boxplot of the annual average hourly wind speed is presented in Figure 4b. The observations indicate that there was a large variance in the annual average wind speed in Ottawa during this period, with a median of 3.8m/s. The raw RCM predicts a lower median wind speed at 3.6m/s, and with a much smaller variance year to year. The bias corrected datasets marginally overestimate the wind speed, each with a median of approximately 4.0m/s.

Figure 4c and d show boxplots of the annual average relatively humidity and temperature during the observational period in Ottawa. According to the observations, the median relative humidity and temperature is 71.9% and 7.1°C, respectively. In both cases, the RCM overestimates the median value compared to the observational data. The bias correction of relative humidity is well done by all the methods as they estimate a median of around 73%. The performance of the methods to correct for temperature are not as good. Even though the bias corrected datasets perform much better than the raw RCM, the corrected temperature predicts a lower median and has a much larger variability with lower lows and higher highs than the observations.

The solar irradiance variables have a more nuanced distribution compared to the other climate variables since it highly depends on the diurnal cycle, which the MBC methods do not account for when the time series gets shuffled during the bias correction procedure.

Consequently, to reproduce a more realistic distribution, the bias corrected values resulting from multivariate methods are replaced with the time series generated by QDM, which does not distort the diurnal cycle because the time series do not get shuffled at all. Figure 5a, b, and d show the annual average diffuse horizontal (DHI), direct normal irradiance (DNI), and global horizontal irradiance (GHI) in Ottawa during the observational period. In both cases, the QDM, MBCn, and R2D2 datasets are identical since the solar irradiance data from QDM is used. It is evident in Figure 5d that morphing and bias correcting raw RCM data yields significant improvements to the GHI, where RCM has a median of over 1100Kj/m^2 compared to the observed 556Kj/m^2. After splitting the GHI into components of DHI and DNI, the median hourly DHI is calculated to be 66Kj/m^2 while the RCM predicts a median of 70Kj/m^2. The Morphing and QDM correction methods both overestimate this, yielding a median of 74Kj/m^2. Similarly, the RCM also overestimates the median DNI at 167Kj/m^2, compared to the observed median of 80Kj/m^2.

The total annual wind-driven rain on the wall assembly in Ottawa facing 270° is also illustrated in Figure 5c. The most accurate dataset in this case is presented by the Morphing method with a median of 0.0318Kg/m^2 compared to the observed 0.0317Kg/m^2, with a very similar spread as well. This is likely due to the nature of how the Morphing correction procedure is performed since the changes are applied to the observational dataset, as opposed to the RCM data by other bias correction methods. The RCM slightly underpredicts the total WDR, with a median of 0.0278Kg/m^2. The performance of QDM, MBCn, and R2D2 are quite varied, with medians of 0.0188Kg/m^2, 0.0256Kg/m^2, and 0.0375Kg/m^2, respectively.

The results of the bias corrected climate data indicate that an improvement is made from the raw RCM data, although the degree of success varies depending on the chosen method and climate variable. Generally, the raw RCM data compares the worst against the observations; while the bias corrected data adequately corrects for biases in the RCM, which result in better agreement with the observed data. The morphing method does not perform as well as the bias corrected data in some respects, such as in the calculation of wind speed and temperature, which were either over or underestimated.

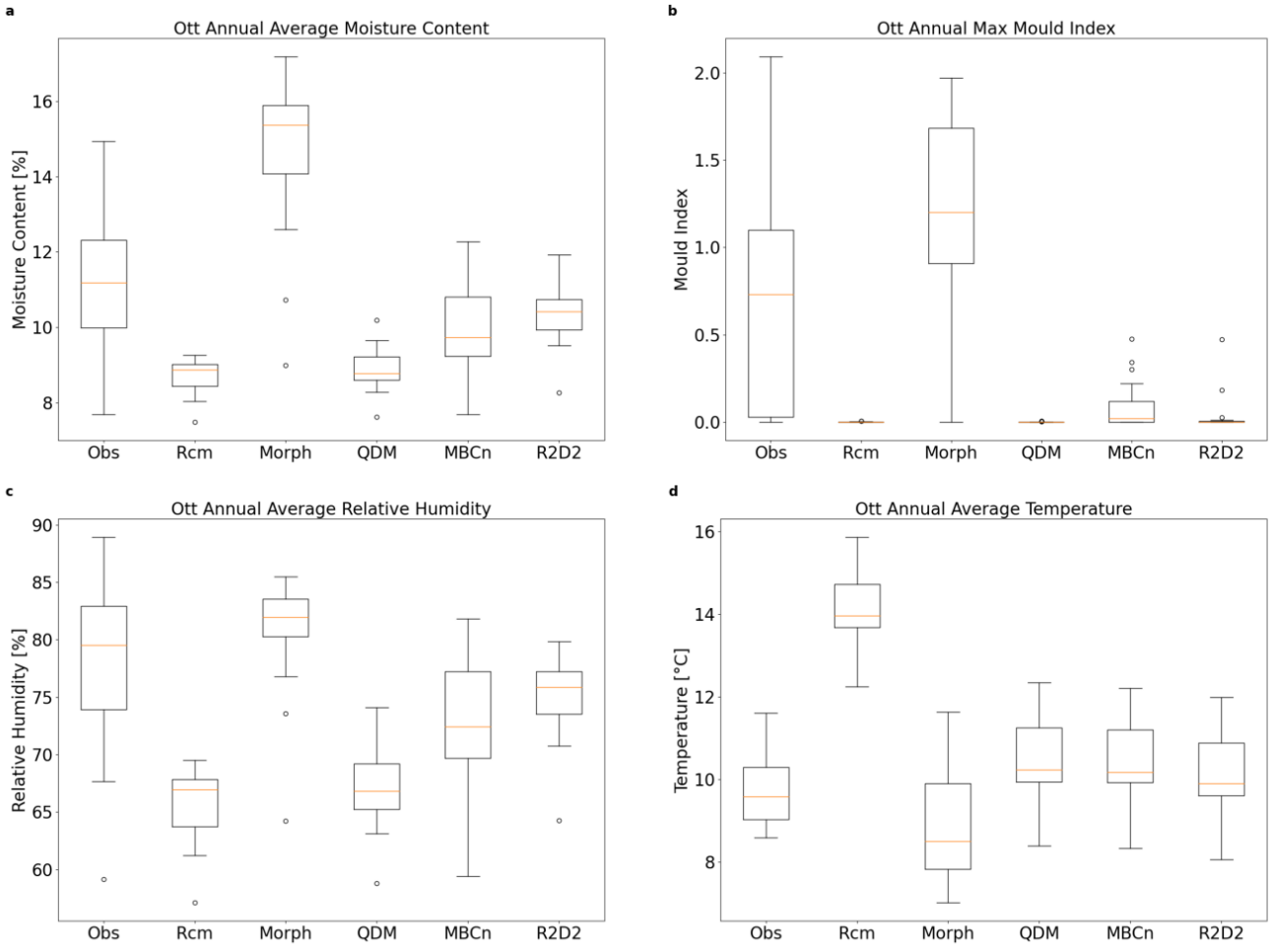

Figure 6. Ottawa annual average: moisture content (a), relative humidity (b), temperature (c), and maximum mould index (d) on the exterior of the OSB sheathing (1998-2017)

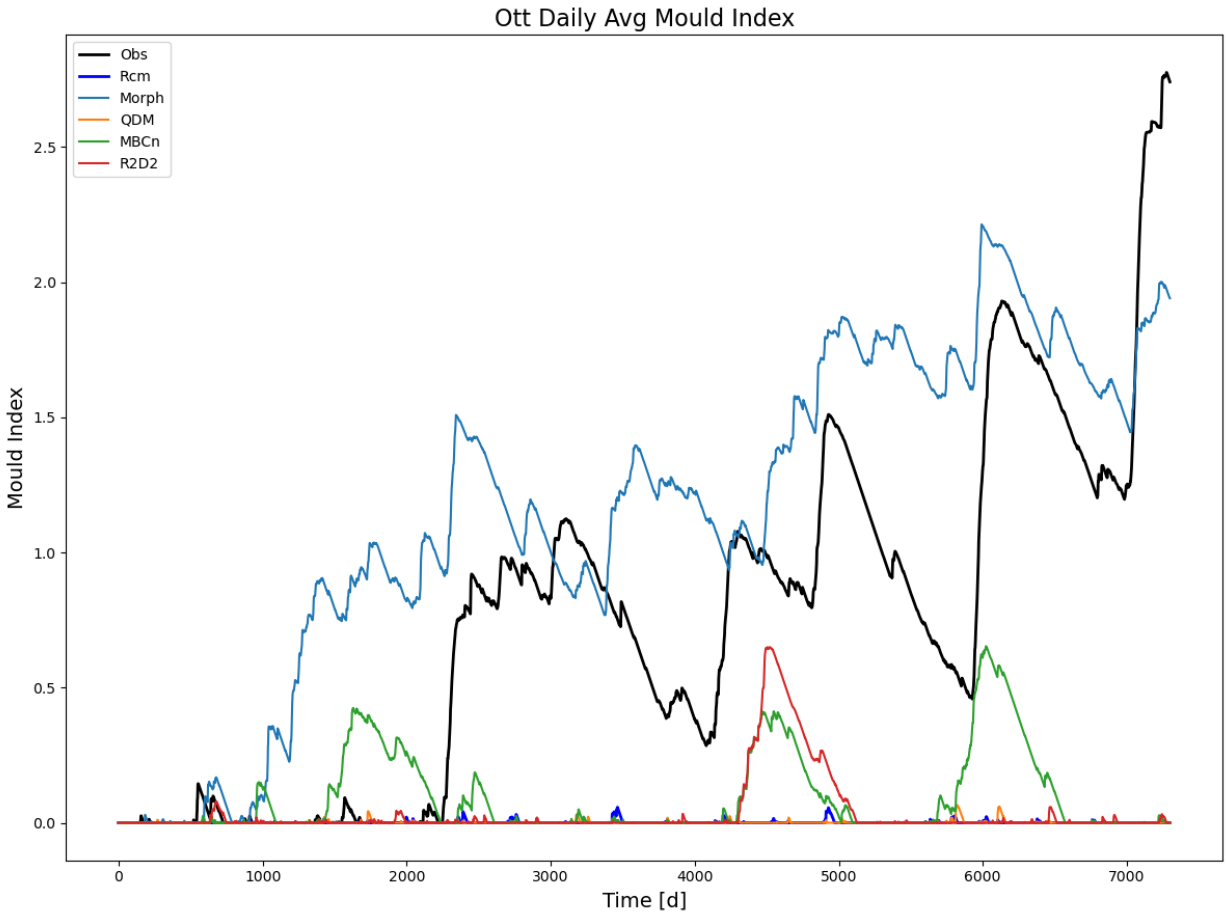

Figure 7. Ottawa daily average mould index on the exterior of OSB sheathing (1998-2017)

The effects of using different climate datasets on the hygrothermal response as simulated by Delphin is compared in Figure 6. The results show the annual average temperature and relative humidity, and maximum mould index on the exterior of the OSB sheathing. The moisture content (MC) of the entire OSB as a percentage of the mass is also presented in this figure. The annual average MC of the OSB varied greatly during the 1998-2017 period according to the observational data, with a minimum of 7.7%, median of 11.2%, and maximum of 14.9%. The hygrothermal simulations with the RCM data yielded quite different results, which greatly underestimates the MC present in the OSB, with a median of 8.9% and

maximum of only 9.3%. This is likely because the RCM's air temperature and global horizontal irradiance is significantly inflated compared to the observed climate, leading to a relatively drier OSB. The morphing method yields a relatively higher MC at a median of 15.4%. The overestimation in this case is due to the larger amount of annual WDR on the assembly. For similar reasons, the MC simulated from QDM, MBCn, and R2D2 closely follow the WDR trends presented in Figure 5 as well.

The median annual relative humidity simulated using the observational dataset is 79.5% with a minimum of 59.1% is shown in Figure 6c. In comparison, the RCM has a median of 66.9% across these 20 years. Despite the near identical performance of the bias correction methods to reproduce the outdoor RH, the corrected datasets achieved varying degrees of success at simulating the RH at the OSB sheathing in the wall assembly. The Morphing method has the most accurate median at 81.9%. Meanwhile, the QDM method mimics the RCM's performance, with a median of 66.8%. Multivariate methods perform marginally better than the univariate QDM method with medians of 72.4% and 75.9% for MBCn and R2D2, respectively.

Observational data indicates an annual average median temperature of 9.5°C on the outer layer of the OSB sheathing in Figure 6d. The RCM significantly overestimates this median by 4.3°C at a median of 13.9°C, which can be attributed to a lesser overestimation of the outdoor air temperature. However, after bias correction by QDM, MBCn, and R2D2, the results yield a more accurate performance as compared to the observed data, bringing down the median temperature on the OSB to within approximately 1°C of the observed dataset. For the same reason, the Morphing method underpredicts the temperature at the OSB, with an annual median value of 8.5°C.

An analysis of the mould index (MI) is presented in Figure 6b and Figure 7. Figure 6b shows the annual maximum mould index, whereas Figure 7 illustrates the daily average value over the entire simulation period from 1998-2017. It is immediately clear that there is a large variation in the mould index between different datasets. The observational data indicates that significant mould growth begins approximately 6 years into the simulation, and continuously experiences favourable mould conditions over the study period peaking at a value of 2.7 at the end of the simulation. The RCM and QDM simulations yielded a completely different result than the observations, showing that there is little to no mould growth at all throughout the entire period. Similarly, the MBCn and R2D2 simulations do not indicate any significant mould growth for most of the time with a couple minor exceptions which subsequently decrease afterwards.

The Morphing method exhibits the most similar behaviour to the observed data; however, the mould growth begins much earlier on in the simulation, starting around 3 years in. The mould growth is strongly driven by the moisture conditions on the OSB sheathing. Certainly, the amount of WDR estimated by the Morphing method is larger than the other datasets, however, another crucial variable to consider is the persistence of moisture, and how long it lingers before other climatic factors dry it. In this regard, the Morphing method would yield the most comparable results to the observed data since the corrections are applied to the observational data to yield the corrected climate dataset.

The hygrothermal results varied much more between datasets than the climate variables did, but the accuracy of the climate data was indicative of the hygrothermal performance. The other datasets, Morph, QDM, MBCn, and R2D2 present reasonably accurate results for the MC, RH, and temperature of the OSB. However, for a more complex variable

such as the mould growth index, which takes into consideration many different climatic conditions, there is varying degrees of success in the correction of climate data. Most notably, QDM, MBCn, and R2D2 fail to replicate the same degree of mould growth present in the simulation with observational data. However, the morphing method is somewhat able to reproduce the mould growth in the simulation. The relative success of the morphing method during the validation period is strongly associated with the fact that RCM data used to calculate the morphing shift/stretch factors are very close to the observed data in time. Therefore, the calculated factors applied to the observational dataset would only introduce minute changes to the underlying data.

4.1.2 Projected Future Period

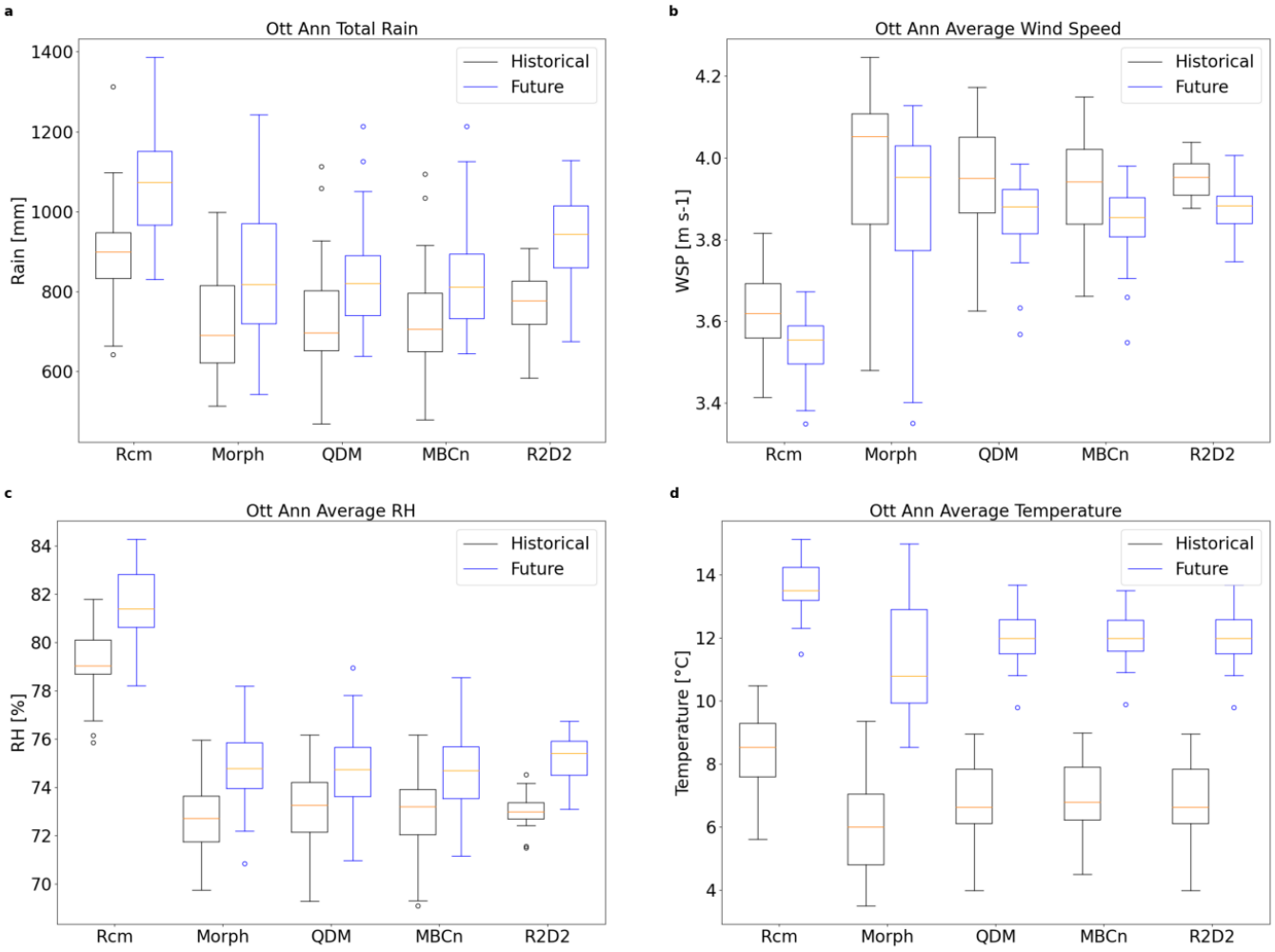

Figure 8. Ottawa boxplots of annual total rain (a), and average wind speed (b), relative humidity (c), and temperature (d), over a baseline historical period from 1991-2021 (black) and a future projected period from 2064-2094 (blue)

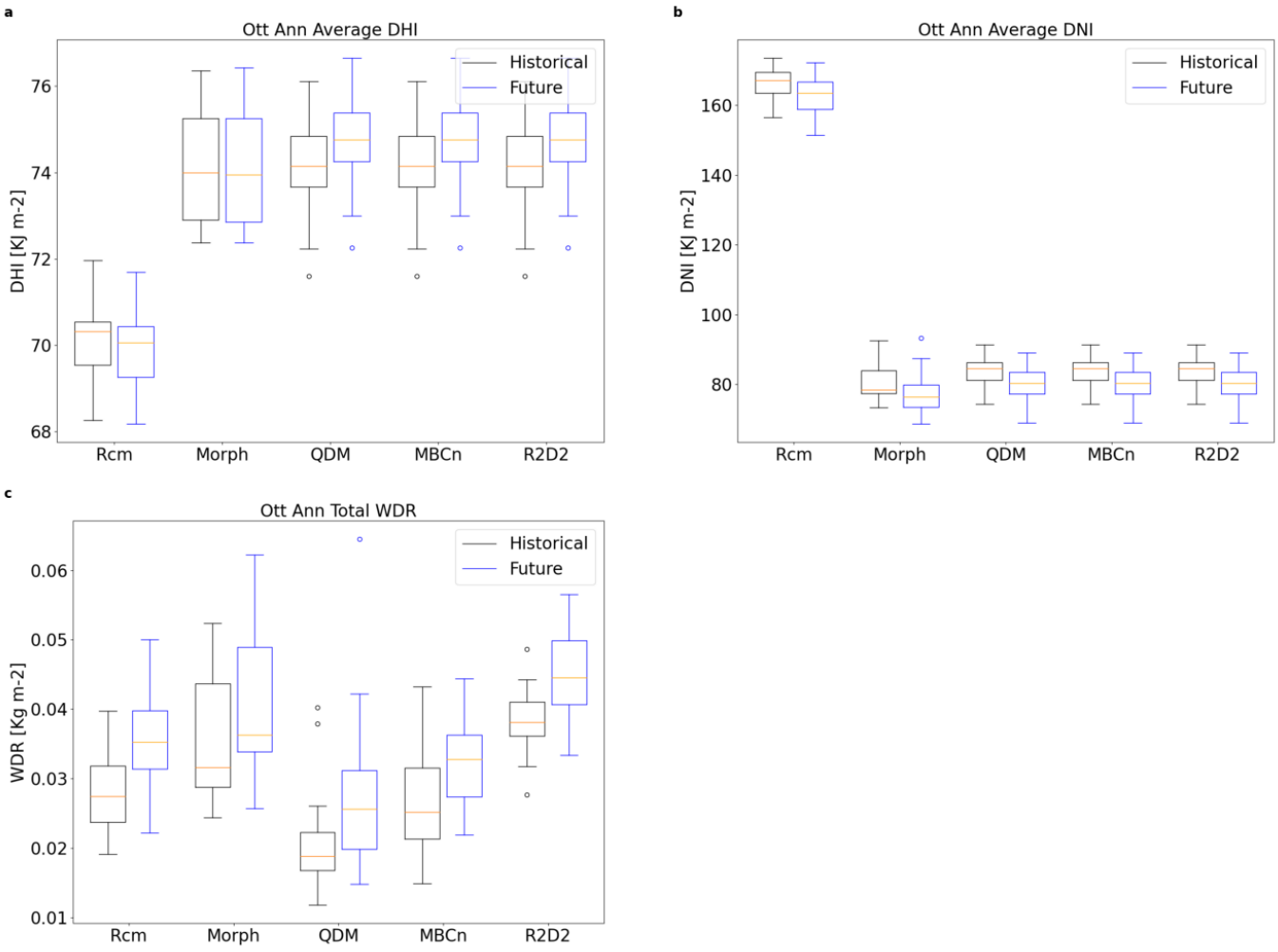

Figure 9. Ottawa boxplots of annual average DHI (a), DNI (b), and WDR (c) over a historical (1991-2021) and future (2064-2094) period

Figure 8a shows the annual total rainfall in 1991-2021 (black) and 2064-2094 (blue). Keeping in mind that the RCM tends to overestimate the amount of rainfall in Ottawa; during the historical period, the RCM predicted a median annual total of 898mm, while the projected rainfall is forecast to increase by 19.4% to 1073mm. In general, bias correction reduces the absolute amount of annual rainfall; however, the relative difference between the two periods is similar, only varying slightly among datasets. For example, Morphing calculates an increase of

18.5% in rainfall, QDM predicts an increase of 17.7%, 15% is expected by MBCn, and 21.4% by R2D2.

A similar comparison of the wind speed is presented in Figure 8b. The raw RCM climate data predicts a median windspeed of 3.6m/s for the 1991-2021 period. Following results from the observational period, it is expected that the RCM generally underestimates wind speed while bias correction tends to bring up the median. All the bias corrected datasets expect a higher wind speed for this period, with a median of approximately 4.0m/s. Future wind speed in Ottawa is projected to decrease marginally by 1.8% to 3.5/s according to the RCM data. All the bias corrected datasets also follow a similar trend, where the projected wind speed decrease by approximately 2%.

During the historical period, the median annual relatively humidity is 79% according to the RCM and increasing to 81.4% in the future. Each bias correction method consistently lowers that median to approximately 73%, however, the values of R2D2 does not vary as much as the other methods. The resulting boxplots are shown in Figure 8c. Overall, future relative humidity will not increase significantly, with the largest relative change at 3.3% from R2D2, and a low of 1.9% predicted by QDM.

Figure 8d shows the annual average temperatures during the historical and future time period. The median annual average temperature during the historical period is 8.5°C. Based on results seen in the observational period, the results from RCM tend to overestimate the temperature. Consequently, the bias correction reduces the median to 5.9°C, 6.6°C, 6.8°C, and 6.6°C, presented in order of Morph, QDM, MBCn, R2D2, during the historical period. Following

a global warming scenario of 3.5°C, the median annual temperature in the future is significantly higher than its historical counterpart at 13.5°C, according to the raw RCM. Estimates of the future temperature from bias corrected data is equally extreme, if not more so. The Morphing method reports a median of 10.8°C, while the other methods show a median of approximately 11.9°C.

Figure 9a and 6b compares the historical and future DHI and DNI. As in the observational period, the solar irradiance variables generated by QDM are used in place of values calculated using the MBCn or R2D2 method as they do not preserve the diurnal cycle. According to the RCM, the median DHI does not change by much between the two periods, with a value of 70Kj/m^2. Due to the extremely small change present in the RCM, the DHI calculated by Morphing remains virtually the same. In both time periods, the median DHI is 74Kj/m^2. On the contrary, according to QDM, the DHI is expected to increase from a median of 74Kj/m^2 to 75Kj/m^2. Considering that the RCM exaggerates the average DNI, the results are relatively consistent between the Morphing and QDM methods which bring down the median value. With a historical median of 78Kj/m^2 and 85Kj/m^2, and 76Kj/m2 and 80Kj/m^2 during the projected period, respectively.

Each dataset consistently predicts an increase in the annual total WDR. A median of 0.0271Kg/m^2 is calculated from the historical RCM data and increasing by 28.5% to 0.0352Kg/m^2. Other datasets experience a similar change to vary degrees, ranging from 14.8% (Morph) to 36.2% (QDM). The changes are a close reflection of the surge in projected total annual rainfall, and the relatively minor decrease in wind speed.

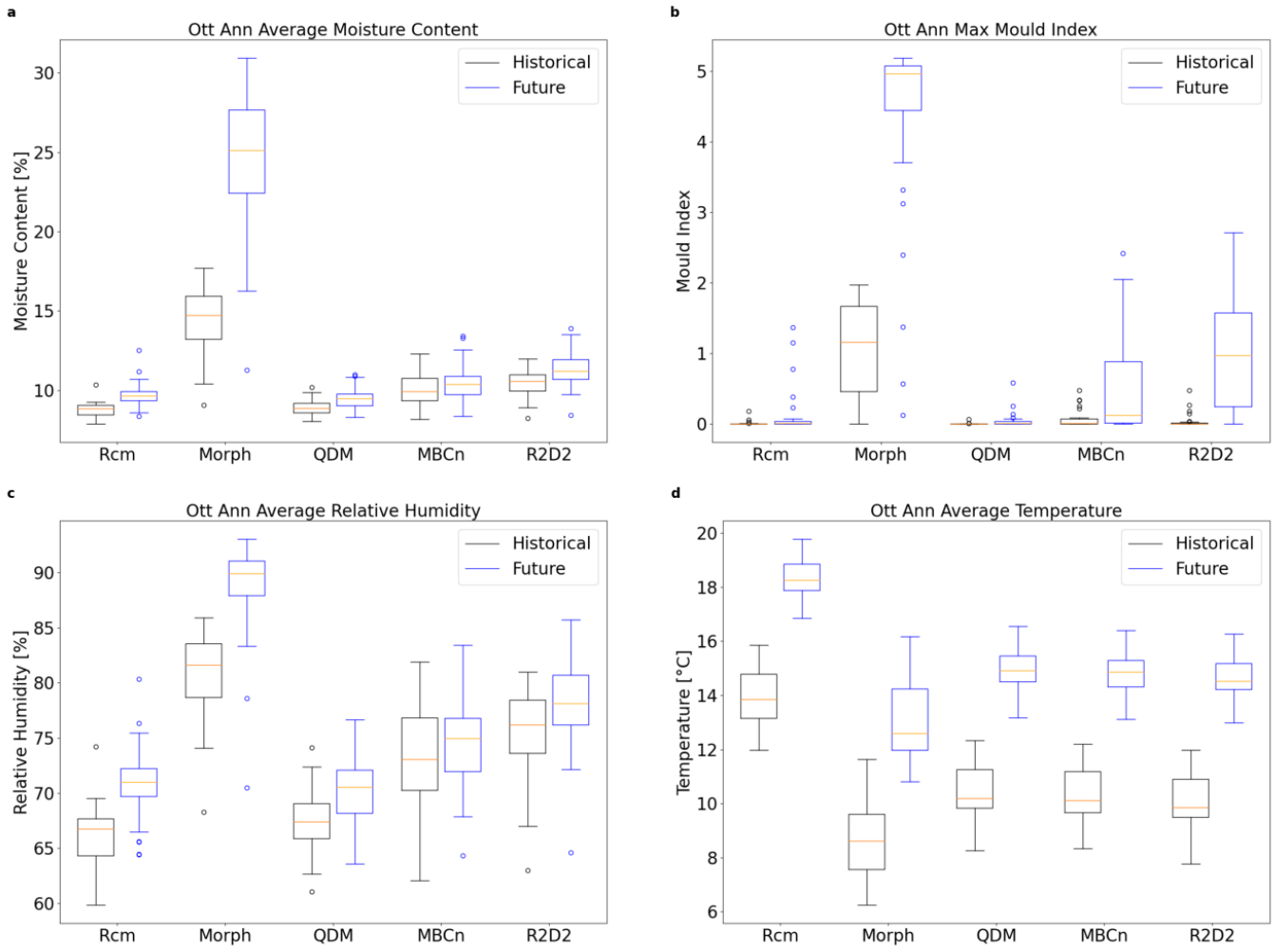

Figure 10. Ottawa annual moisture content (a), relative humidity (c), temperature (d), and maximum mould index (b) of the OSB sheathing of the wall assembly, for a historical (1991-2021) and future (2064-2094) period

A comparison of various aspects of the hygrothermal performance of the wall assembly in Ottawa is presented in Figure 10. The differences in moisture content between the historical and future period, as a percentage of mass of the OSB, is presented in Figure 10a. The simulated hygrothermal response from the RCM, QDM, MBCn, and R2D2 indicate small relative increases in the moisture content between the two time periods. Importantly, the MC from

these datasets do not exceed the critical threshold of 16% in either scenario. Despite higher temperatures due to global warming and thus increased drying potential, the morphing method is estimated to increase, with a historical median of 14.7% and projected median of 25.1%. The increase can largely be attributed to the simultaneous increase in RH and annual total WDR during this period, as these factors would dampen the drying effects of solar irradiance and temperature on the OSB sheathing.

In general, conditions favourable to mould growth will become more common in the future; according to the results comparing the mould index on the OSB in Figure 10b. In the case of the RCM and QDM data, the mould index remains relatively low despite extreme increases in the median. In the most extreme case, the historical R2D2 data estimates a median mould index of 0.002 while the median future projected mould index is 0.92. However, it is important to note that the MI calculated from QDM, MBCn, and R2D2 does not exceed the critical value of 3.0 in either period. The MI is closely tied to the moisture content as the more moisture there is in the OSB, the better the conditions are for mould growth. For this reason, it is no surprised that the Morphing method predicts the most mould growth in either time period. For the same reason, the MI calculated from the other bias correction methods will increase to a lesser extent. These changes indicate that the climate in Ottawa will become wetter for longer durations, which gives the OSB sheathing less time to dry. This in combination with warmer temperatures will result in more favourable mould growth conditions.

In Figure 10c, the simulated relative humidity for the historical and future time period on the exterior side of the OSB sheathing is illustrated in boxplots. The historical median annual average relative humidity according to the RCM is 66.8%, while projected relative humidity is

expected to increase to 70.8%. The QDM data predicts nearly the same values to the RCM in both time periods, while the trend presented in MBCn and R2D2 are comparable to the RCM if starting from a higher baseline. Indeed, that should be expected as the RCM underpredicted the RH on the OSB during the validation period. The Morphing method exhibits the most difference between the datasets and time periods as it predicts a historical median RH of 81.6% and has the largest relative increase of 10.1%.

A similar analysis is performed for the temperature on the exterior of the OSB, the results of which are illustrated in Figure 10d. Generally, the trend in temperature is foreseeable as the climate data already indicated an increase in the median temperature which would be strongly correlated to the temperature on the OSB. The simulation with RCM data shows that the median annual average temperature is expected to increase from 13.9°C to 18.3°C. Similar trends can be found in the QDM, MBCn, and R2D2 datasets, with a baseline historical median temperature of approximately 10°C, and projected increases up to 15°C. During the validation period, the RCM overestimated the temperature on the OSB, while the Morphing method slightly underperforms compared to the other methods. That is also true in this case, where the Morphed dataset corrected the historical median annual temperature to 8.6°C and increases to 12.6°C in the future.

4.2 Montreal

4.2.1 Baseline Validation Period

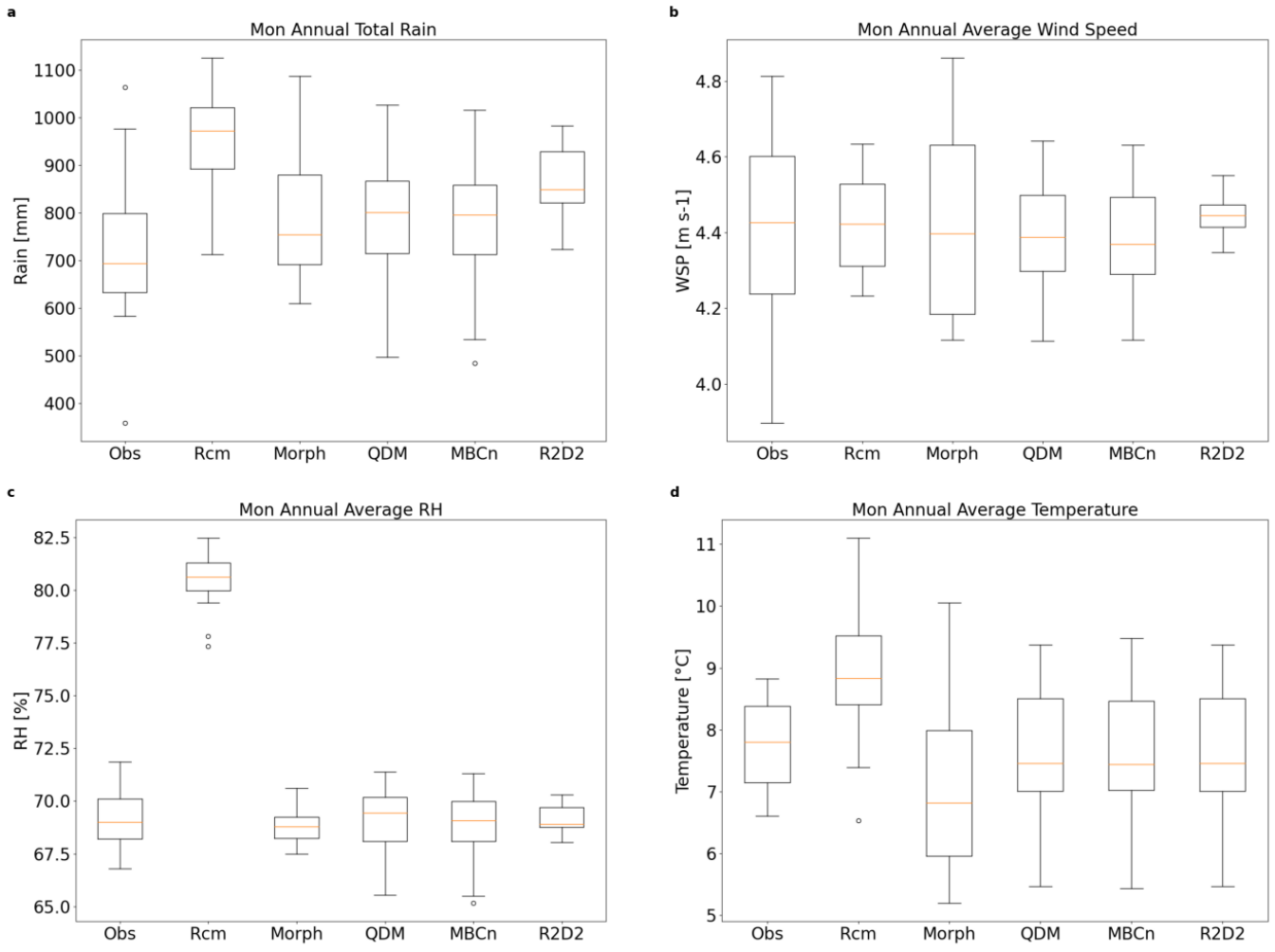

Figure 11. Montreal annual total horizontal rainfall (a), and average wind speed (b), relative humidity (c), and temperature (d) during the observational period (1998-2017)

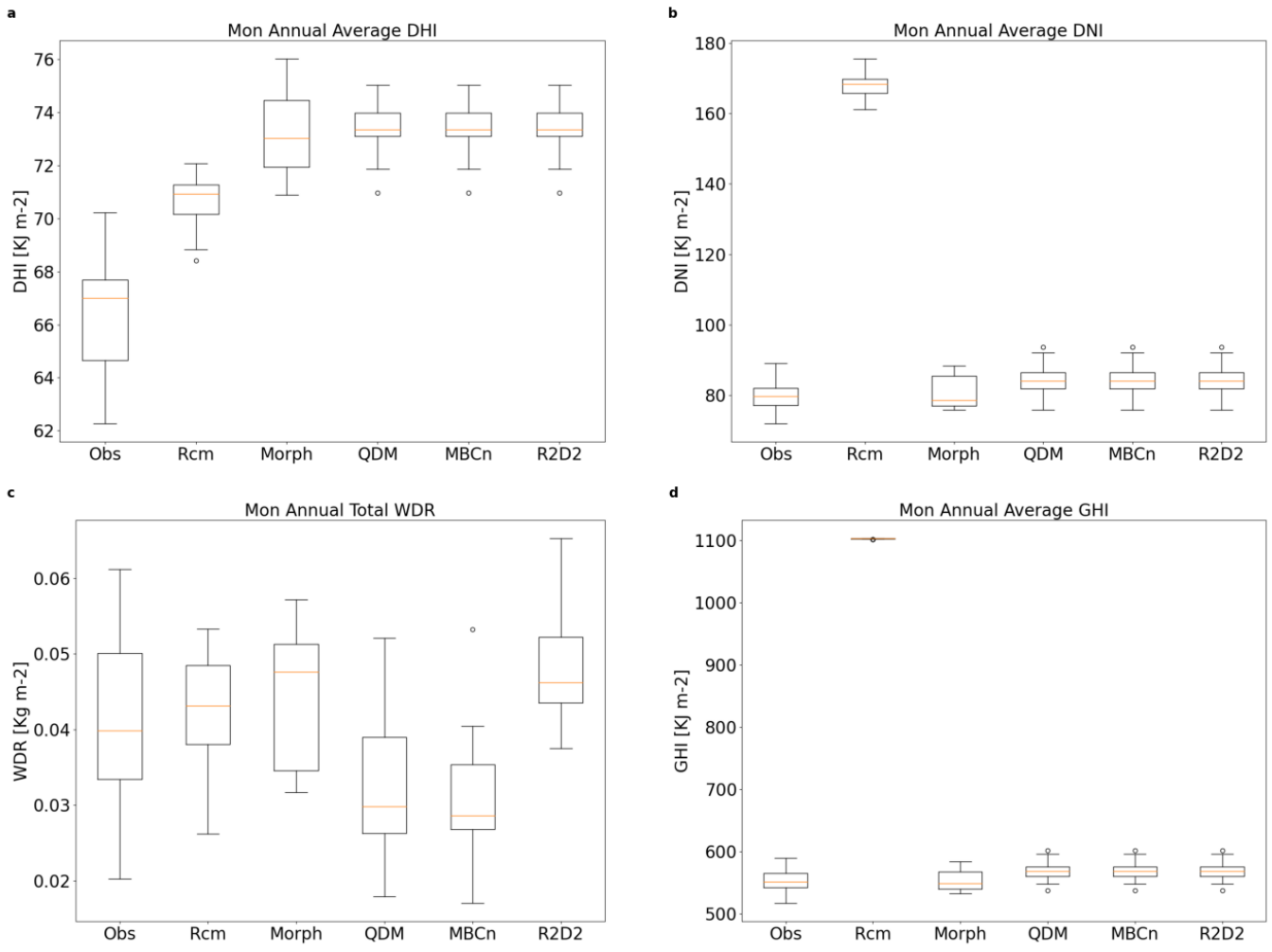

Figure 12. Vancouver annual average DHI (a), DNI (b), total WDR (c) on the wall assembly, and DHI (d) (1998-2017)

The annual total rainfall, average wind speed, relative humidity, and temperature in Montreal during the observational period is analyzed in Figure 11. Similar to the previous results for Ottawa, Figure 11a shows the RCM overpredicting the amount of rainfall (972mm) during this period as compared to the observed median of 694mm. Consequently, the corrected datasets lower the estimated rainfall to around 800mm, improving on the raw climate model data. The average wind speed shown in Figure 11b yields relatively good

agreement in the median wind speed at approximately 4.4m/s across all datasets. However, some datasets report greater variability than others in this 20-year period. Similarly, the average temperature presented in Figure 11d show an observed median of 7.8°C, with a slight overestimation by the RCM at 8.8°C. The QDM, MBCn, and R2D2 datasets yield nearly identical medians at approximately 7.5°C, and the Morphing at an even lower 6.8°C. The resulting relative humidity poses a divergent case between datasets, where the RCM significantly overpredicts the RH, with a median of 80% compared to the others which vary only slightly around 69%.

Figure 12d shows significant improvement in estimated GHI in the corrected data, where raw RCM data overestimates the average GHI with a median value of over 1100Kj/m^2 compared to the observed 553Kj/m^2. Figure 12a and b shows the result of splitting GHI into DHI and DNI in Montreal during the observational time period. In both cases, the QDM, MBCn, and R2D2 datasets are identical since the values from QDM were used. The DHI is overestimated by morphed and QDM datasets when compared to the observations, which has a median of 67Kj/m^2, while the RCM has a median of 71Kj/m^2, and 74Kj/m^2 for Morph and QDM. Alternatively, the DNI is overestimated by the RCM with a median of 168Kj/m^2, while all the other datasets have a median closer to 80Kj/m^2. Finally, the total WDR during this period is presented in Figure 12c, where quite a bit of variation can be seen between the datasets. The RCM, Morph, and R2D2 datasets expect large amounts of WDR deposited on the exterior of the OSB sheathing at medians of 0.0432Kg/m^2, 0.0476Kg/m^2, and 0.0462Kg/m^2, respectively. Compared to that of the observations which indicate 0.0398Kg/m^2. While the QDM and MBCn data predicts significantly lower amounts with median annual averages of 0.0298Kg/m^2 and

0.0286Kg/m^2. Despite the relatively similar climatic conditions, the fluctuations in the WDR can be attributed to the shuffling of the time series that MBCn and R2D2 perform during the bias correction process, which creates a different alignment of rainfall, windspeed, and wind direction, and therefore changes the resultant total WDR deposited on the exterior of the OSB sheathing.

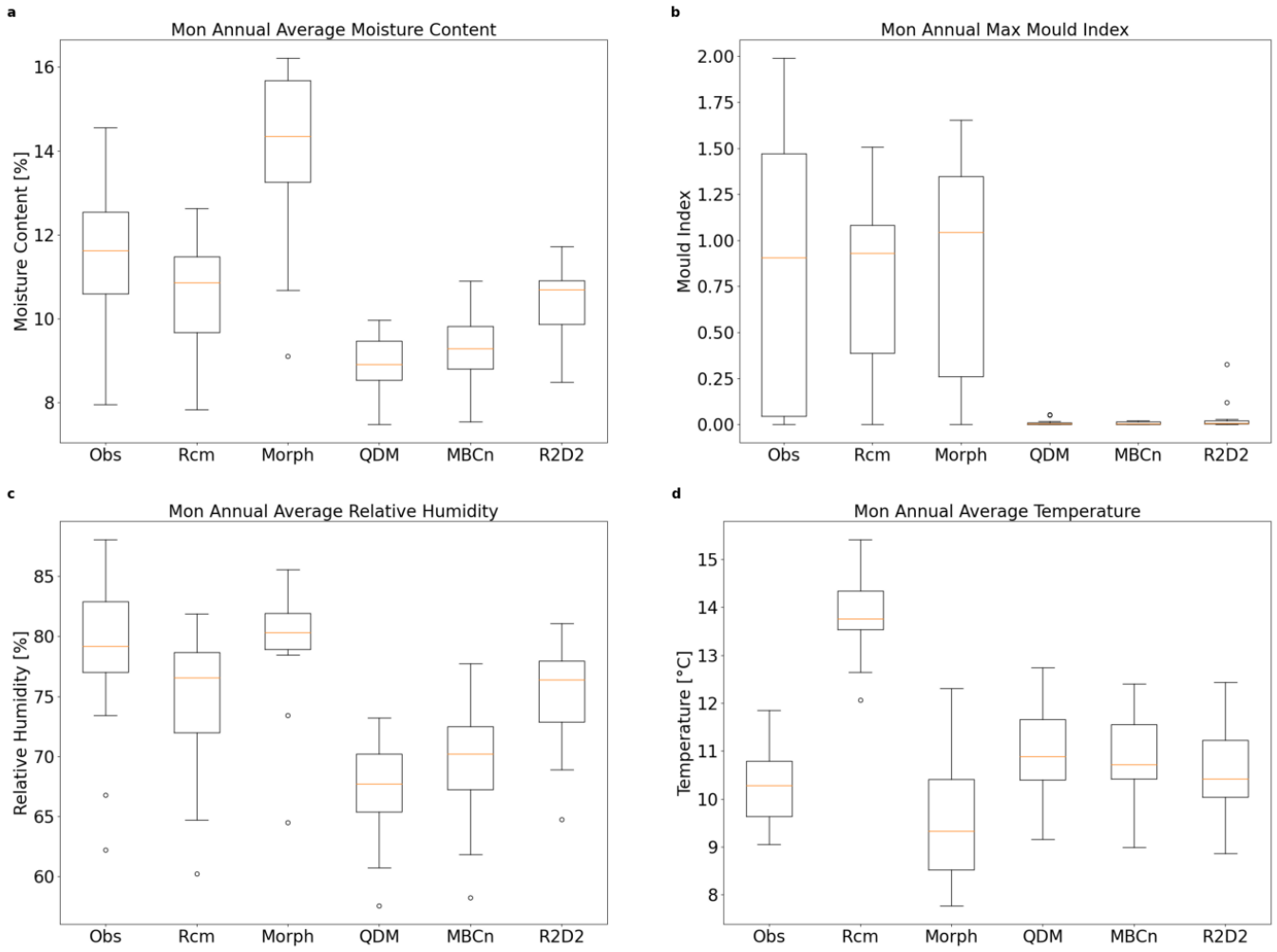

Figure 13. Montreal annual average: moisture content (a), relative humidity (b), temperature (c), and maximum mould index (d) on the exterior of the OSB sheathing (1998-2017)

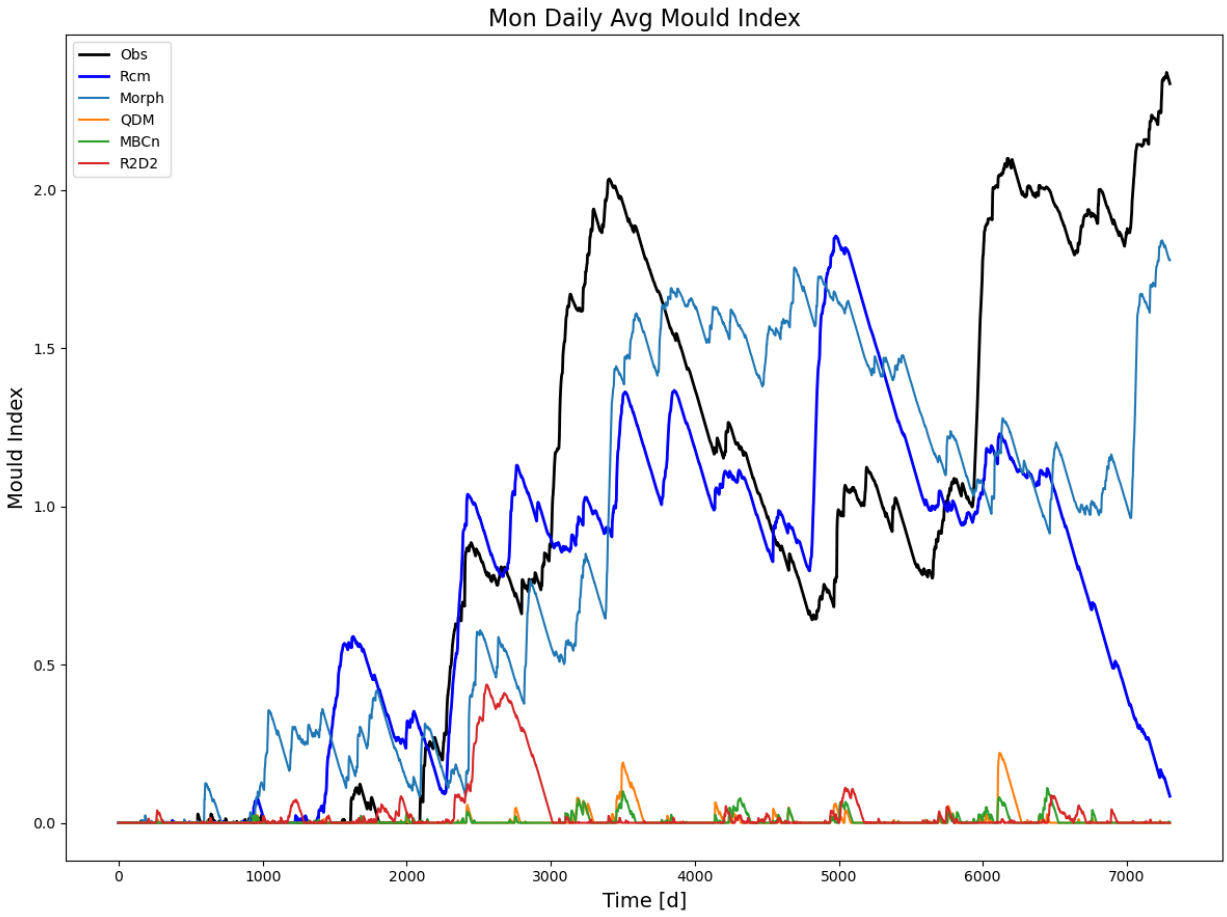

Figure 14. Montreal daily average mould index on the exterior of OSB sheathing (1998-2017)

The results of the hygrothermal simulations using climate data presented in Figure 11 and Figure 12 are illustrated in Figure 13, where the average MC, MI, RH, and temperature are shown. The moisture content as a percent mass of the OSB is analyzed in Figure 13a. The simulations using morphed data results in the highest average moisture content in the OSB, with a median MC of 14.1% compared to the observed 11.7%. This is expected since the MC is directly influenced by the amount of deposited WDR, and morphed data forecasts comparatively higher WDR than the other datasets. Similarly, the QDM and MBCn methods

predict relatively lower WDR, and thus also have relatively lower MC at around 9%. The total WDR calculated from RCM and R2D2 compared similarly, consequently they also have a similar median MC of 10%. The median RH on the OSB simulated using observational data is 79.6% shown in Figure 13c. Despite the relatively similar values for the climatic RH in Figure 12c, the simulated RH on the OSB results in large variations between datasets. For instance, the relative humidity obtained through morphed data yield a higher median at 81.3%. On the other hand, the QDM, MBCn, and R2D2 datasets also underestimate the RH on the OSB. Additionally, the RCM predicts a surprisingly lower RH with a median of 76.4%. On the other hand, RCM data overestimates the temperature on the OSB, calculating an annual average median temperature near 14°C in Figure 13d. However, after correction, the data yields more accurate results, with medians of around 11°C, compared to the observed value of 10°C.

An analysis of the MI on the OSB in Montreal is presented in Figure 13b and Figure 14, showing the annual maximum MI and the daily average value, respectively. There is much variation in the MI between different datasets. The observed and morphed data exhibit a similar trajectory which indicates significant mould growth beginning around 6 years into the simulation and peaks at the end of the simulation at a value of 2.4 and 1.9, respectively. In both these cases, there are periods of decline, but it eventually increases again. However, mould growth begins earlier according to the RCM, starting around 3 years into the simulation, with a peak value of 1.8, and decaying towards the end of the simulation. Contrastingly, simulated mould growth using the bias corrected data resulted in little to no mould growth for large parts of the simulation, with a few minor exceptions, but these subsequently decrease afterwards for the duration of the study period. Despite the similarities seen in the climate in Figure 11 and

Figure 12, the mould growth simulated by observed, RCM, and morphed data can be largely attributed to the significantly wetter conditions in terms of higher RH and moisture loading, resulting in longer periods where favourable mould growth conditions occur, compared to the bias corrected datasets such as QDM, MBCn, or R2D2. Morphed data appears to be the most accurate when calculating the mould index because the temporal variability of the climatic parameters is identical to that found in the observation data since the correction factors are applied to the observed data.

The results of the climate data processing techniques showed that some improvement was made to the raw RCM data in terms of their means, although the degree to which depends on the method and variable. For example, significant improvements were made to the annual total rainfall, RH, and DNI, whereas wind speed and WDR was already in reasonably good agreement with the observations. However, in the context of hygrothermal simulations, bias corrected data had varied results. For instance, there was not much agreement even among the simpler parameters such as RH and temperature on the OSB. For a more complex parameter such as the mould index, only morphed climate data was able to replicate the temporal variability of the observed data, resulting in the most accurate simulation, outperforming the RCM, which eventually diverges from the observations. Due to the nature of the morphing process, it's no surprise that morphed data performs the best in this context, which more accurately simulates the persistence of moisture conditions on the OSB.

4.2.2 Projected Future Period

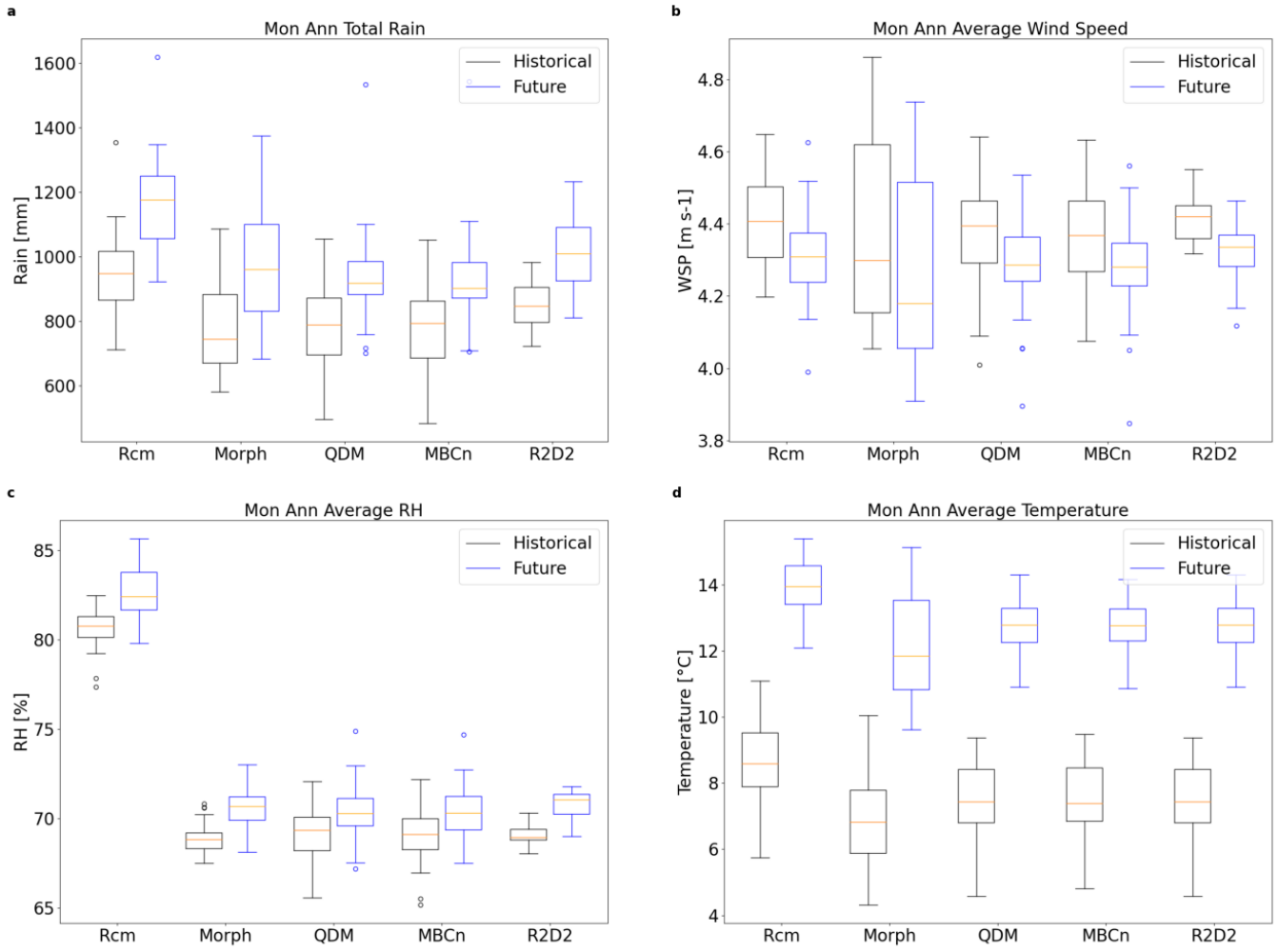

Figure 15. Montreal boxplots of annual total rain (a), and average wind speed (b), relative humidity (c), and temperature (d), over a baseline historical period from 1991-2021 and a future projected period from 2064-2094

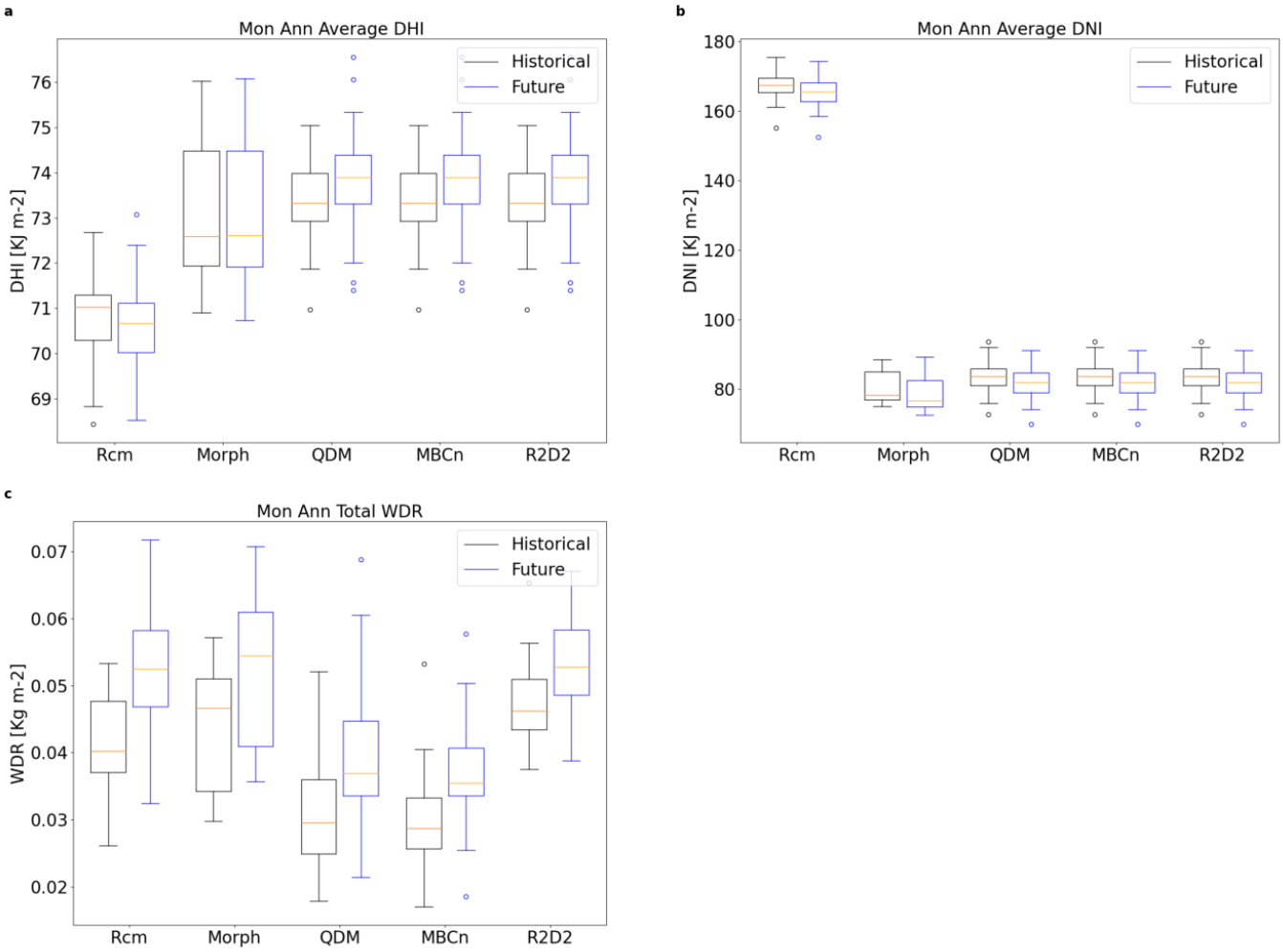

Figure 16. Montreal boxplots of annual average DHI (a), DNI (b), and WDR (c) over a historical (1991-2021) and future (2064-2094) period

Figure 15a shows the annual total rainfall during the historical period against the future projected period under 3.5°C of global warming. Across the 30-year period, the RCM predicts a median annual average of 949mm, increasing by 24% to 1177mm in the second half of the century. Since the RCM tends to overestimate total rainfall, the corrected datasets predict lower average total rainfall. The Morphed data yields the highest percent increase in the median at 29%, from 745mm to 960mm. QDM and MBCn both have a historical median of

approximately 790mm which subsequently increase by 16% and 14% respectively to 921mm and 902mm. Lastly, R2D2 predicts the highest median by far compared to the other correction methods with a historical median of 847mm and future projected median 1010mm. The average wind speed illustrated in Figure 15b implies that the RCM simulates the windspeed fairly accurately since there is not much variation between the corrected datasets and the RCM. Consequently, a minute 2.5% decrease in windspeed calculated by the RCM is followed by the corrected datasets as well, with a historical median of approximately 4.4m/s across the board. The Morphed data has a slightly lower historical median at 4.3m/s. According to the validation section, the RH and temperature are overestimated by the RCM. Therefore, the corrections will tend to lower the average values, which can be seen in the case of Figure 15c and 12d. Indeed, the RCM has a historical median RH of 81.1% while every other dataset has a median of 69.3%, but in each case, small increases in the future RH is expected at 2%. On the other hand, large increases in temperature should be expected in Montreal due to climate change, where the RCM predicts an increase from 8.6°C to 14°C. Similarly, corrected datasets forecast a similar magnitude increase, where QDM, MBCn, and R2D2 start from a median of 7.4°C to approximately 10.9°C. The Morphed temperature starts at a lower historical median at 6.8°C and increasing to 11.9°C.

The historical and future DHI are compared in Figure 16a. The RCM is the only data the predicts a decrease in DHI over these two time periods from 71Kj/m^2 to 70Kj/m^2. Little to no change is calculated through the Morphed data with a median annual average DHI of 73Kj/m^2. Naturally, due to how the solar radiation variables are processed, the shown results of MBCn and R2D2 are identical to those from QDM, which only yield a small increase from 73Kj/m^2 to

74Kj/m^2. Similar changes are found in the DNI as well, with only minor differences between the two time periods. As was seen during the validation period, the RCM largely overestimates the DNI in Montreal with a median of approximately 165Kj/m^2 during both periods. The Morph and QDM data decrease from 78Kj/m^2 to 76Kj/m^2 and 84Kj/m^2 to 82Kj/m^2, respectively. Lastly, the average annual total WDR is presented in Figure 16c. The relative performance between the datasets closely resembles those found in the validation period. The RCM projects the largest increase in annual WDR from 0.0402Kg/m^2 to 0.524Kg/m^2. However, the Morphed data yields the highest absolute values, with a historical median of 0.0466Kg/m^2, increasing to 0.0544Kg/m^2. While the lowest predict values came from MBCn, rising from 0.0287Kg/m^2 to 0.0354Kg/m^2.

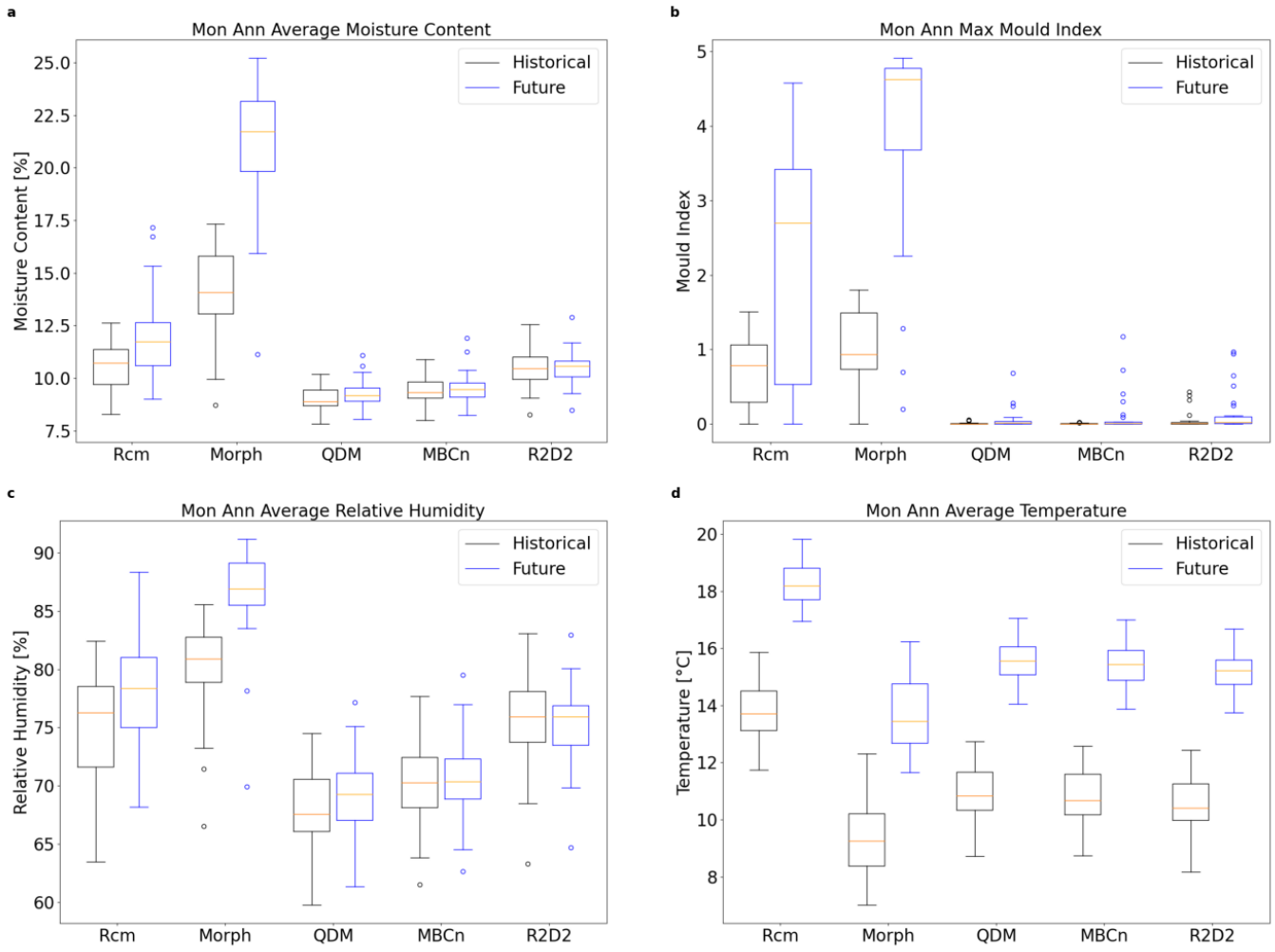

Figure 17. Montreal annual MC (a), RH (c), temperature (d), and maximum MI (b) of the OSB sheathing of the wall assembly, for a historical (1991-2021) and future (2064-2094) period

A similar comparison between the two periods on the hygrothermal performance of the wall assembly in Montreal is presented in Figure 17. There is a large variation between datasets when simulating the MC of the OSB sheathing. The RCM, QDM, MBCn, and R2D2 data are all relatively low compared to Morph, where it estimates the highest MC among them at 10.7% and 11.7% for the historical and future periods, respectively. Hygrothermal simulations with the

Morphed data predicts an even greater historical median MC at 14.1% and increasing to 21.7%. Consequently, it's not surprising that the simulated mould index is largest using Morphed and RCM data. In all cases, the mould index does not exceed the critical threshold of 3.0 during the historical period. However, due to climate change, there will be increased mould growth across all datasets, but increases in QDM, MBCn, and R2D2 are not critical. On the other hand, both RCM and Morph project significant increases in mould growth with a median mould index value of 2.7 and 4.6, respectively. The increases in MC and MI can be attributed to the relatively large increases in the WDR deposited on the exterior OSB sheathing, which result in more moisture absorption. Future projected changes of the RH on the exterior side of the OSB are expected to increase. The RCM indicates an increase in the median RH from 76.3% to 78.4%, while Morphed data predicts a larger relative increase from 80.9% to 86.9%, and smaller changes are measured by the bias corrected datasets. The average outdoor temperature in Montreal is expected to increase by approximately 6°C, consequently, a similar development is seen after simulating the temperature on the exterior of the OSB. The highest historical median produced by RCM yields a value of 13.7°C, which increases by 4.5°C in the future. Other datasets start with a much lower average temperature, where Morph is at 9.3°C, and the bias corrected data average around 10.6°C; subsequently increasing to 13.5°C and 15.3°C.

4.3 St. John's

4.3.1 Baseline Validation Period

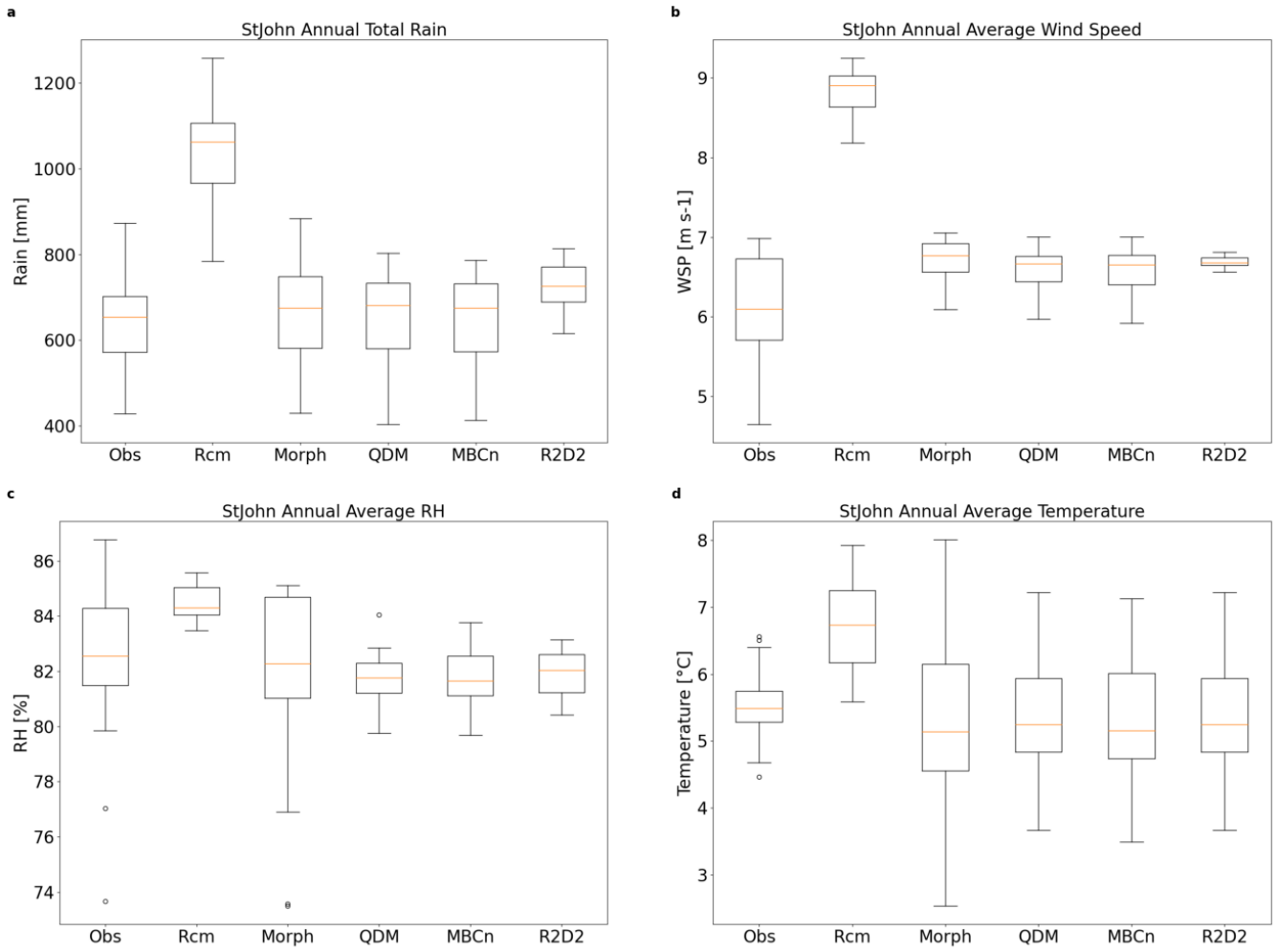

Figure 18. St. John's annual total horizontal rainfall (a), and average wind speed (b), relative humidity (c), and temperature (d) during the observational period (1998-2017)

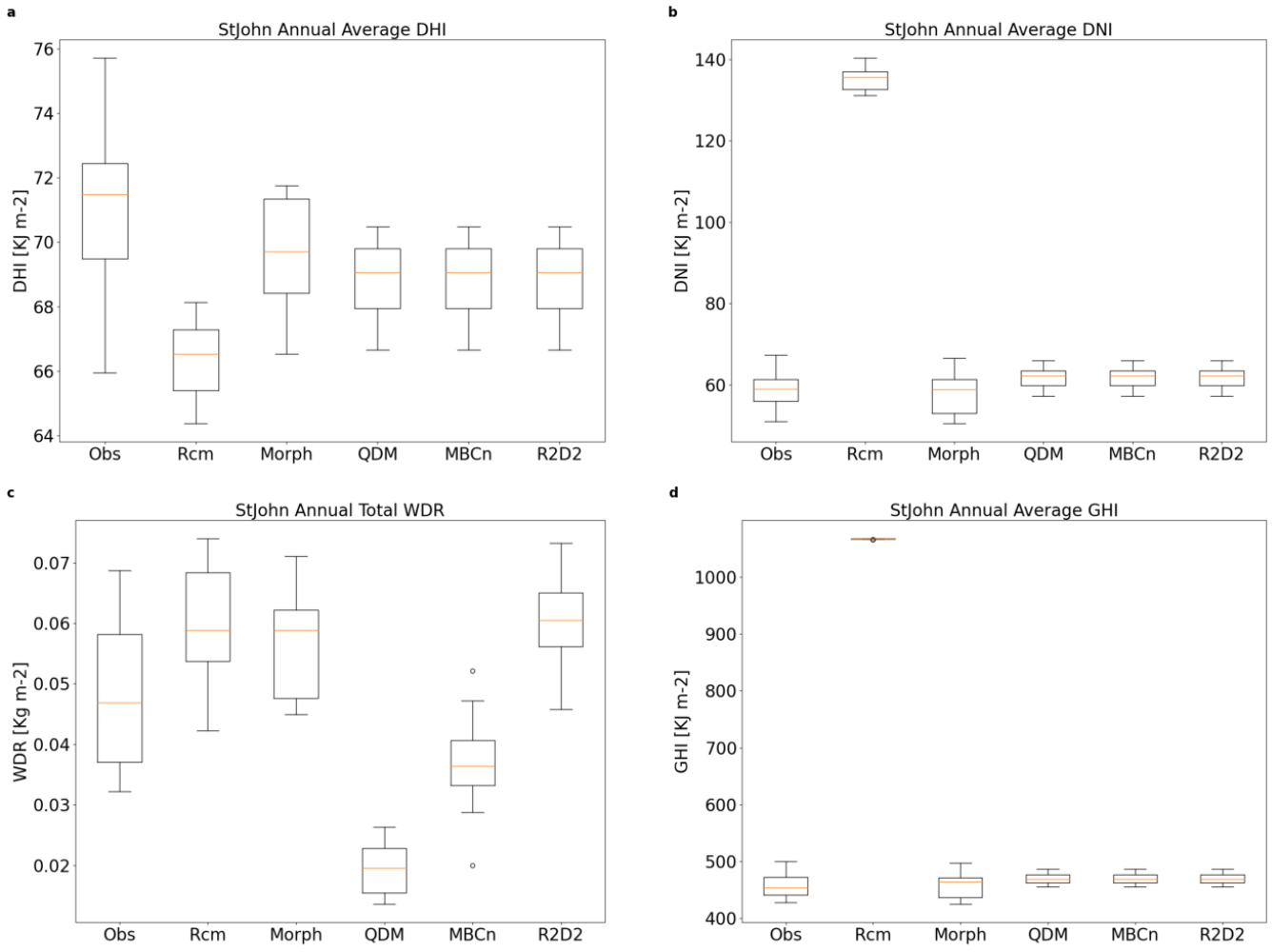

Figure 19. St. John's annual average DHI (a), DNI (b), total WDR (c) on the wall assembly, and DHI (d) (1998-2017)

The conditions in St. John's are comparatively wetter, according to the RCM, considering the studied locations so far. For instance, Figure 18a shows the total annual horizontal rainfall during the entire 20-year observational period from 1998-2017. Within these 20-years, the RCM total annual rainfall calculated a median of 1063mm, which is significantly greater than the observed 654.6mm. Subsequently, morphed and bias corrected data significantly improves on the estimation of annual total rainfall with medians of 675mm, 681mm, 675mm, and

727mm. Additionally, the wind speed is also overestimated by raw RCM data with a median of 8.9m/s. Corrected data lowers the estimated wind speed to approximately 6.7m/s, compared to the actual observed 6.1m/s. The RH is also overestimated by the RCM, however to a lesser extent than the previous parameters. As a result, the RCM predicts a median value of 84.3% against the observed 82.6%. Meanwhile, corrected data yields a median around 82%, with morphed data displaying somewhat larger variability from year to year. Observed temperatures at St. John's resulted in a median of 5.5°C while corrected data yield very similar medians at 5.2°C, which reduces the overestimation by the RCM from a median of 6.7°C.

Like previous locations, the RCM predicts significantly higher GHI than any other dataset shown in Figure 19d, with a median of 1067Kj/m^2, compared to the observed 455Kj/m^2. Morphed and QDM corrected results in medians around 456Kj/m^2. A solar split is performed on the GHI resulting in components such as the DHI and DNI. The average DHI calculate through observed data, shown in Figure 19a, resulted in the highest median at 72Kj/m^2, while RCM data calculated the lowest of all the datasets at a median of 67Kj/m^2. On the other hand, morphed and QDM data both calculated a median of approximately 69Kj/m^2. Like other locations, the RCM simulated DNI at St. John's is extremely overestimated at a median of 136Kj/m^2, while observed, morphed, and QDM corrected data yields a median closer to 60Kj/m^2. Lastly, the sum of annual WDR presented in Figure 19c displays a large variability among the many datasets. The most obvious outlier in this case is presented by QDM, with the lowest median of 0.0195Kg/m^2 of WDR per year. Meanwhile the other bias corrected datasets expected more WDR at 0.0364 Kg/m^2 and 0.0605 Kg/m^2 for MBCn and R2D2, respectively. Morphed and RCM

climate data calculated median annual WDR at 0.0588Kg/m^2, compared to the observed 0.0468Kg/m^2.

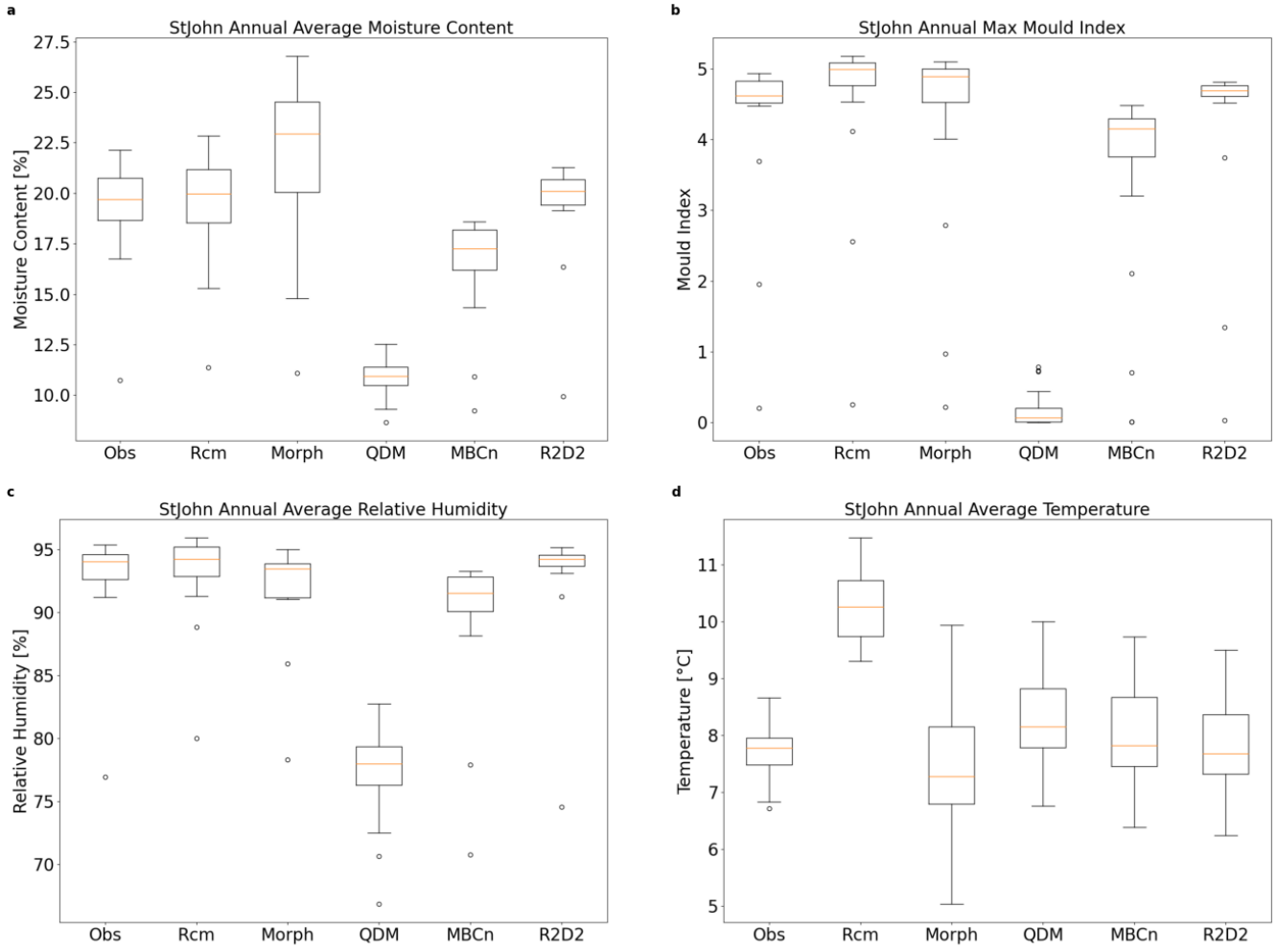

Figure 20. St. John's annual average: moisture content (a), relative humidity (b), temperature (c), and maximum mould index (d) on the exterior of the OSB sheathing (1998-2017)

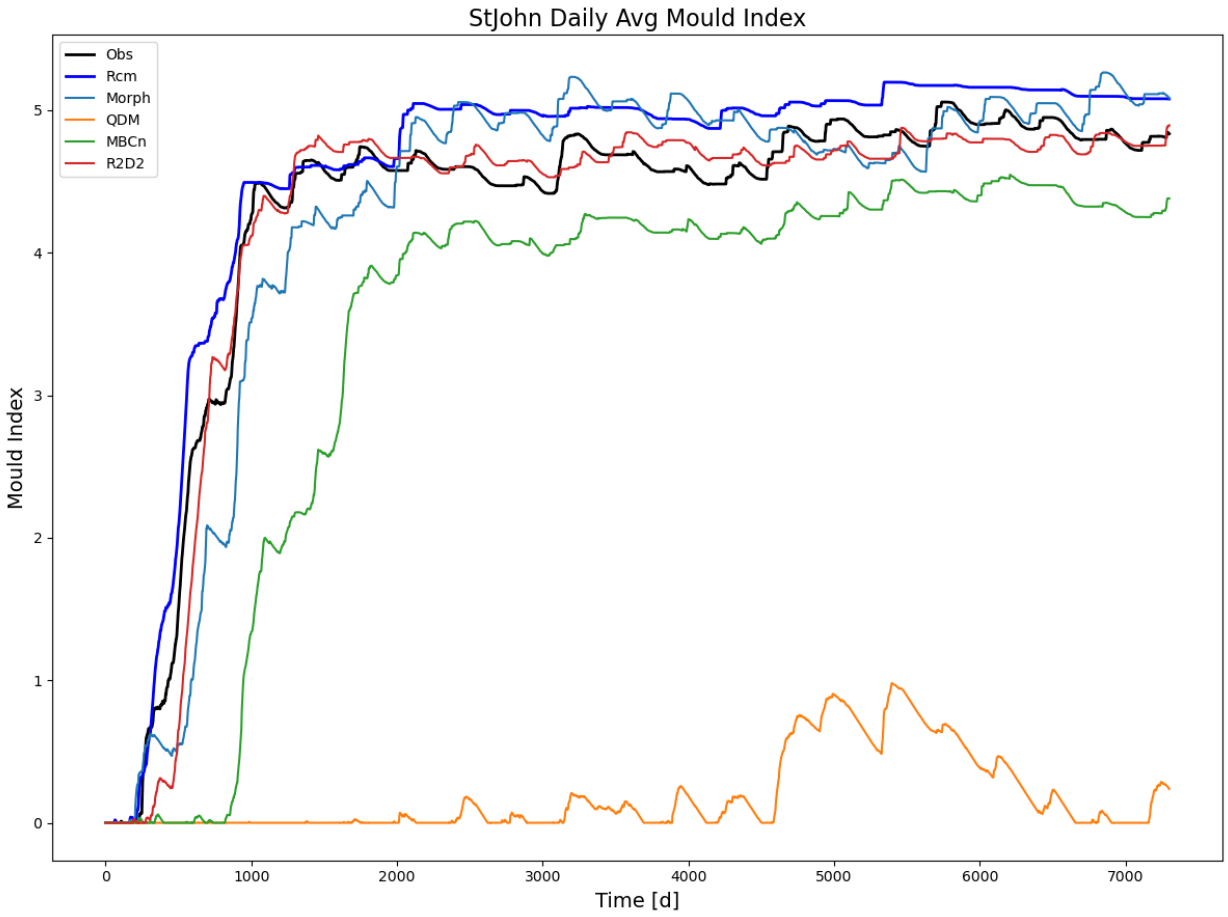

Figure 21. St. John's daily average mould index on the exterior of OSB sheathing (1998-2017)

Through hygrothermal simulations using DELPHIN, the MC of the OSB sheathing was simulated and the results of which are illustrated in Figure 20a for the observational period from 1998-2017. These results closely resemble the relative performance of the various datasets in Figure 19c, which showed the annual total WDR. Consequently, the hygrothermal simulations using QDM corrected climate data resulted in the lowest MC by far, with a median of 10.9%. Which is distantly followed by MBCn and R2D2 at medians of 17.2% and 19.9%. Similarly, observed and RCM simulations indicated a median MC of 19.5%, while morphed data

resulted in an even greater 23.1% median. Therefore, during the observational time period, since the MC generally exceeds the critical threshold of 16%, it is likely that the OSB sheathing will experience decay during this study period due to excessive moisture in the OSB. Calculations of the mould index presented in Figure 20b shows a similar relative performance between the datasets, with the least mould growth predicted by QDM at a median annual maximum mould index of only 0.03. Which is again distantly followed by MBCn and R2D2 with medians of 4.1 and 4.7. Simulations with observed weather data resulted in a median of 4.6 across the whole study period while morphed data produced more mould growth with a median index of 4.9. The RCM simulation resulted in the most mould growth overall, at a median of 5. According to Figure 21, significant mould growth begins approximately 3 years into the simulation, with each set of simulations reaching their peak and a relative steady state afterwards, excepting the QDM simulations. Overall, due to consistently high humidity and wet conditions in St. John's, significant mould growth will occur on the exterior of the OSB during this period. The relative humidity on the exterior of the OSB sheathing is generally quite high compared to that at other cities. Most of the datasets excepting QDM yielded median values above 90.6%, while 78.3% was simulated using QDM corrected data. Temperature on the OSB is also presented in Figure 20d, where observational data indicted a median of 7.3°C, contrasting with the comparatively higher estimation of 9.6°C made my RCM data. Meanwhile, bias corrected data resulted in slightly higher estimates at 8.1°C, 7.7°C, and 7.5°C for QDM, MBCn, and R2D2, respectively. Lastly, morphed data simulated the lowest median temperature on the OSB at 6.7°C.

The results of the processed climate data indicate that a significant improvement is made alleviating some of the bias present in the raw RCM data. Nearly all the climate parameters presented are improved upon, except for the annual total WDR, which resulted in some variability between the datasets. Despite the relative accuracy in climate variables, the hygrothermal performance of the various datasets produce some variability. In this case, the QDM data produces the most obvious outlier, in many of the parameters that were studied, including the RH, MC, and MI. In St. John's, the RCM simulates the variability of the climate parameters relatively accurately compared to some of the other studied locations, which results in a mould profile similar to that calculated using observation data. Overall, the climate in St. John's is shown to be quite wet, which may result in potential wood decay and mould growth problems.

4.3.2 Projected Future Period

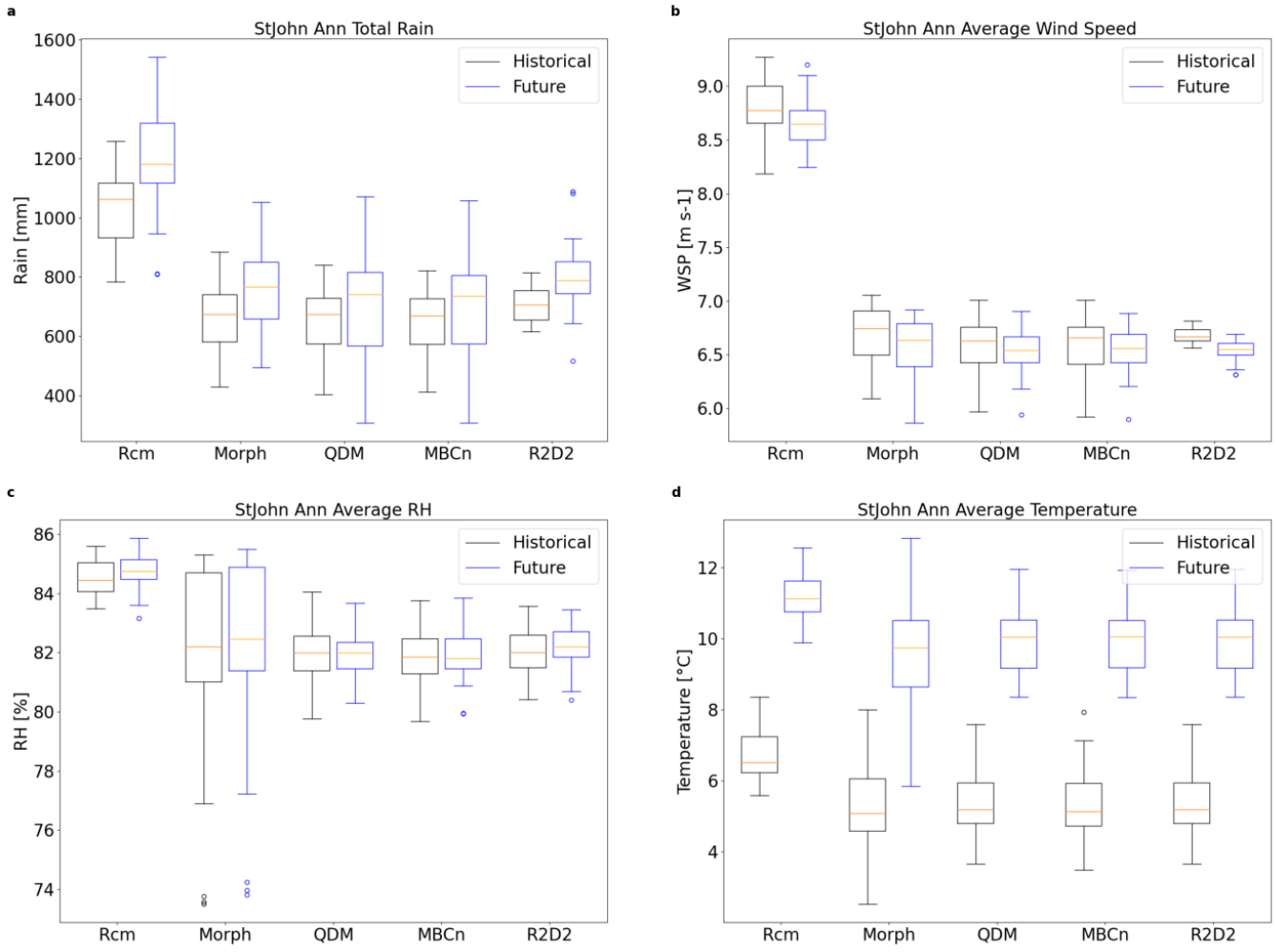

Figure 22. St. John's boxplots of annual total rain (a), and average wind speed (b), relative humidity (c), and temperature (d), over a baseline historical period from 1991-2021 and a future projected period from 2064-2094

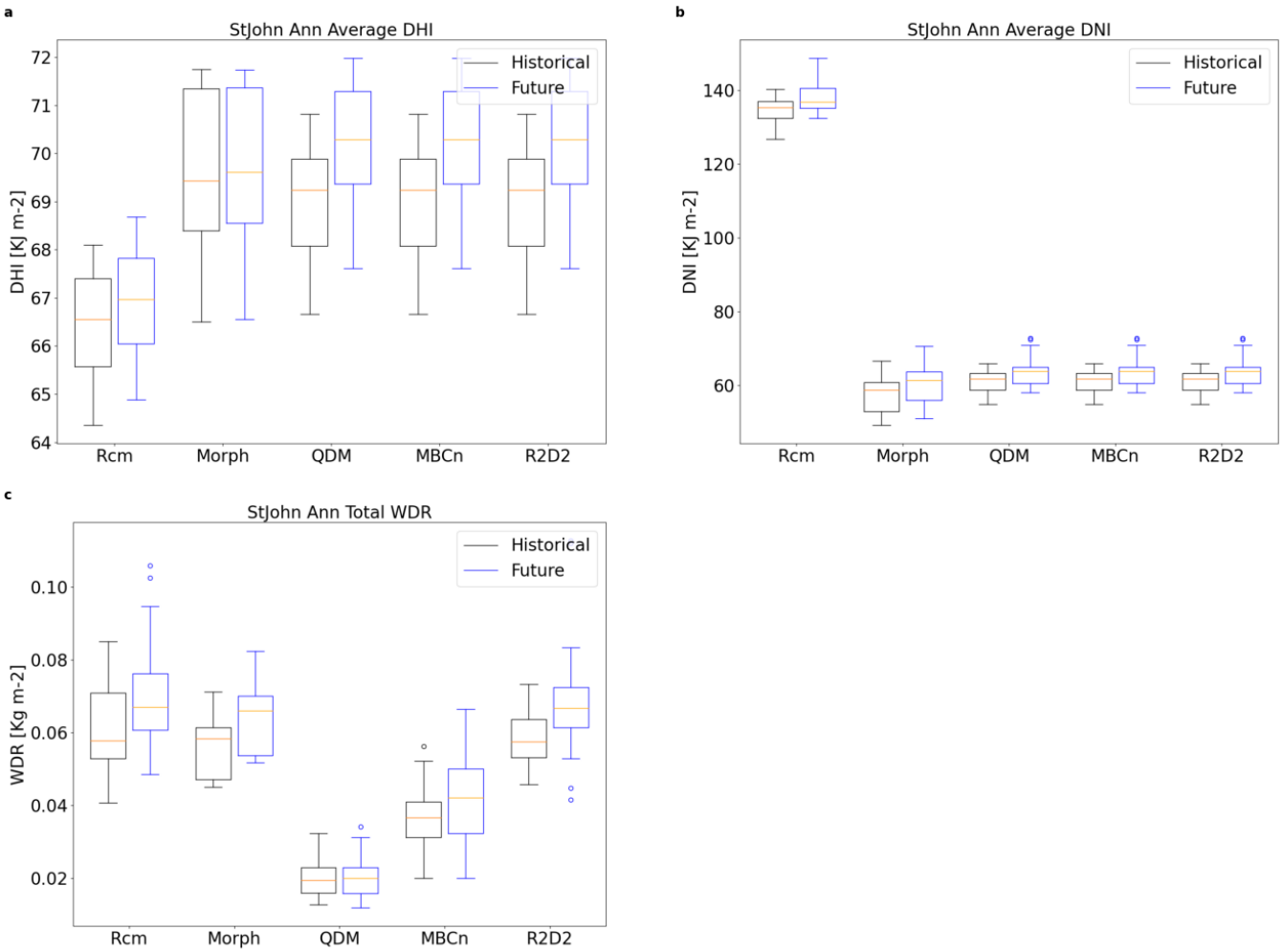

Figure 23. St. John's boxplots of annual average DHI (a), DNI (b), and WDR (c) over a historical (1991-2021) and future (2064-2094) period

Based on the validation period, the RCM overestimates the amount of horizontal rainfall. In this case, during the historical period a median annual total of 1062mm was expected, which is projected to increase to 1181mm in 2064-2094. Whereas morphed and bias corrected results bring the median to a lower 700mm for the historical period and 751mm for the future. A similar trend is seen in the RH and temperature shown in Figure 22c and Figure 22d, where each parameter is forecast to increase due to climate change, and the fact that bias

correction reduces the overall mean value. The RH does not change much regardless of which dataset was used, with only a 1% difference between the two periods. On the other hand, temperature changes drastically in comparison, where the RCM gains from a historical median of 6.5°C to 11.1°C. Corrected datasets reduce the absolute temperature in each case, with a similar historical median at 5.1°C and increasing to 10°C in the future. Projected changes in wind speed are minimal, going from 8.8m/s to 8.6m/s, according to the RCM. As with during the validation period, wind speed is overestimated by the RCM. Therefore, morphed and bias corrected data yield lower wind speeds around 6.7m/s historically and lowering to 6.6m/s in the future.

Similar results are presented for the DHI, DNI, and WDR in Figure 23. As in the observational period, the solar irradiance variables generated by QDM are used in place of values calculated using the MBCn or R2D2 method as they do not preserve the diurnal cycle. According to the RCM, the median DHI does not change by much between the two periods, with a value of 67Kj/m^2 historically, and 66.9Kj/m^2 in the future. Due to the extremely small change present in the RCM, the DHI calculated by Morphing remains virtually the same at 70Kj/m^2. The same can be said about QDM corrected data going from 69Kj/m^2 to 70Kj/m^2. Considering that the RCM exaggerates the average DNI at 135Kj/m^2, the results are relatively consistent between morphing and QDM data which bring down the median value. With a historical median of 59Kj/m^2 and 62Kj/m^2, and 61Kj/m2 and 64Kj/m^2 during the projected period, respectively. The annual total WDR predicted by raw RCM, morph, and R2D2 data near identical with medians around 0.057Kg/m^2 and 0.066Kg/m^2 for the historical and future period, respectively. On the other hand, despite relatively similar performance that QDM and MBCn

data showed among the other climatic parameters, they both forecast less WDR in both time periods.

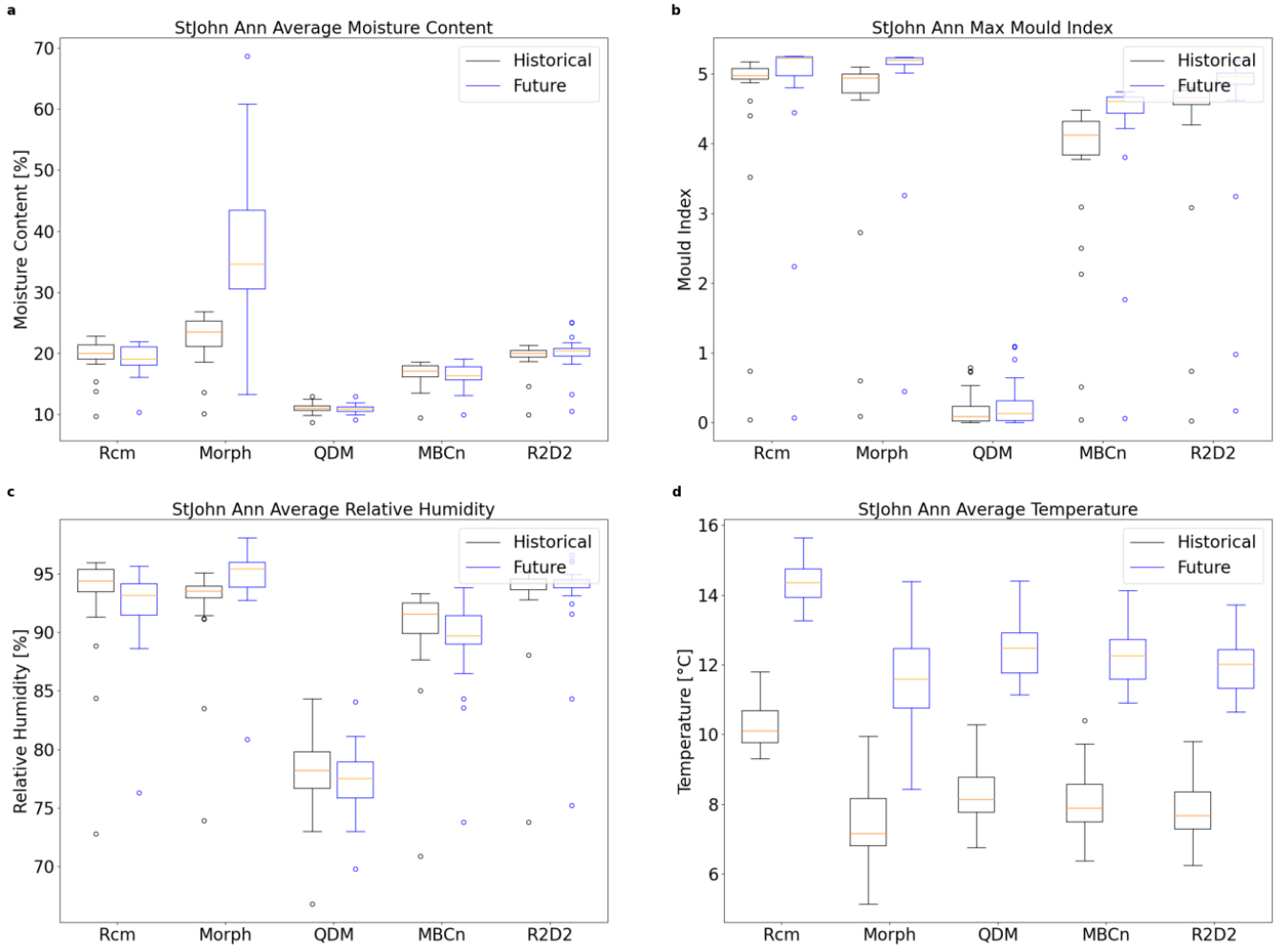

Figure 24. St. John's annual MC (a), RH (c), temperature (d), and maximum MI (b) of the OSB sheathing of the wall assembly, for a historical (1991-2021) and future (2064-2094) period

A comparison of the hygrothermal performance of the wall assembly in St. John's is presented in Figure 24, which includes the MC, MI, RH, and temperature. The simulated hygrothermal response presents a lot of variation between the datasets. While the RCM

simulated a historical MC of 20.1%, it projects a decrease into the future to 19%. On the other hand, morphed data results in quite the extreme which projects increase in median MC from 23.3% to 34.9%. Other datasets such as MBCn and R2D2 also calculated historical and future MC of the OSB exceeding the critical threshold, meaning the OSB will experience decay in both periods. Despite increases seen in the amount of WDR, some of the datasets simulated a decrease in future MC, likely due to the increase in ambient drying conditions. Mould growth was already an issue, with extremely high mould index values, close to 5 in most cases, during the historical period. However, due to climate change, mould growth will worsen as conditions favourable to mould growth become of prevalent in the future, subsequently resulting in increased mould index values. While QDM also simulated increase mould growth, the magnitude is not the same as the other datasets. As was seen during the validation period, QDM does present the same climatic conditions as the other datasets in St. John's. Consequently, QDM predict RH on the exterior of the OSB is relatively lower than those predict by other data, with a historical median of 78.6%, which is expected to decrease to 77.3%. Similar changes are forecast by other datasets, however starting from a much higher historical RH with a median historical value of approximately 93%. The simulated temperature on the OSB is expected to increase. According to the RCM, from 10.1°C to 14.4°C, whereas other datasets start from a lower historical median. Historically, morph simulations resulted in a median of 7.17°C rising to 11.6°C. Bias corrected data perform similarly, with a historical median of 8°C rising to approximately 14°C.

4.4 Calgary

4.4.1 Baseline Validation Period

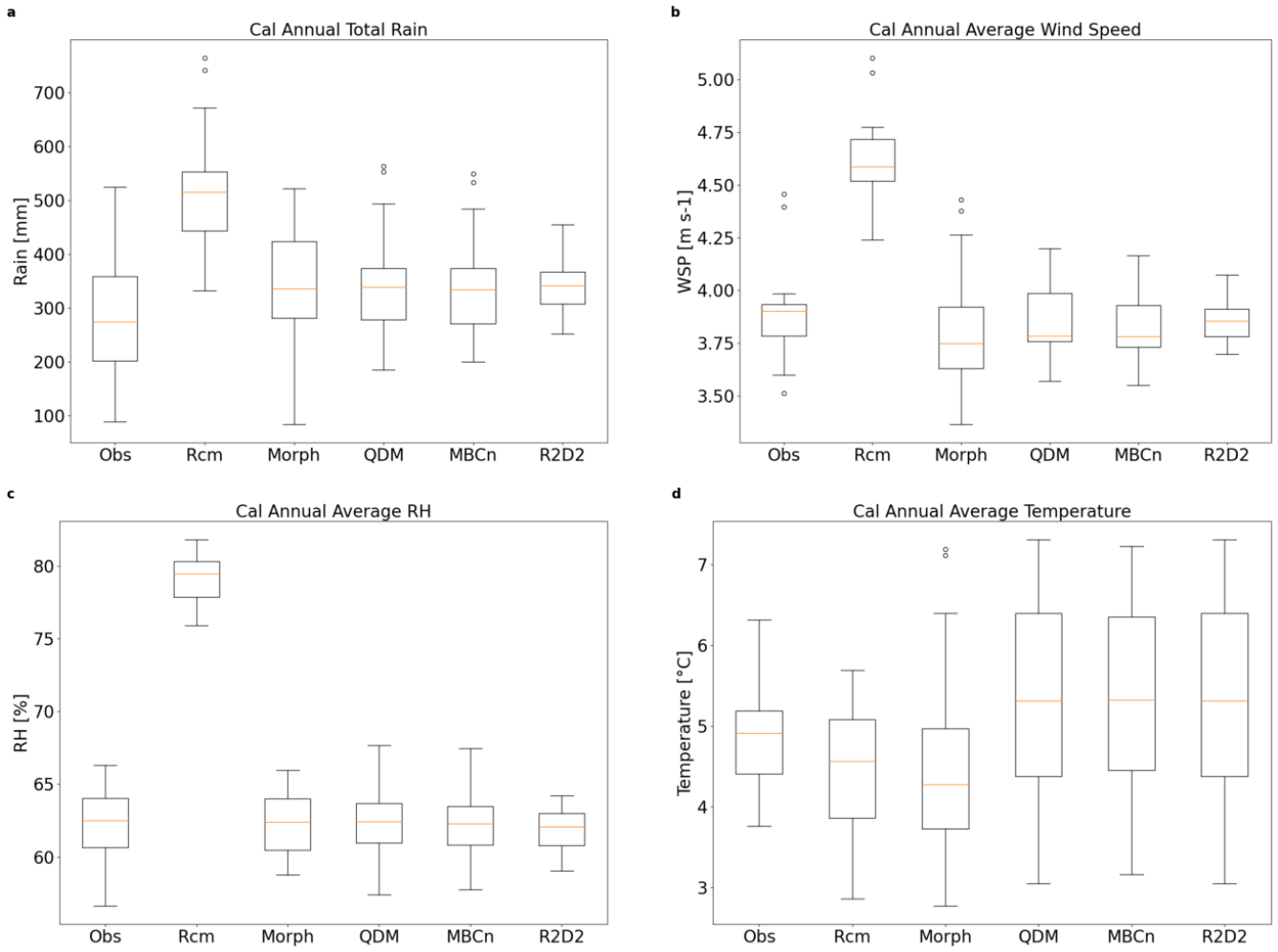

Figure 25. Calgary annual total horizontal rainfall (a), and average wind speed (b), relative humidity (c), and temperature (d) during the observational period (1998-2017)

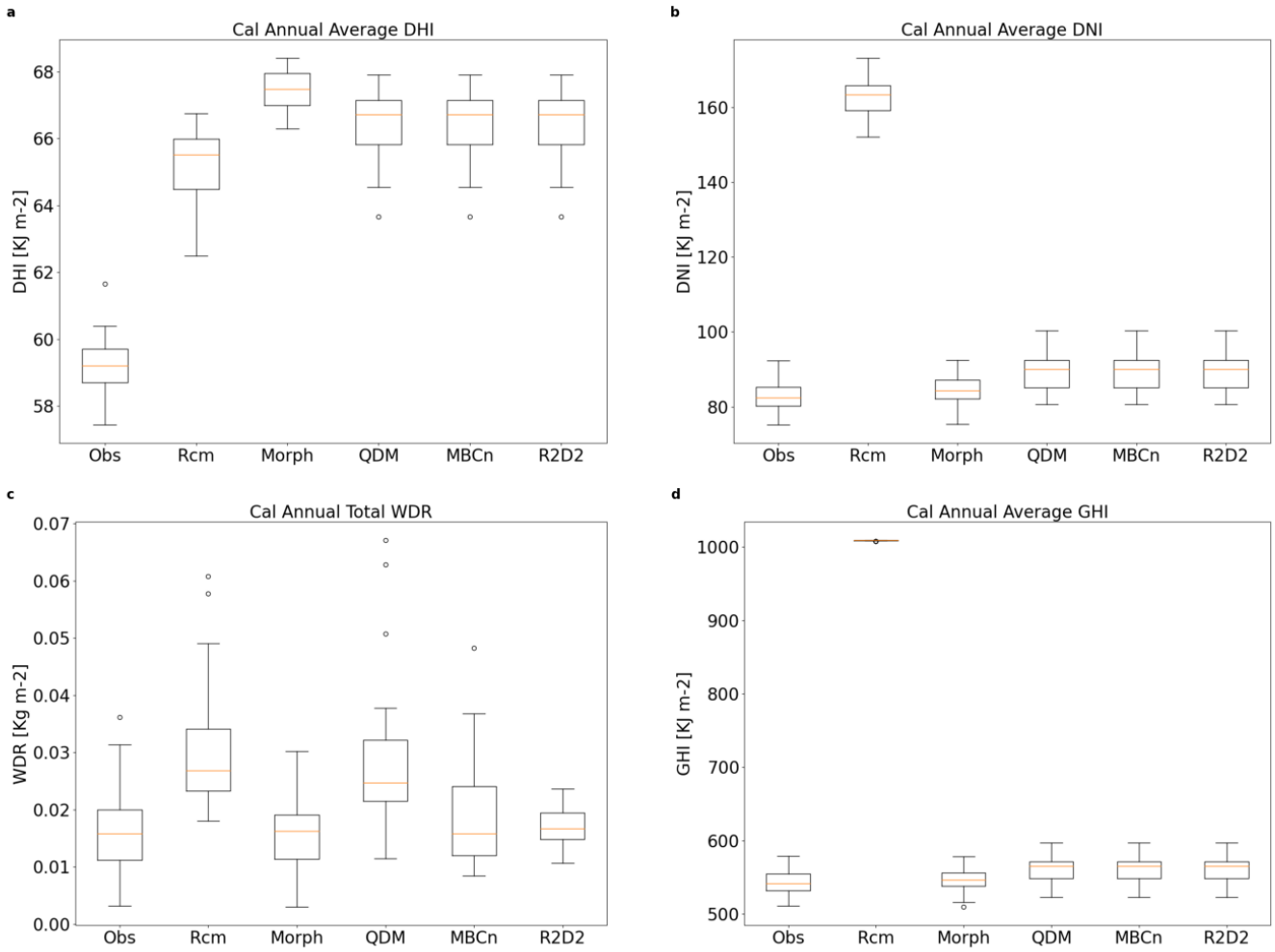

Figure 26. Calgary annual average DHI (a), DNI (b), total WDR (c) on the wall assembly, and DHI (d) (1998-2017)

A summary of the climatic variables in Calgary during the observational period is presented in Figure 25 and Figure 26, including the rainfall, wind speed, relative humidity, temperature, diffuse horizontal and direct normal irradiance, and wind driven rain experience by the simulated wall assembly. The observational records indicate a median annual average total rainfall of 274mm while the morphed and bias corrected data result in relatively similar values at approximately 336mm, which is a reduction compared to the raw RCM data at

515mm. Similarly, for the wind speed, the RCM overpredicts it at 4.6m/s while the other datasets are in relatively good agreement with the observed data at a median of 3.9m/s, however with larger variations from year to year. Continuing this trend, the RH is extremely overestimated by the RCM, with a median of 79.5%, whereas observed and corrected data all yield a median of approximately 62%. The temperature is better simulated by the RCM, resulting a median of 4.5°C, while observed data shows a median of 4.9°C. Morphed data underestimates slightly at 4.3°C, and the bias corrected datasets are nearly identical in median and variability at 5.3°C.

GHI is significantly overestimated by raw RCM data in Calgary, with nearly twice the observed value at a median of 1009Kj/m^2, compared to 543Kj/m^2. Consequently, morphed and bias corrected data lower the median average value to 547Kj/m^2 and 565Kj/m^2, respectively. GHI is split into DHI and DNI, where the average DHI is shown in Figure 26a, with the observational data presenting an overall lower DHI at a median of 59Kj/m^2 while RCM data predicts a value of 66Kj/m^2, morphed data at 68Kj/m^2, and QDM at 67Kj/m^2. The DNI as calculated by RCM data is extremely overestimated compared to the observed data at 163Kj/m^2 versus the observed 82Kj/m^2. Similarly, morphed data calculated a median of 84Kj/m^2 while QDM inches higher at 90Kj/m^2. As with previous illustrations of solar radiation variables, the QDM corrected solar data is used in place of MBCn and R2D2. Lastly, the annual total WDR deposited on the exterior of the OSB across the 20-year observational period is illustrated in Figure 26b. Observational data indicates a median value of 0.0158Kg/m^2, while RCM and QDM data predict a much higher median of 0.0268Kg/m^2 and 0.0247Kg/m^2, respectively. Other

datasets predict much closer medians to the observed data at 0.0162Kg/m^2, 0.0158Kg/m^2, and 0.0167Kg/m^2, for morph, MBCn, and R2D2 respectively.

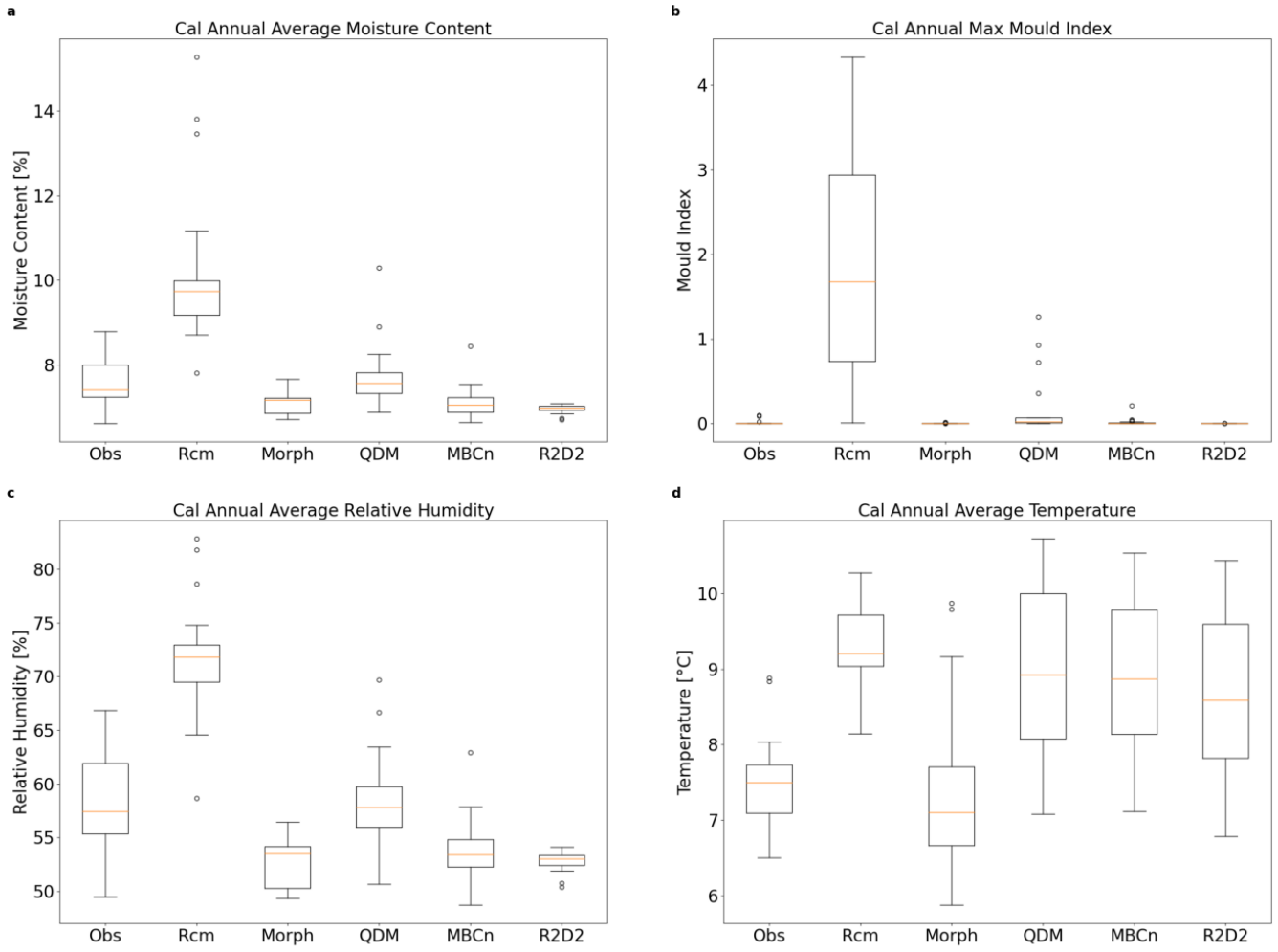

Figure 27. Calgary annual average: moisture content (a), relative humidity (b), temperature (c), and maximum mould index (d) on the exterior of the OSB sheathing (1998-2017)

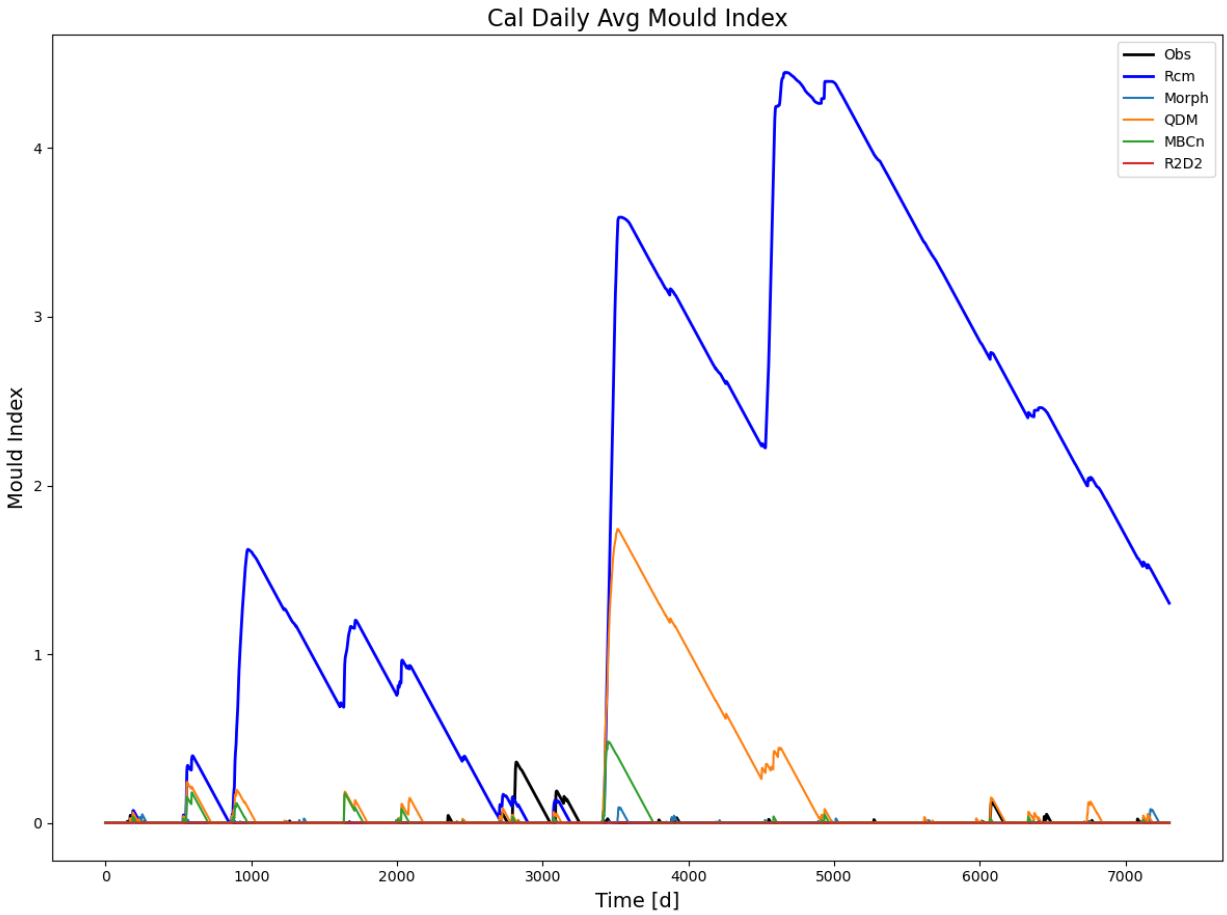

Figure 28. Calgary daily average mould index on the exterior of OSB sheathing (1998-2017)

The simulated MC of the OSB in Calgary is presented in Figure 27a. Considering the greater amount of deposited WDR experienced through the RCM data, the MC of the OSB predicted by the RCM is higher than the other datasets at a median of 9.7%. The simulation using observed and QDM data resulted in a median MC of 7.6%, while those of morph, MBCn, and R2D2 resulted in roughly the same median at 7%. For similar reasons, the RCM predicts a greater RH on the exterior side of the OSB sheathing at a median of 71.8%, compared to the observed and QDM data at 57.2%. MBCn and R2D2 predicts near identical RH at 53%, with

morphed data slightly lower at 51.3%. The temperature on the exterior of the OSB surprisingly varies quite a lot compared to the relatively good agreement in the ambient air temperature. Subsequently, the observed median temperature on the OSB is calculated to be 7.5°C while morphed data predicts a slightly lower temperature at a median of 7.1°C, but the variation from year to year is larger. The RCM calculated a median temperature of 9.2°C, and the three bias corrected datasets yielded similar medians, where QDM and MBCn had a value of approximately 8.9°C, and R2D2 slightly lower at 8.6°C.

The simulated mould index is presented in two formats in Figure 27b which shows the highest value reached in each year and in Figure 28 where the daily average value is presented for the length of the validation period. The RCM is an outlier in this case as it is the only dataset that resulted in any significant mould growth, with the exception of QDM which at one point calculated a moderate amount of mould growth, before subsequently decaying. The combination of relatively wetter conditions on the OSB in concert with a significantly higher ambient RH is the likely culprit causing the considerable difference in mould growth between the RCM and the other datasets.

The results of the bias correcting climate data indicate that an improvement is made from the raw RCM data, although the degree of success varies depending on the chosen method and climate variable. Generally, the raw RCM data compares the worst against the observations; while the bias corrected data can adequately correct for biases in the RCM, which result in better agreement with the observed data, especially in the case of rainfall and RH. Similarly, morphed data performs as well as those bias corrected. Hygrothermal performance of the various climate datasets simulated using DELPHIN showed varying degrees of success

depending on the parameter. However, overall, morphed and bias corrected data does yield more accurate results than the RCM data, especially in the case of mould growth. Where the raw RCM simulated wetter conditions than any other dataset and was the only one to predict any significant mould growth at all.

4.4.2 Projected Future Period

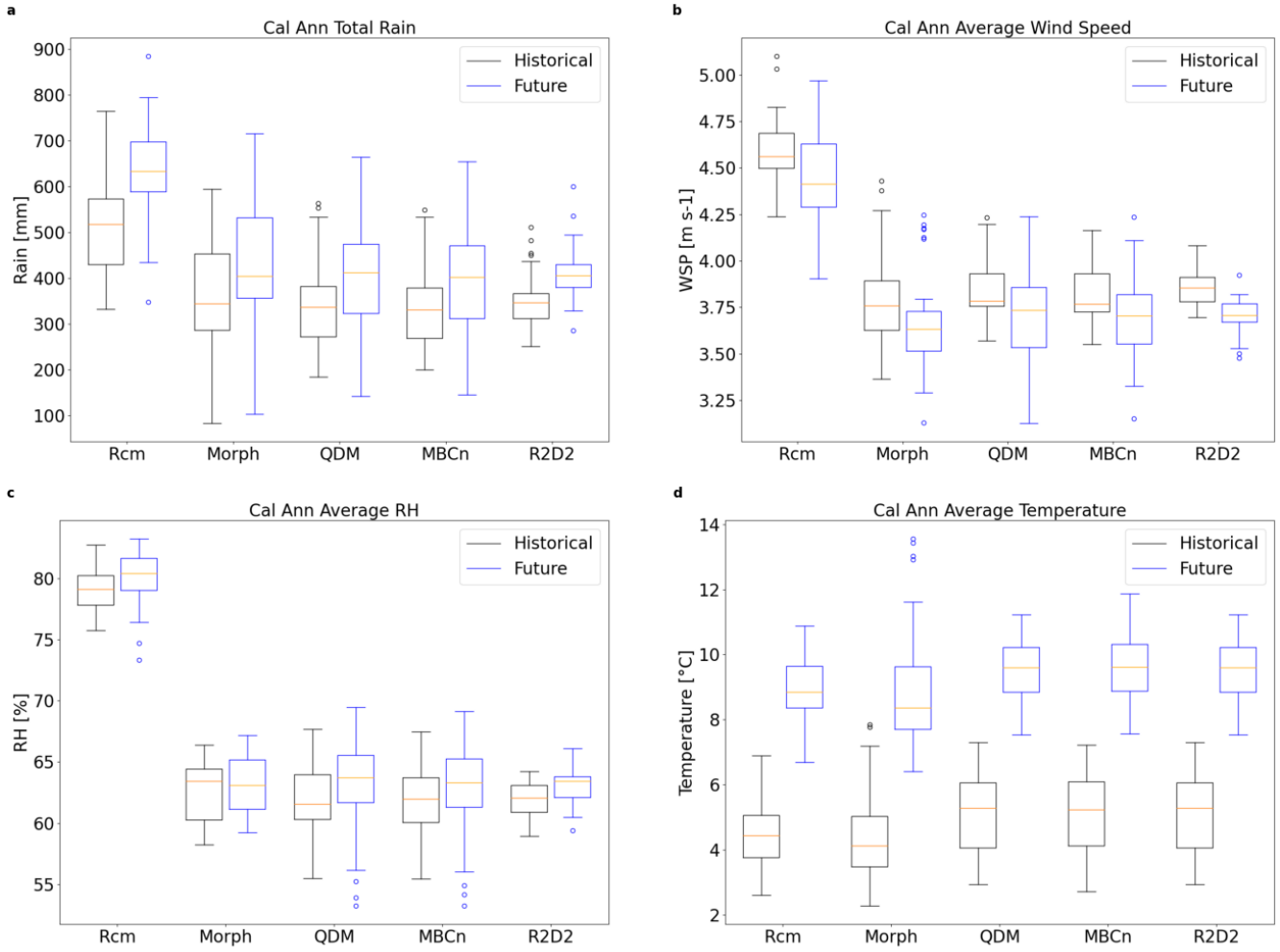

Figure 29. Calgary boxplots of annual total rain (a), and average wind speed (b), relative humidity (c), and temperature (d), over a baseline historical period from 1991-2021 and a future projected period from 2064-2094

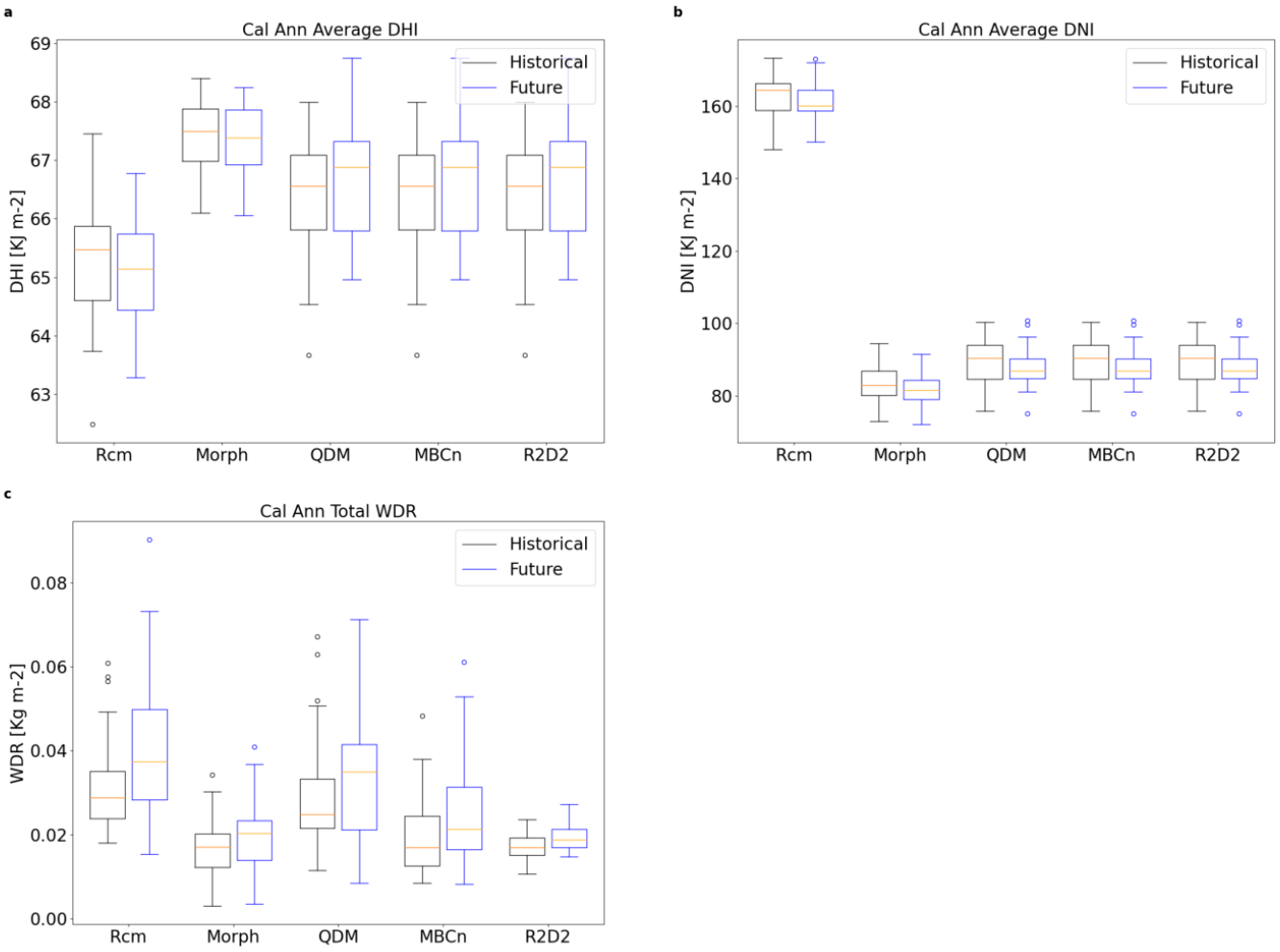

Figure 30. Calgary boxplots of annual average DHI (a), DNI (b), and WDR (c) over a historical (1991-2021) and future (2064-2094) period

Based on the previous analysis, total rainfall is typically overestimated by the RCM. In this case, the historical and future projected annual total rainfall forecasts a median of 518mm and 634mm, illustrated in Figure 29a. Morphed data reduces these projects to 345mm and 405mm for the historical and projected periods respectively. QDM, MBCn, and R2D2 predict similar medians in both time periods at 336mm and 405mm. Consequently, there is a net increase in annual total rainfall between the historical and future period. A similar behaviour is

seen in the wind speed shown in Figure 29b, in terms of the relatively performance of the datasets. According to the RCM, wind speed is anticipated to decrease from 4.6m/s to 4.4m/s. Meanwhile, performance of the other datasets is quite similar, decreasing from a median of approximately 3.8m/s to 3.7m/s in the future. Similarly, RH in Calgary is known to be overestimated by the RCM, with a historical value of 79.1%, and forecast to increase in the future to a median of 80.4%. On the other hand, QDM, MBCn, and R2D2 bias corrected RH yields a historical median of 62% rising to 63.5%. Meanwhile, little change is forecast by morphed climate data with an annual median RH of 63%. Again, temperature appears to be quite well simulated by the RCM, with a historical median of 4.4°C, and rising to 8.9°C due to climate change. Similarly, morphed data calculates a median of 4.1°C during the historical period while increasing to 8.4°C. Additionally, R2D2, MBCn, and QDM data forecasts similar temperatures in both periods increasing to 9.6°C from 5.3°C.

The RCM projects decrease in both the solar radiation variables, DHI and DNI, in the future. Figure 30a shows RCM estimates of the DHI with a historical median of 65Kj/m^2 lowering to 65Kj/m^2. An even smaller decrease in found between morphed data from 68Kj/m^2 to 67Kj/m^2. Conversely, QDM estimates an increase from 66Kj/m^2 to 67Kj/m^2. The behaviour of DNI is more consistent with all datasets predicting a decrease in the median. There is quite a lot of variation in the WDR between the datasets, however a consistent increase into the future is forecasted. In the case of the RCM, median WDR will increase from 0.0288Kg/m^2 to 0.0373Kg/m^2. QDM performs similarly with a historical median of 0.0248Kg/m^2 rising to 0.0349Kg/m^2. The other three datasets morph, MBCn, and R2D2 start with a historical median of close to 0.017 Kg/m^2 which increases to approximately 0.02Kg/m^2.

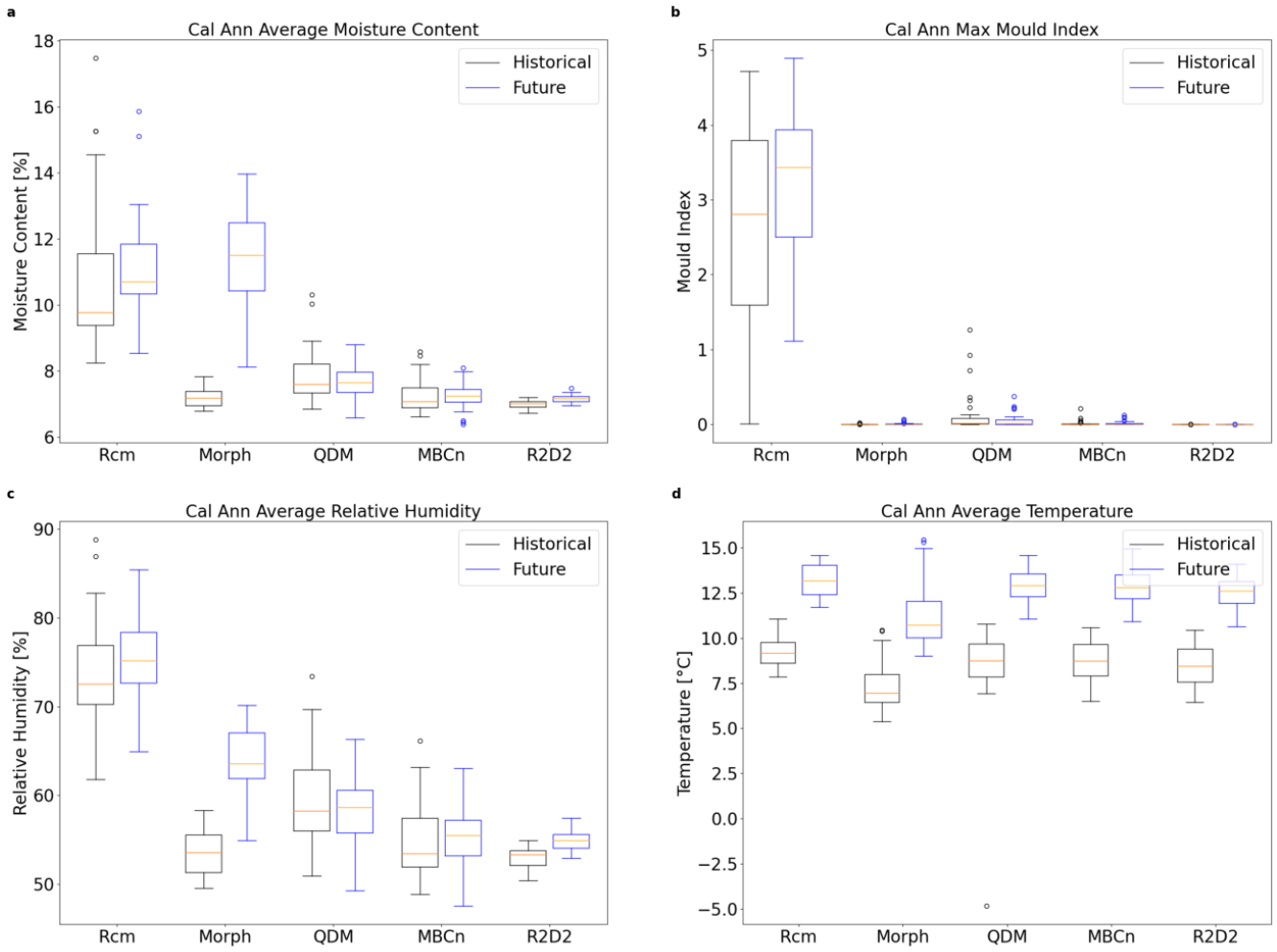

Figure 31. Calgary annual MC (a), RH (c), temperature (d), and maximum MI (b) of the OSB sheathing of the wall assembly, for a historical (1991-2021) and future (2064-2094) period

As expected, the MC of the OSB is projected to increase in the future climate, the degree to which varies significantly depending on the climate dataset used in the hygrothermal simulation. For the RCM, MC is projected to increase from 9.8% to 10.7%, whereas much smaller gains are expected from QDM, MBCn, and R2D2 data. Simulations with QDM data resulted in a historical median MC of 7.6% with only a marginal increase in the future.

Meanwhile, MBCn and R2D2 start from 7% rising to 7.2%. Results simulated using morphed climate date shows the most drastic difference going from 7.2% to a median value of 11.5%. Following results from the observational period, its no surprise that the RCM simulated mould index would yield significantly more growth than the process climate data, with the historical distribution closely match those from the observational period. As a consequence of wetter conditions, and increased RH and temperature, the conditions conducive to mould growth become more prevalent in the future, resulting in even more mould growth within a 30-year period. Similarly, the RH and temperature on the exterior of the OSB presented in Figure 31c and Figure 31d, closely follow the changes in climatic conditions illustrated in Figure 29. Consequently, RH on the OSB is forecasted to increase to varying degrees. RCM predicts a historical median of 72.5% rising to 75.2%, while the most drastic change follows from morphed data, rising from 53.6% to 63.6%. The temperature predicted by QDM, MBCn, and R2D2 behave similarly increasing from approximately 8.7°C to 12.8°C. Morphed data start with a lower historical median temperature at 6.9°C rising to 10.7°C. Lastly, the RCM forecasts an increase in of nearly 4°C, starting at a historical median of 9.2°C.

4.5 Vancouver

4.5.1 Baseline Validation Period

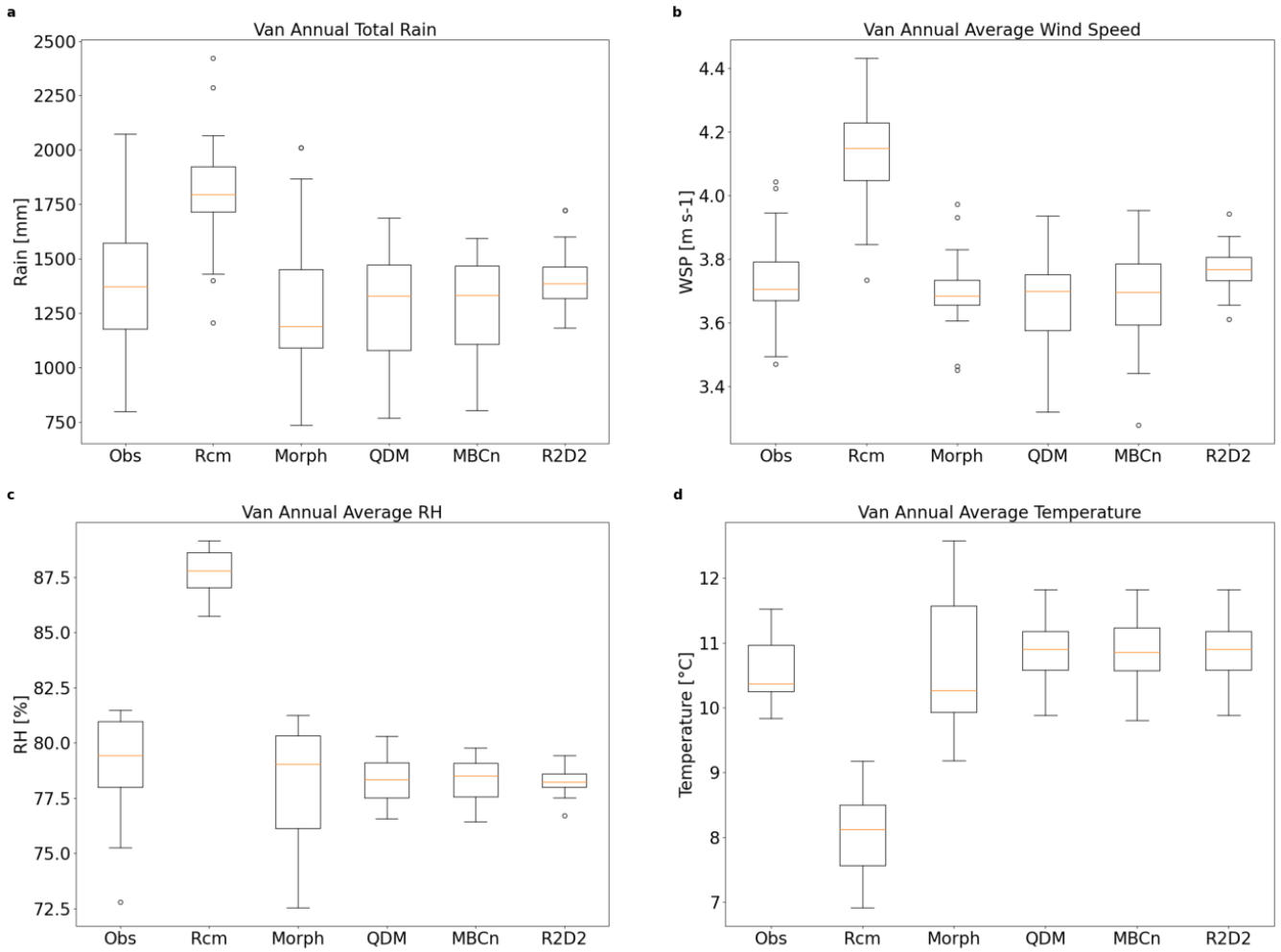

Figure 32. Vancouver annual total horizontal rainfall (a), and average wind speed (b), relative humidity (c), and temperature (d) during the observational period (1998-2017)

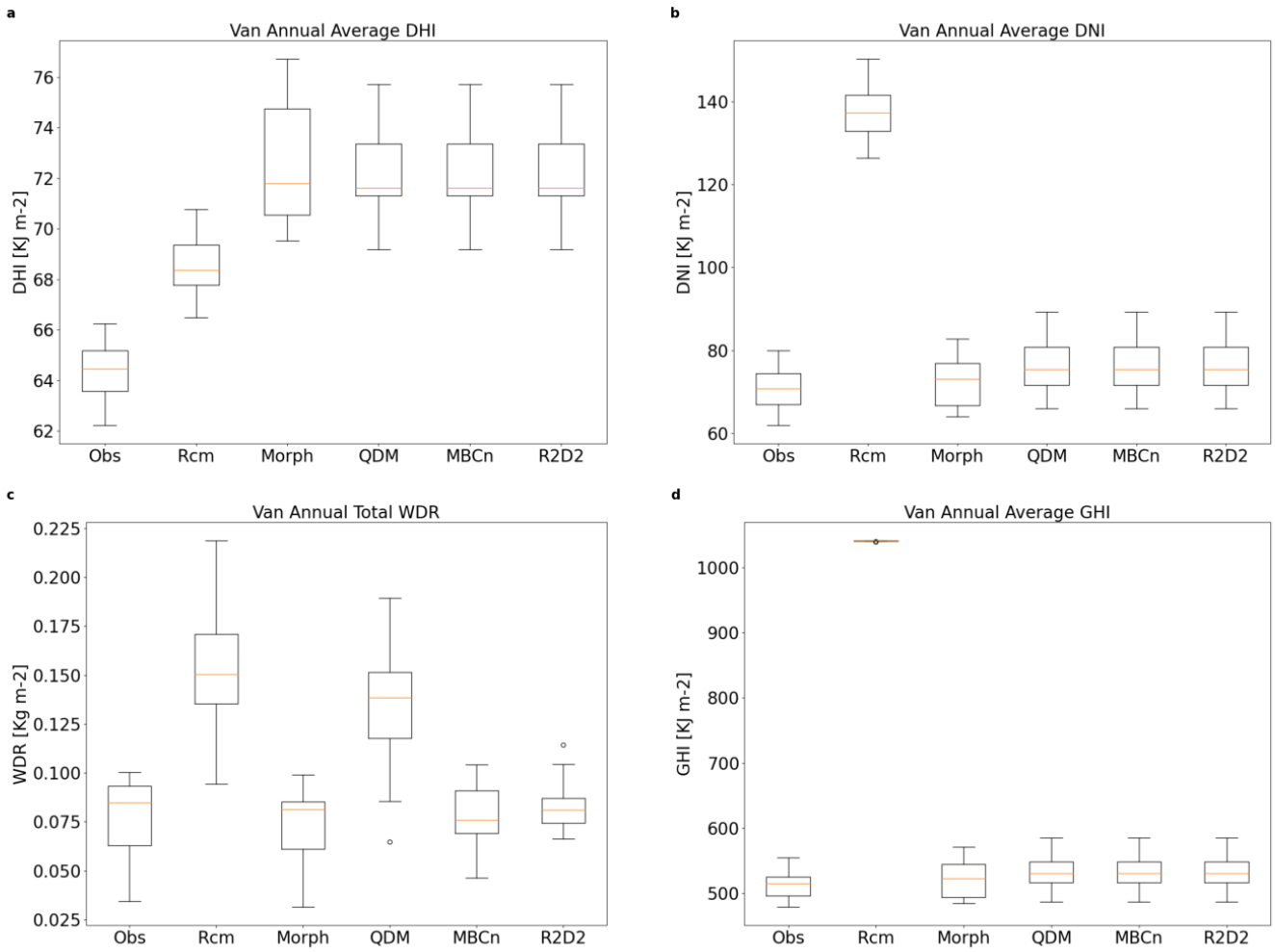

Figure 33. Vancouver annual average DHI (a), DNI (b), total WDR (c) on the wall assembly, and DHI (d) (1998-2017)

Vancouver experiences significantly more rain during the observational period compared to any of the other studied locations. In Figure 32a, observed data indicates a median annual total rainfall of 1372mm. As with other locations, raw RCM data overestimates the horizontal rainfall. In this case, the RCM estimates a median of 1796mm. QDM, MBCn, and R2D2 corrected rainfall calculated a median annual value of approximately 1351mm, while morphed data predicts the least rainfall at 1189mm. There is relatively good agreement

between the morphed and bias corrected datasets with the observations, each with a median of approximately 3.7m/s, where R2D2 is slightly higher at 3.8m/s. However, RCM data indicates faster wind speeds at a median of 4.1m/s. Similar relative performance in the RH can be seen in Figure 32c, where again the RCM overestimates the RH at a median value of 87.8%. On the other hand, median from observed, morphed, and bias corrected datasets was calculated to be approximately 78%. Contrastingly, RCM simulated air temperature is lower than the other datasets, with a median of 8.1°C. Observed and morphed data shows a higher median temperature at 10.3°C, while the other bias corrected data are near identical with a median of 10.9°C with a similar year to year variability as well.

Vancouver is no exception to overestimation of GHI by the raw CanRCM4 data, where significant adjustments are made by morphing and QDM to reduce the median values closer to the observations of 515Kj/m^2. Once GHI is split into components, the morphed and bias corrected DHI result in similar medians, close to 72Kj/m^2. However, observational data indicates a lower DHI, with a median of 65Kj/m^2, while RCM data is between, resulting in a median of 68Kj/m^2. As with all solar radiation related parameters used in this work, QDM corrected data is used in place of MBCn and R2D2 for reasons mentioned previously. Which is why the results in Figure 33a are identical for those datasets. Average DNI is severely overestimated by raw RCM data, like it was for other locations as well. Consequently, resulting in a median of 138Kj/m^2, while all other data presents a median closer to 70Kj/m^2. Due to the large of amount of horizontal rainfall predicted by the RCM during the observational period, its not surprise that the RCM also forecasts the most WDR, with a median annual value of

0.151Kg/m^2. Which is followed closely by QDM corrected data at a value of 0.138Kg/m^2. Other datasets estimate values close to the observed data at approximately 0.08Kg/m^2.

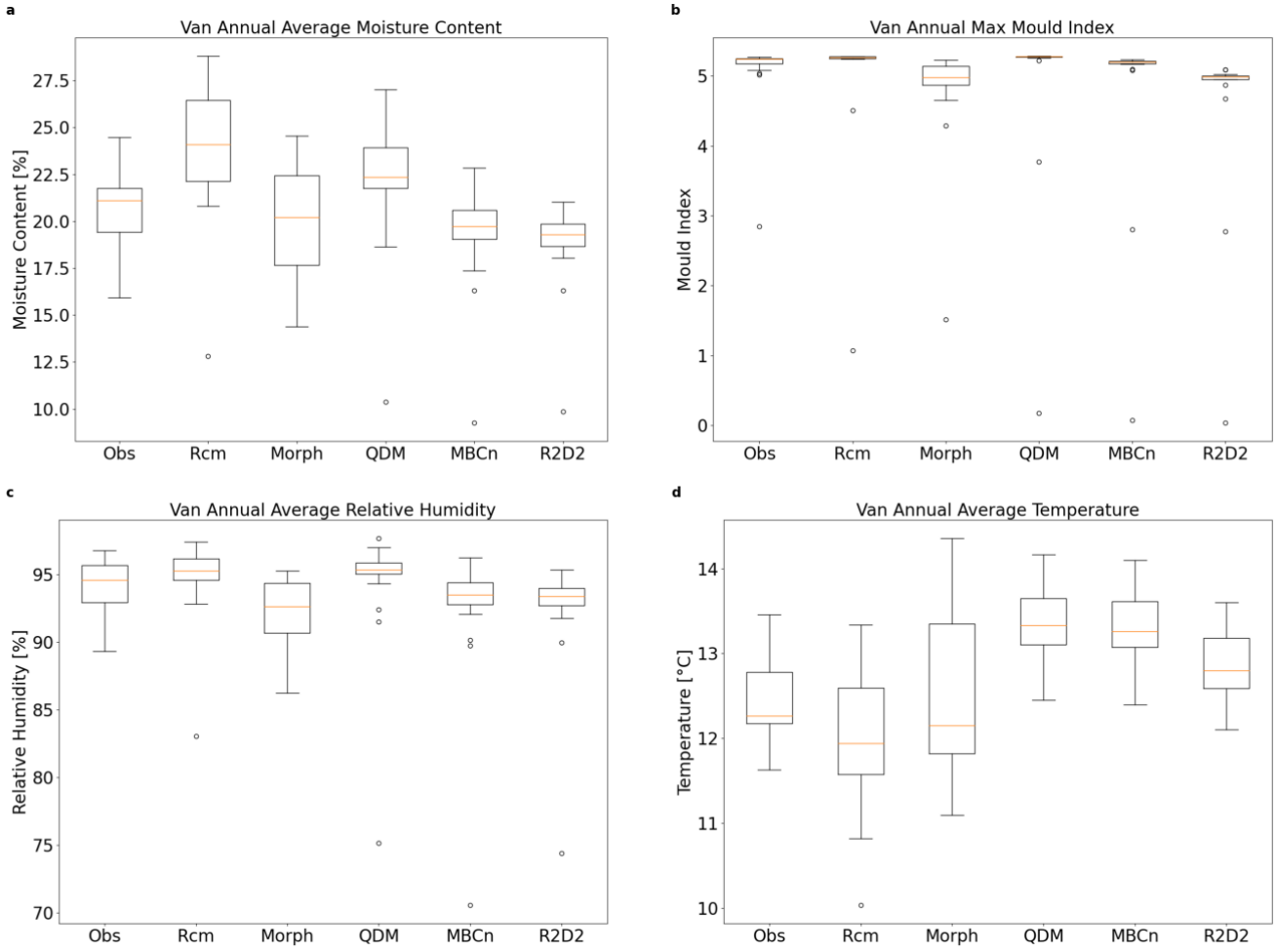

Figure 34. Vancouver annual average: moisture content (a), relative humidity (b), temperature (c), and maximum mould index (d) on the exterior of the OSB sheathing (1998-2017)

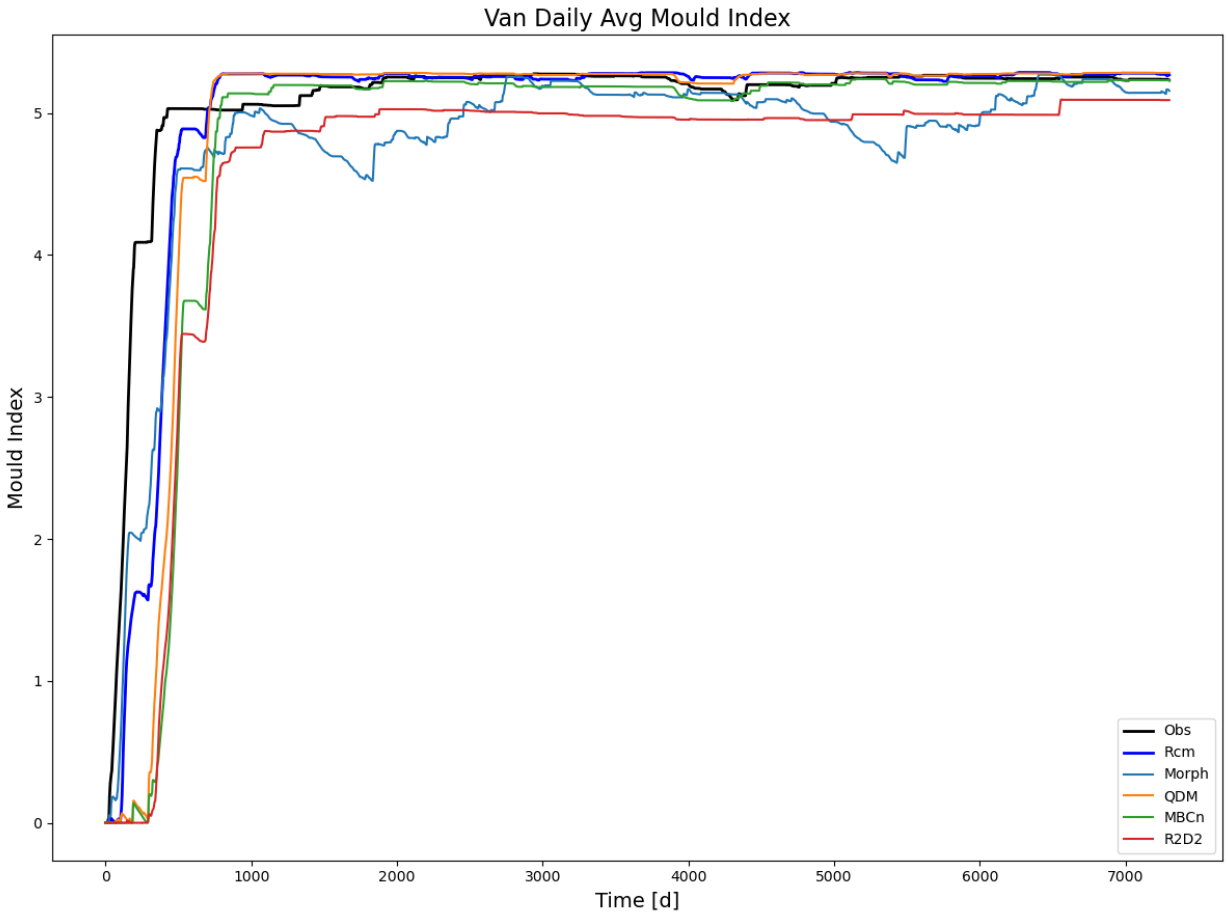

Figure 35. Vancouver daily average mould index on the exterior of OSB sheathing (1998-2017)

The MC of the OSB is quite high in Vancouver, compared to other cities. DELPHIN simulations using observed data yield a median annual average MC of 21.4%, while RCM estimates a value of 24.2%. There is some variability between the processed climate data, where the multivariate methods, MBCn and R2D2, and morphing yield a median of approximately 20%, while QDM corrected data is closer to the RCM at 23.1%. Regardless of the dataset, the OSB will experience decay since the moisture content surpasses the critical threshold of 16%. The simulated RH on the exterior of the OSB is very high, with almost all

datasets predicting a median greater than 95%, except for morphed data at which has a median of 94.5%. Observational and morphed data indicates a median temperature on the exterior of the OSB of 12.1°C, while RCM simulated a lower temperature at 10.9°C. R2D2 calculates a slightly higher median at 11.9°C, and QDM and MBCn result in the highest simulated temperature with a median annual average of 12.7°C. Due to the moderate climate in Vancouver, consistent high relatively and warm temperatures lead to a high risk of mould growth. According to Figure 35, within a year from the start of the simulation, significant mould growth begins. Subsequently peaking at a mould index of 5 before reaching a relative steady state. This phenomenon is experienced no matter which set of climate data was used in the hygrothermal simulation.

Significant improvements are made to raw model data when processing climate data in Vancouver through the presented methods. Generally, the raw RCM data compares the worst against the observations; while the bias corrected data adequately corrects for biases in the RCM, which result in better agreement with the observations. However, despite the relatively accurate annual average of rainfall, wind speed, RH, and temperature, there is significant variability in the deposited WDR on the OSB sheathing. Consequently, hygrothermal simulations indicate a similar variation in MC of the OSB. The results show that Vancouver has a relatively wet climate, which is likely to result in wood decay and mould growth issues on the OSB.

4.5.2 Projected Future Period

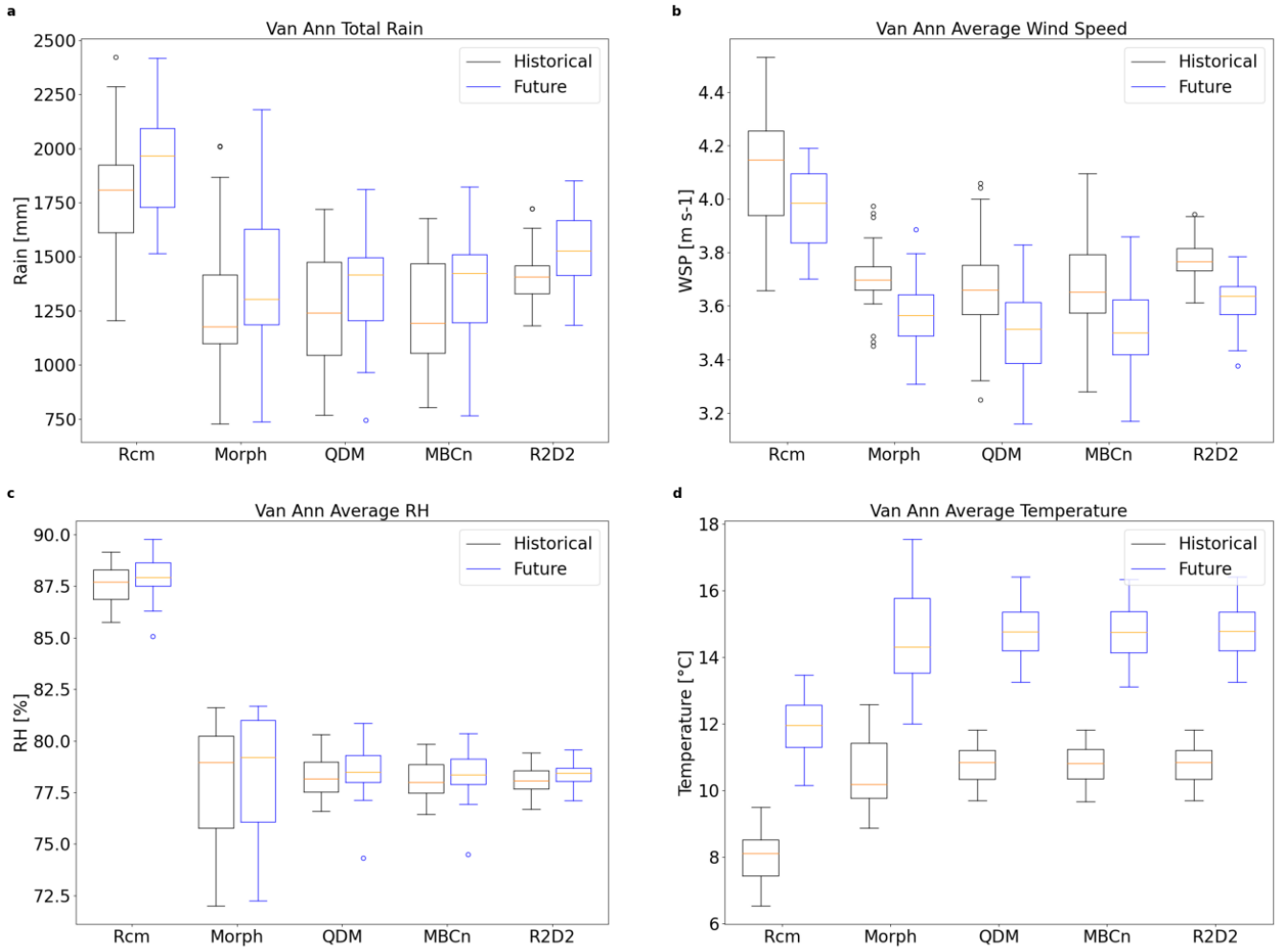

Figure 36. Vancouver boxplots of annual total rain (a), and average wind speed (b), relative humidity (c), and temperature (d), over a baseline historical period from 1991-2021 and a future projected period from 2064-2094

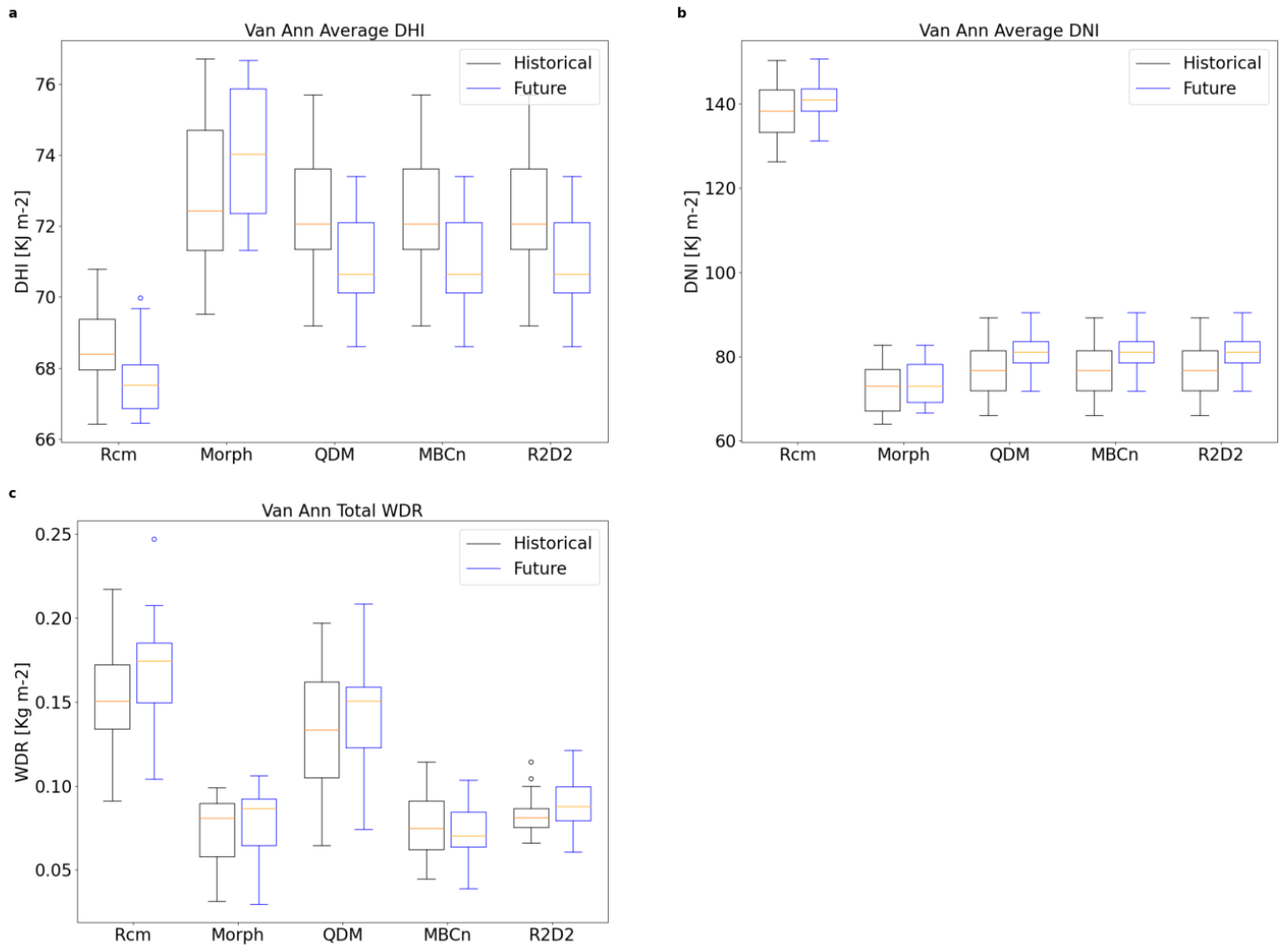

Figure 37. Vancouver boxplots of annual average DHI (a), DNI (b), and WDR (c) over a historical (1991-2021) and future (2064-2094) period

Historically, Vancouver received the most rain out of the 6 studied locations, and according to the RCM in Figure 36a, it is poised to increase in the future from 1808mm to 1967mm. Due to the model bias, rainfall is typically overestimated by the RCM. Consequently, corrected datasets present lower historical median annual totals which range from a low of 1179mm calculated with morphed data to a higher of 1407mm according to R2D2. Similarly, the future projected rainfall is forecast to increase, where the largest difference is presented by

the MBCn data, at 20.2%, rising from 1195mm to 1423mm. RCM projects a decrease in future wind speed from a median of 4.2m/s to 4.0m/s. Hygrothermal simulations with the pre-processed data also illustrate decrease in average wind speed, in general going from a median of around 3.7m/s to 3.6m/s. Ambient RH and temperature are both projected to increase in the 2064-2094 period, although RH to a lesser extent, which is illustrated in Figure 36. RH is largely unchanged with the RCM estimate a historical median of 87.7% while processed data calculated a median of 78.6%. In comparison, temperature is expected to increase significantly more. RCM forecasts that the temperature will go from a historical median of 8.11°C to 11.9°C. Similarly, morphed and bias corrected data indicates temperatures rising from 10.2°C and 10.8°C to 14.3°C and 14.8°C, respectively.

RCM estimated DHI will decrease in the projected period from 68Kj/m^2 to 67Kj/m^2. A similar adjustment calculated by QDM corrected data is also observed, however, from a higher historical value of 72Kj/m^2. Contrarily, morphed climate data indicates an increase in average DHI, rising from 72Kj/m^2 to 74Kj/m^2. Slight increases in DNI are projected for the future in Vancouver seen in Figure 37b. As with other locations, RCM produces large values in the DNI around 140Kj/m^2. Morphed and bias corrected values result in medians closer to 80Kj/m^2 in both periods. WDR is expected to increase following climate change according to the RCM, rising from a median annual total of 0.151Kg/m^2 to 0.175Kg/m^2. Morph, MBCn, and R2D2 do not present the same level of WDR, with historical means closer to 0.08Kg/m^2, with minute increases in the future, excepting MBCn where a slight decrease is calculated. On the other hand, QDM data exhibit nearly as much WDR as the raw RCM data.

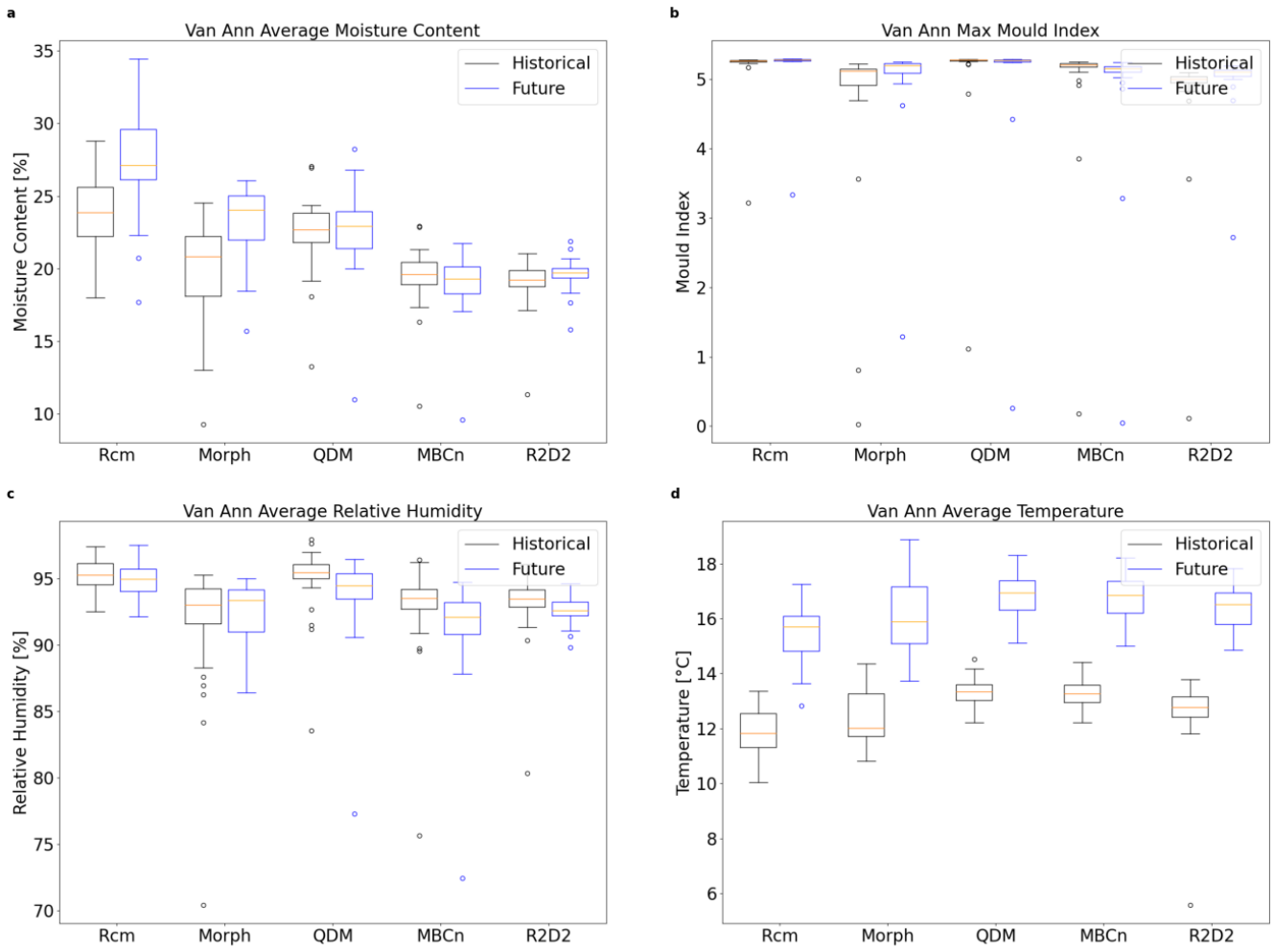

Figure 38. Vancouver annual MC (a), RH (c), temperature (d), and maximum MI (b) of the OSB sheathing of the wall assembly, for a historical (1991-2021) and future (2064-2094) period

Due to the large amounts of WDR deposited on the OSB sheathing, hygrothermal simulations using RCM data show the highest levels of MC in the OSB in Figure 38a. In both cases, deterioration of the OSB should be expected as the MC exceeds the threshold for OSB decay, at a historical median of 23.9% and projected increase to 27.1%. A similar increase is calculated with morphed climate data, resulting in MC of 20.8% and 24.1% for the historical and

future periods, respectively. While simulations with other datasets, namely QDM, MBCn, and R2D2 also show high levels of MC in the OSB, enough to cause deterioration, they are less than that found through RCM data. MBCn is the only set where a minimal decrease in MC is expected, likely because the WDR is also forecast to lessen. Vancouver is known to be of a relatively wet climate for a Canadian city. Consequently, historical mould growth risk is already quite significant, where values exceeding 5 are expected with any of the tested datasets. Climate change will exacerbate this issue, due to increasing temperature leading to longer periods favourable to mould growth. Despite generally decreasing RH forecasted by all but morphed data, the RH in Vancouver is already high enough for mould to grow on the exterior of the OSB.

4.6 Kuujjuaq

4.6.1 Baseline Validation Period

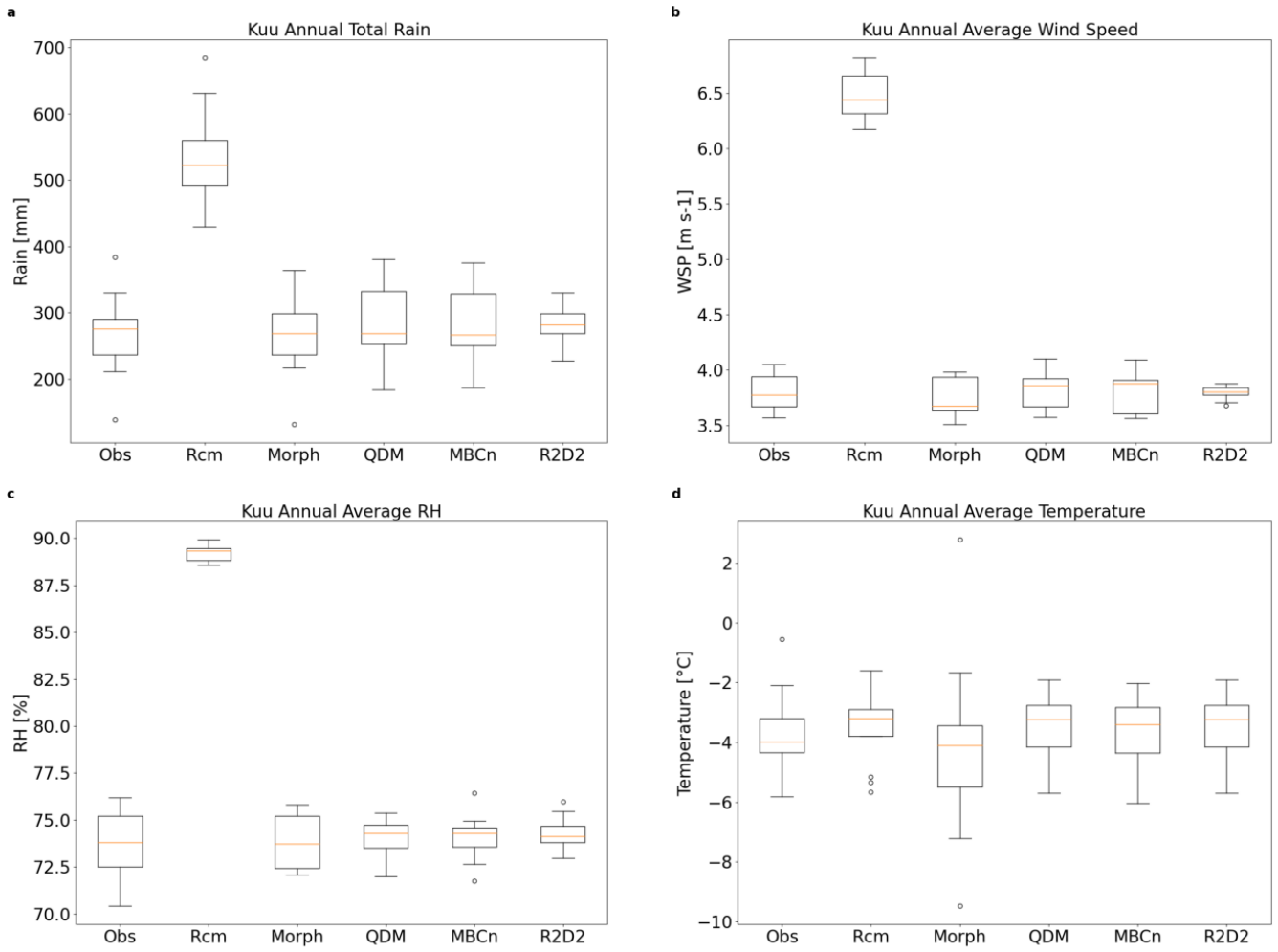

Figure 39. Kuujjuaq annual total horizontal rainfall (a), and average wind speed (b), relative humidity (c), and temperature (d) during the observational period (2005-2017)

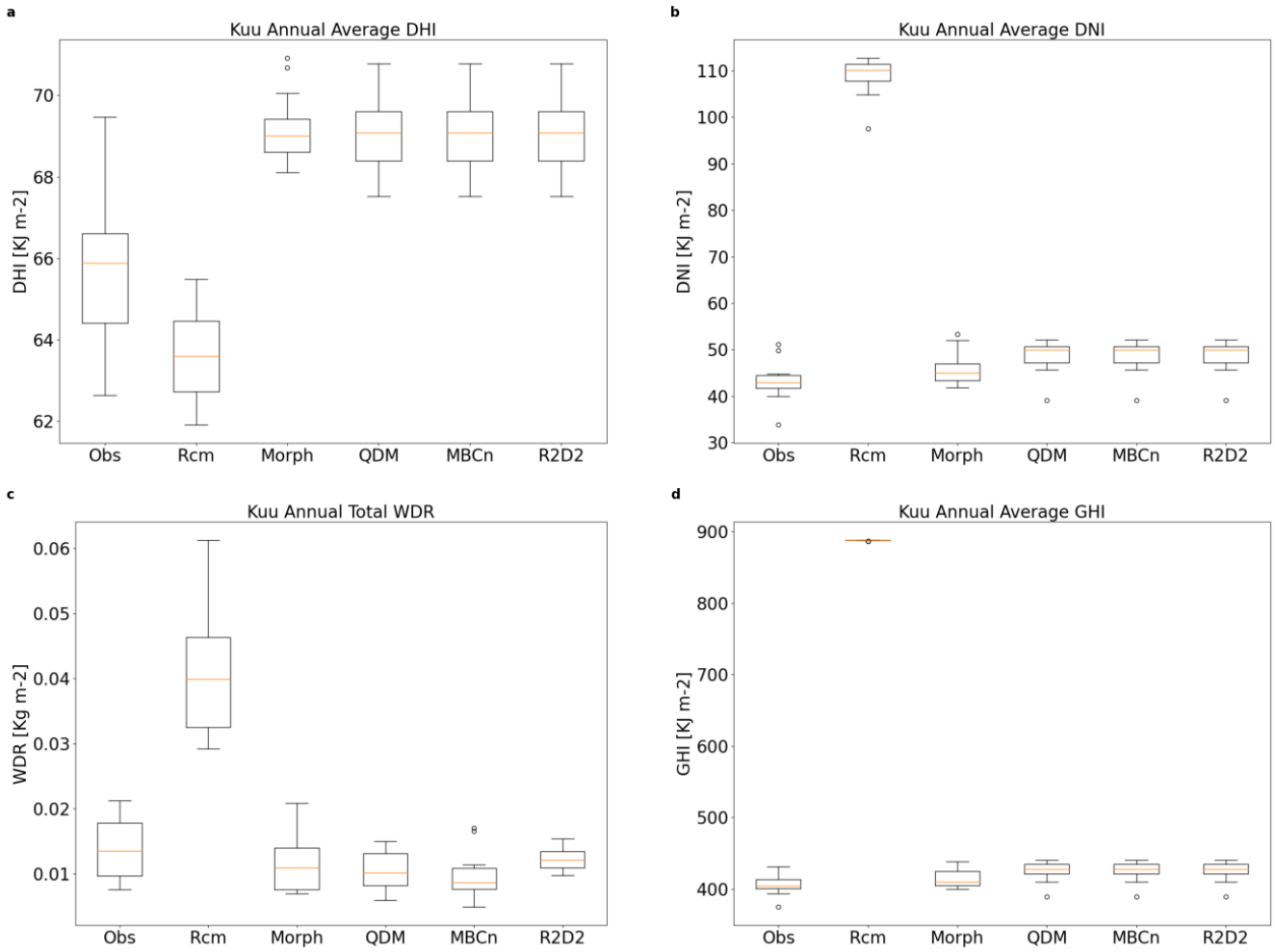

Figure 40. Kuujjuaq annual average DHI (a), DNI (b), total WDR (c) on the wall assembly, and DHI (d) (2005-2017)

The annual total rainfall across the baseline observational period from 2005-2017 is presented in Figure 39a. The RCM consistently overestimates the rainfall for all of the previous locations that were studied, and Kuujjuaq is no different, with a median annual total rainfall of 523mm, as opposed to the observed 276mm. Morphed and bias corrected climate data show similar amounts of rainfall as the observation data with approximately 270mm. Similarly, RCM data significantly overestimates the wind speed, with a calculated median of 6.4m/s whereas

the other datasets indicate a median wind speed closer to 3.8m/s. A similar trend is seen for the relative humidity, shown in Figure 39c, where the RCM estimates an extremely high RH a median of 89.3%. Observed and processed climate data indicate a median closer to 74%. Kuujjuaq is by the far coldest climate out of all the locations included in this work, where the measured average temperature is -4.0°C. Raw RCM data is not far off from the observations with a median of -3.2°C, while morphed data is slightly colder at -4.1°C. Bias corrected data performed similarly with a median temperature around -3.3°C.

Kuujjuaq receives the least solar radiation compared to any of the other locations. Consequently, observed GHI results in a median of 405Kj/m^2. However, RCM still overestimates this at 888Kj/m^2 but morphed and QDM data is able to modify the data and bring down the expected GHI. After splitting GHI into components, morph and QDM predicts a higher DHI than observed and RCM data, with a median annul average of 70Kj/m^2, compared to the 67Kj/m^2 from observations, and 64Kj/m^2 according to raw model data. Following results of other locations, DNI calculated with RCM data also severely overestimate it at Kuujjuaq as well, with a median of 111Kj/m^2, opposed to the observed 43Kj/m^2. Meanwhile, morph and QDM data DNI yields 45Kj/m^2 and 50Kj/m^2, respectively. Due to the relatively colder climate, WDR is less prevalent in Kuujjuaq. Consequently, observation data shows a median annual total WDR of 0.0136Kg/m^2. The processed climate data predicts even less WDR deposited on the OSB sheathing, with medians ranging from 0.008Kg/m^2 to 0.0122Kg/m^2 by MBCn and R2D2, respectively.

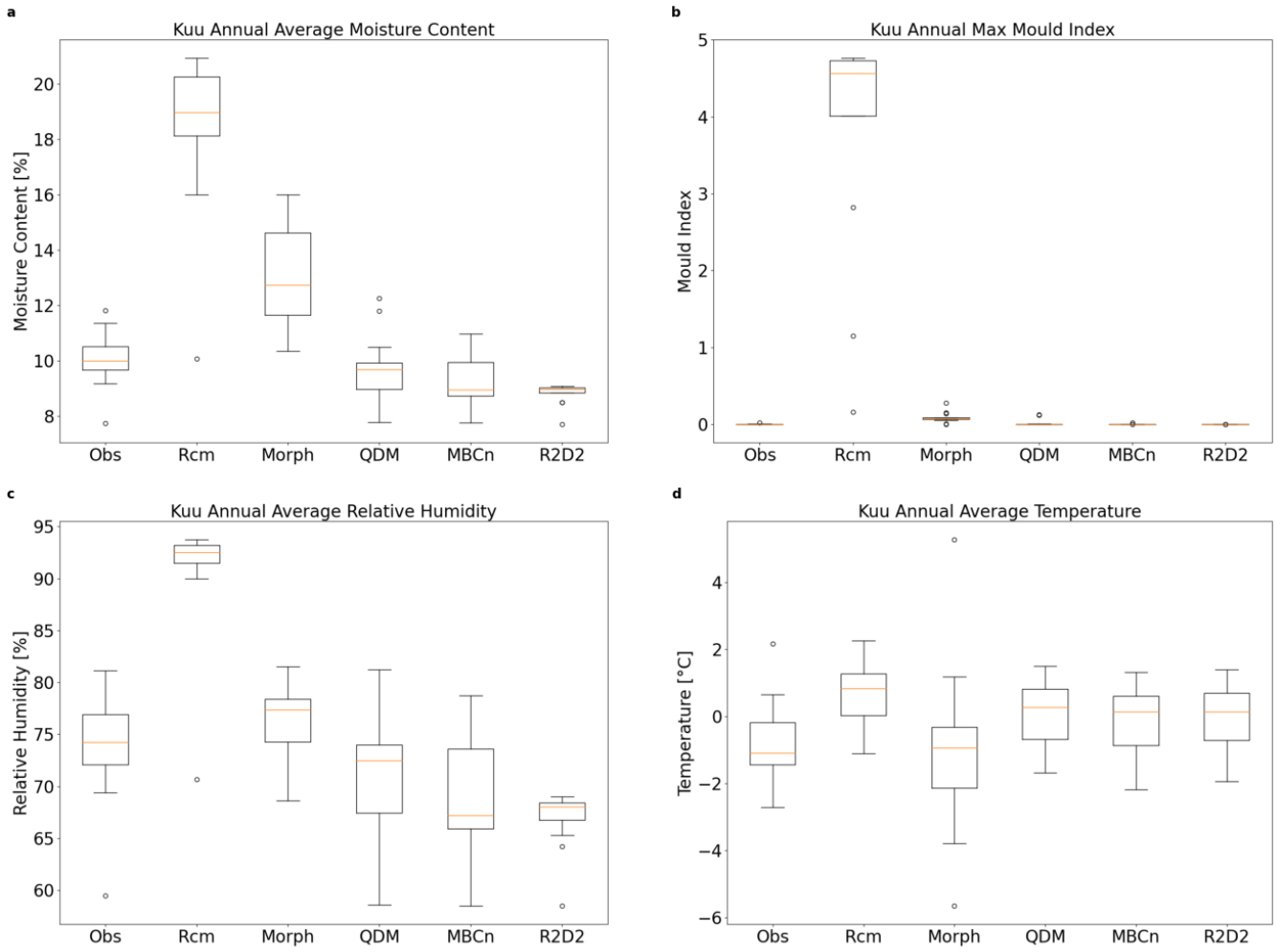

Figure 41. Kuujjuaq annual average: moisture content (a), relative humidity (b), temperature (c), and maximum mould index (d) on the exterior of the OSB sheathing (2005-2017)

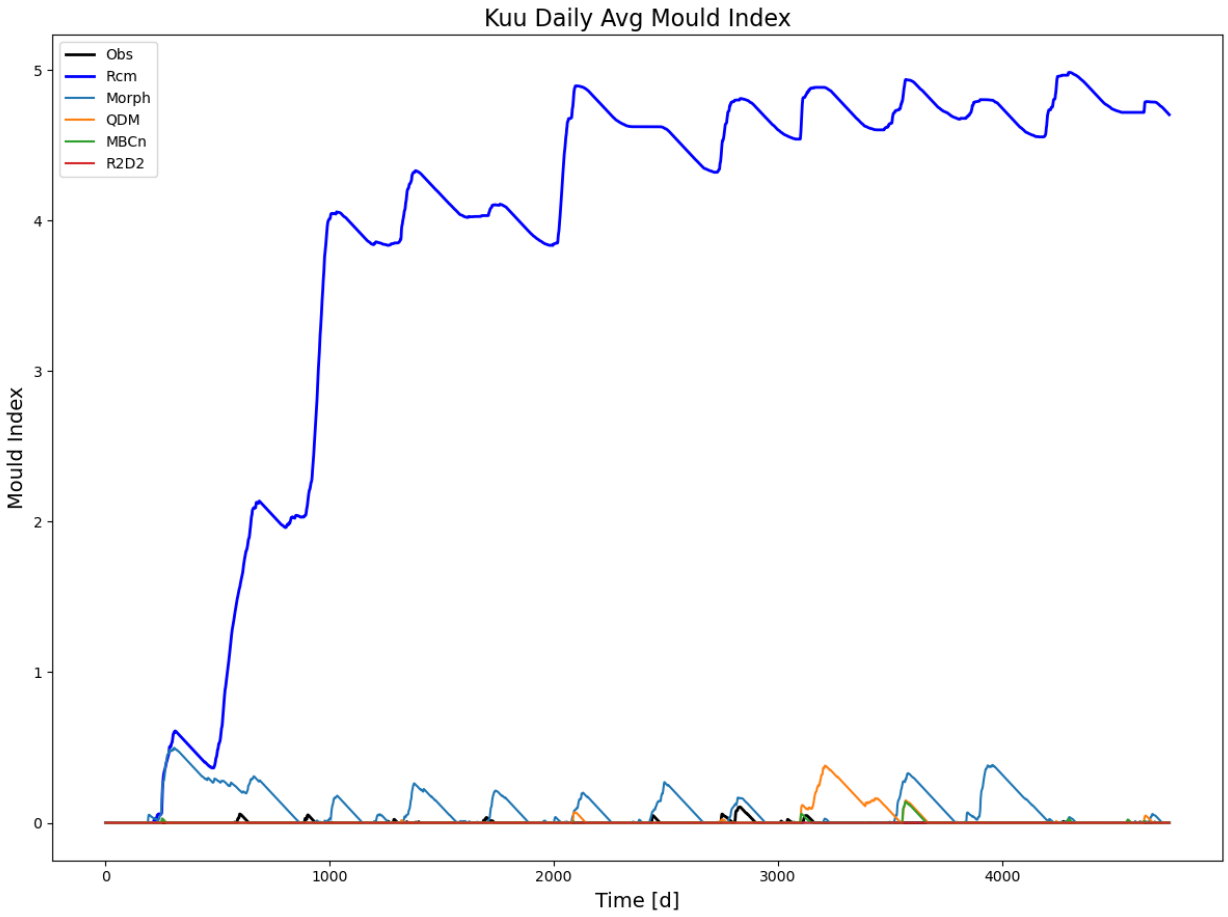

Figure 42. Kuujjuaq daily average mould index on the exterior of OSB sheathing (2005-2017)

The MC is heavily dependant on the amount of deposited WDR on the OSB. Therefore, the simulated MC of the OSB in Figure 41a somewhat follow the forecasts of WDR from Figure 40c. Consequently, the largest prediction of MC of the OSB comes from the RCM inputs, resulting in a median MC of 18.9%, clearly exceed the critical threshold, which would likely result in deterioration of the OSB over this observational period. Meanwhile observed and bias corrected data predicts a MC of around 9%. Despite morphed data forecasting relatively similar levels of deposited WDR, the MC resulted in comparatively higher values than the other

datasets, with a median of 12.7%. Simulated RH on the exterior surface of the OSB is also quite high according to the RCM, with a median annual average of 91.8%, compared to the observed 74.5%. Morphed data presents a median close to the observations at 77.3%, while QDM predicts a lower RH at 72.5%. The multivariate bias corrected data yielded lower RH on the OSB around 68%. The simulated temperature on the OSB is in relatively good agreement compared to the other parameters. For example, the observed temperature is -1.1°C, where the highest value seen is through the RCM at 0.8°C, and the lowest temperature was simulated from morphed data, which had a median annual average of -0.9°C. The comparatively wet conditions simulated using raw RCM climate data resulted in significant mould growth occurring relatively early on in the simulation and reaching a steady state around a mould index value of 4.5 for the rest of the study period. Contrastingly, no significant mould growth was seen when the hygrothermal simulations used other climate datasets.

The results of the bias corrected climate data indicate that a significant improvement is made from the raw RCM data. In this case, the annual total horizontal rainfall, annual average wind speed, relative humidity, temperature, DNI, and WDR compared better than the RCM. Hygrothermal simulations using pre-process climate data resulted in more accurate representations on the exterior of the OSB sheathing. Consequently, RCM simulations compares the worst against the observations, which overestimates the MC, MI, and RH on the OSB.

4.6.2 Projected Future Period

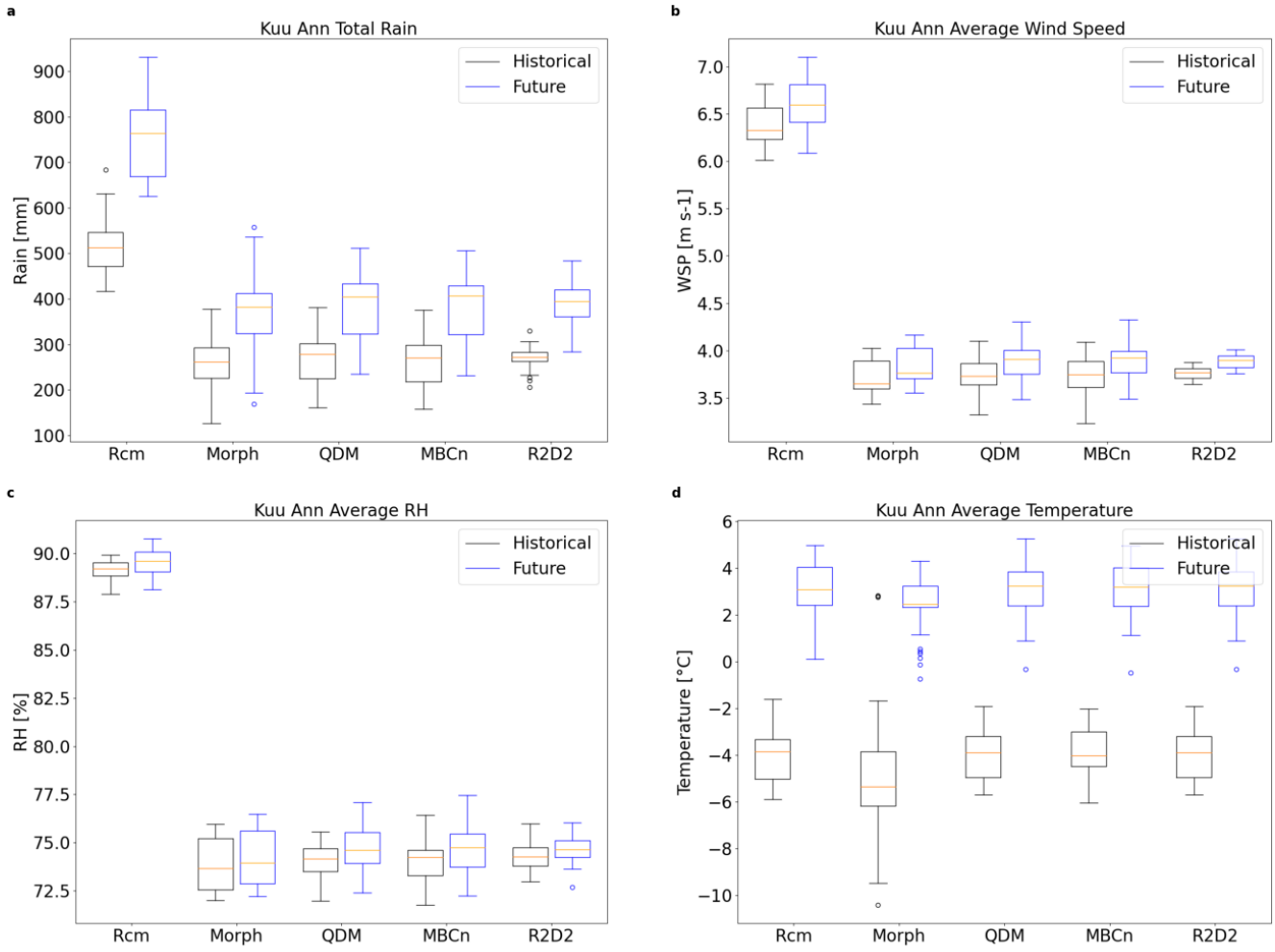

Figure 43. Kuujjuaq boxplots of annual total rain (a), and average wind speed (b), relative humidity (c), and temperature (d), over a baseline historical period from 1991-2021 and a future projected period from 2064-2094

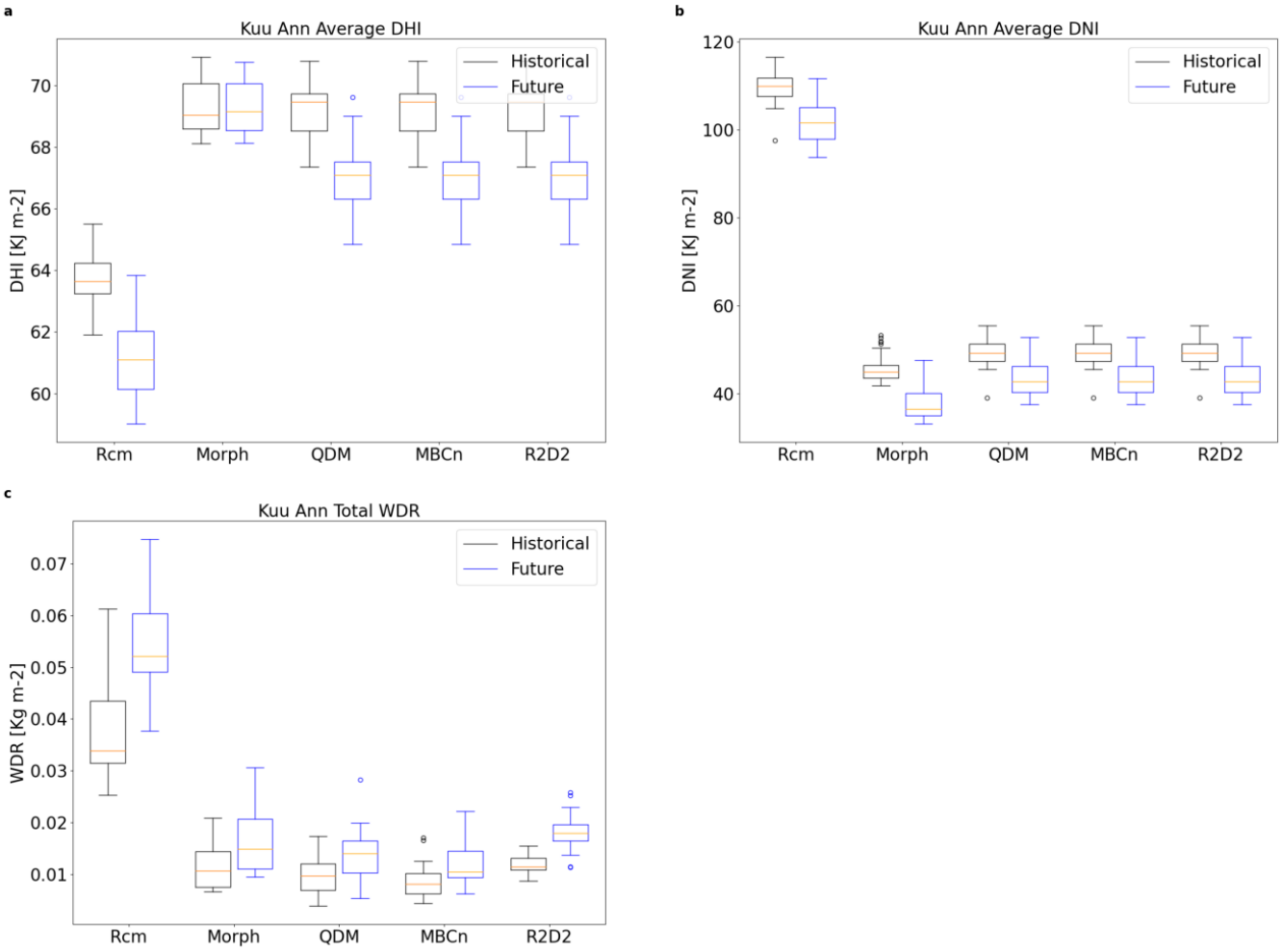

Figure 44. Kuujjuaq boxplots of annual average DHI (a), DNI (b), and WDR (c) over a historical (1991-2021) and future (2064-2094) period

Figure 43a shows the annual total rainfall in 1991-2021 and 2064-2094. According to the results in the validation period, the RCM is known to overestimate the amount of rainfall in Kuujjuaq. During the historical period, the RCM predicted a median annual total of 514mm, while the projected rainfall is forecast to increase by 49% to 764mm. Generally, processed data reduces the absolute amount of rainfall, but the relative different between the historical and future periods is similar, with a historical median annual total rainfall of approximately 270mm

and increasing to 400mm. RCM also overestimates the wind speed which falls from 6.3m/s to 3.7m/s calculated with morphed or bias corrected data. Wind speed is projected to increase in the future where processed datasets indicate a median around 3.9m/s. RCM simulated RH is extremely high compared to the corrected data with historical and future medians of 89.7%. On the other hand, corrected data indicates a median closer to 74% in both periods. Kuujjuaq is the coldest climate studied in this work, consequently it's the only location with sub-zero average temperatures, at least during the historical period before significant global warming effects. Calculations with RCM data indicate a historical median annual average temperature of -3.8°C, which is forecast to increase to 3.1°C. Similar estimates are made by QDM, MBCn, and R2D2, while morphed data presents colder conditions rising from -5.3°C to 2.47°C.

Figure 44a and b compares the historical and future DHI and DNI. As in the observational period, the solar irradiance variables generated by QDM are used in place of values calculated using the MBCn or R2D2 method as they do not preserve the diurnal cycle. According to morphed data, the median DHI does not change by much between the two periods, with a value of 69Kj/m^2. The morphing method was the only data to indicate an increase in DHI. RCM and QDM both forecast decreases in DHI. Considering that the RCM exaggerates the average DNI, the results are relatively consistent between the morphing and QDM methods which bring down the median value. With a historical median of 45Kj/m^2 and 49Kj/m^2, and 37Kj/m2 and 43Kj/m^2 during the projected period, respectively. Lastly, Figure 44c presents the annual total WDR during the historical and future periods. The magnitude of WDR forecast by RCM is the greatest in either time period, with a historical median of 0.0339Kg/m^2, which increases to 0.0521Kg/m^2. On the other hand, morphed and bias corrected data yield

historical values closer to 0.01Kg/m^2, which subsequently increases to approximately 0.014Kg/m^2.

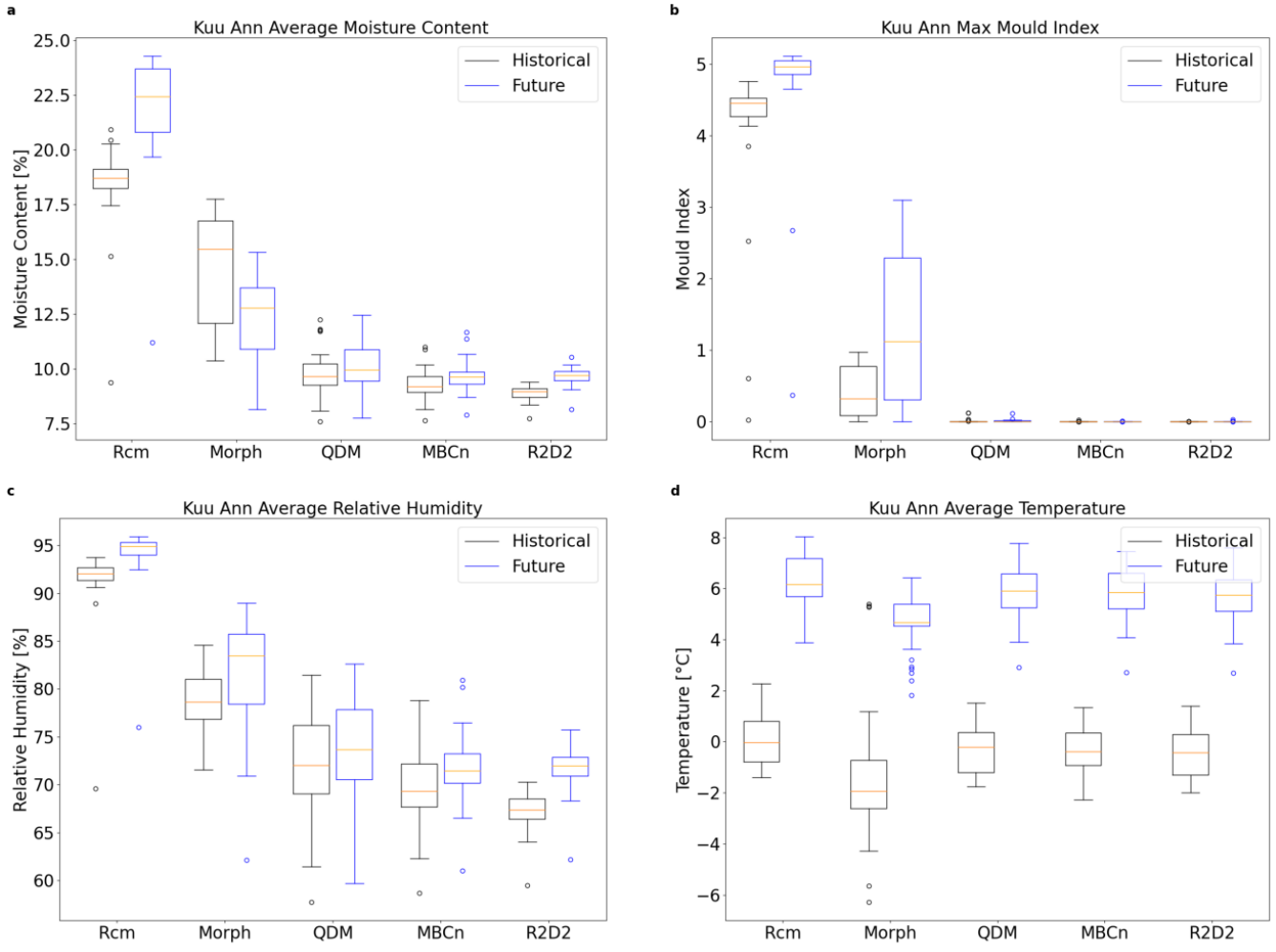

Figure 45. Kuujjuaq annual MC (a), RH (c), temperature (d), and maximum MI (b) of the OSB sheathing of the wall assembly, for a historical (1991-2021) and future (2064-2094) period

A comparison of the simulated hygrothermal response is presented in Figure 45, where the MC, MI, RH, and temperature is analyzed. The differences in moisture content between the historical and future period, as a percentage of mass of the OSB, is presented in Figure 45a. Due

to the significantly higher amounts of deposited WDR on the OSB, the hygrothermal simulations with RCM data present the highest MC with a historical median of 18.7%, subsequently increasing to 22.4%. Therefore, simulation with RCM data is the only set that indicates potential deterioration of the OSB. Bias corrected data shows lower MC in the OSB with historical values around 9.5% and future median annual averages of 9.8%. Contrastingly, morphed data indicates a decrease in MC from a median of 15.7% to 12.8%. An analysis of the mould growth in Kuujjuaq during the validation period indicated that little to no mould growth should occur in the during the historical period. Howeverer, RCM data results in significant mould growth during this period, which worsens in the future, going from a median of 4.5 to 4.9 in annual maximum mould index. This is a consequence of the increased RH and temperature, which increase the conditions conducive to mould growth. Morphed data predicts moderate levels of mould growth in the historical period with a median value of 0.3, subsequently increasing to 1.1 following 3.5°C of global warming. Bias corrected datasets do not show any significant mould growth in either time periods. RH and temperature are both forecast to increase in this climate change scenario, where the annual average temperature on the exterior of the OSB is shown in Figure 45d. RCM and bias corrected data yield similar results in both historical and future time periods, starting with approximately -0.3°C and subsequently rising to 6°C. Morphed data exhibit overall lower temperatures with a historical median of -1.9°C and rising to 4.7°C. There is more variability between the datasets when simulating the RH on the OSB. For example, raw RCM data predict the highest RH at 92.1% historically and rising to 95.8%. On the other hand, morphed predicts a lower RH with a historical median of 78.6% and increasing to 83.5%. R2D2 data simulated the lowest RH by far where it increases from 67.5% to 72.1%.

4.7 Summary

This chapter investigated the different climatic conditions presented by observed, modelled, and processed climate datasets and their impacts on the hygrothermal performance of a wood-frame wall assembly through DELPHIN simulations. Climate parameters at 6 cities such as the rainfall, windspeed, relative humidity, temperature, and solar radiation were used to judge the accuracy of the various climate data generation methods. A summary of the median annual average values calculated with the 6 datasets over the validation period is presented in Table 9 at each of the studied locations. Through boxplots of the annual average climate parameters, it was shown that the bias correction methods, QDM, MBCn, and R2D2 corrects for the bias in the mean in raw RCM data, resulting in a more accurate set of data when comparing annual averages to the observations during the validation period. The morphing method compares as well as the others, however, this is largely due to the nature of how morphed data is calculated. By using the observational data as a basis for morphing data, this process ensures that morphed data will yield similar results to the observations, especially during the validation period.

Table 9. Summary of median annual average climate variables during the validation period

OTTAWA	**Obs**	**Rcm**	**Morph**	**QDM**	**MBCn**	**R2D2**
Rain [mm]	713	899	680	700	712	770
Wind Speed [m/s]	3.8	3.6	4.1	3.9	3.9	4.0
Relative Humidity [%]	71.9	79.0	72.6	73.5	73.5	73.0
Temperature [°C]	7.1	8.6	5.8	6.6	6.8	6.6
GHI [Kj m-2]	556	1105	548	568	568	568
MONTREAL	**Obs**	**Rcm**	**Morph**	**QDM**	**MBCn**	**R2D2**
Rain [mm]	693	972	755	801	796	849
Wind Speed [m s-1]	4.4	4.4	4.4	4.4	4.4	4.4
Relative Humidity [%]	69.0	80.6	68.8	69.4	69.1	68.9
Temperature [°C]	7.8	8.8	6.8	7.5	7.4	7.5
GHI [Kj m-2]	552	1103	549	568	568	568
ST. JOHN'S	**Obs**	**Rcm**	**Morph**	**QDM**	**MBCn**	**R2D2**
Rain [mm]	654	1062	675	681	675	726
Wind Speed [m s-1]	6	9	7	7	7	7
Relative Humidity [%]	83	84	82	82	82	82
Temperature [°C]	5	7	5	5	5	5
GHI [Kj m-2]	454	1067	465	469	469	469
CALGARY	**Obs**	**Rcm**	**Morph**	**QDM**	**MBCn**	**R2D2**
Rain [mm]	274	515	336	339	334	341
Wind Speed [m s-1]	3.9	4.6	3.7	3.8	3.8	3.9
Relative Humidity [%]	62.5	79.5	62.4	62.4	62.3	62.1
Temperature [°C]	4.9	4.6	4.3	5.3	5.3	5.3
GHI [Kj m-2]	542	1009	547	565	565	565
VANCOUVER	**Obs**	**Rcm**	**Morph**	**QDM**	**MBCn**	**R2D2**
Rain [mm]	1371	1795	1188	1329	1332	1385
Wind Speed [m s-1]	3.7	4.1	3.7	3.7	3.7	3.8
Relative Humidity [%]	79.4	87.8	79.1	78.4	78.5	78.2
Temperature [°C]	10.4	8.1	10.3	10.9	10.9	10.9
GHI [Kj m-2]	515	1041	523	531	531	531
KUUJJUAQ	**Obs**	**Rcm**	**Morph**	**QDM**	**MBCn**	**R2D2**
Rain [mm]	276	522	269	268	266	282
Wind Speed [m s-1]	3.8	6.4	3.7	3.9	3.9	3.8
Relative Humidity [%]	73.8	89.3	73.7	74.3	74.3	74.1
Temperature [°C]	-4.0	-3.2	-4.1	-3.2	-3.4	-3.2
GHI [Kj m-2]	404	888	409	428	428	428

The accuracy of the different climate datasets on the hygrothermal performance of the simulated wall assembly are examined through several parameters including the moisture content of the OSB, mould index, relative humidity, and temperature on the exterior of the OSB sheathing. A summary of the average hygrothermal conditions during the validation period at various locations is presented in Table 10. The results indicated that despite relatively accurate mean climatic conditions produced by morphing and BC, small variations can result in significant differences in the simulated hygrothermal performance of the wall assembly. Since the exposure time is a critical factor that influencing the mould growth, the mould growth risk is poorly characterized by bias corrected data.

A similar analysis during two periods separated by 3.5°C of global warming was conducted to examine the impacts of the various data generation methods on climate change and hygrothermal performance. The consequences of climate change on the climate parameters are illustrated in Table 11 for the RCM, morphed, and bias corrected data. This table shows that the morphing and BC methods are able to capture the projected changes in climate conditions simulated by the RCM, however a difference in the annual averages are observed. As a consequence of climate change, the moisture loads are expected to increase across all the studied locations, resulting in increased mould growth and wood decay risk due to excessive moisture in the OSB, which can be seen in Table 12.

Table 10. Summary of median annual average hygrothermal results during the validation period

OTTAWA	**Obs**	**Rcm**	**Morph**	**QDM**	**MBCn**	**R2D2**
MC [%]	11.1	8.7	15.3	8.9	9.8	10.3
MI	0.8	0.0	1.2	0.0	0.0	0.0
Relative Humidity [%]	79.0	66.7	82.6	67.6	73.0	75.3
Temperature [°C]	10.5	14.4	11.1	11.1	11.0	10.6
MONTREAL	**Obs**	**Rcm**	**Morph**	**QDM**	**MBCn**	**R2D2**
MC [%]	11.3	10.5	14.4	8.9	9.2	10.3
MI	0.9	0.9	1.0	0.0	0.0	0.0
Relative Humidity [%]	79.6	75.7	81.5	67.8	69.9	75.2
Temperature [°C]	10.8	14.4	11.3	11.7	11.5	11.0
ST. JOHN'S	**Obs**	**Rcm**	**Morph**	**QDM**	**MBCn**	**R2D2**
MC [%]	19.4	19.7	23.1	10.9	17.2	19.9
MI	4.6	5.0	4.9	0.0	4.1	4.7
Relative Humidity [%]	93.7	94.2	92.8	78.0	91.9	94.1
Temperature [°C]	7.3	9.6	6.7	8.1	7.7	7.5
CALGARY	**Obs**	**Rcm**	**Morph**	**QDM**	**MBCn**	**R2D2**
MC [%]	7.4	9.7	7.2	7.6	7.1	7.0
MI	0.0	1.7	0.0	0.0	0.0	0.0
Relative Humidity [%]	57.4	71.8	53.5	57.8	53.4	53.1
Temperature [°C]	7.5	9.2	7.1	8.9	8.9	8.6
VANCOUVER	**Obs**	**Rcm**	**Morph**	**QDM**	**MBCn**	**R2D2**
MC [%]	21.4	24.2	20.2	23.1	20.3	19.8
MI	5.2	5.3	5.0	5.3	5.2	5.0
Relative Humidity [%]	95.6	97.6	94.1	96.7	95.5	95.4
Temperature [°C]	12.1	10.9	12.1	12.8	12.6	12.0
KUUJJUAQ	**Obs**	**Rcm**	**Morph**	**QDM**	**MBCn**	**R2D2**
MC [%]	10.0	19.0	12.7	9.7	9.0	9.0
MI	5.2	5.3	5.0	5.3	5.2	5.0
Relative Humidity [%]	95.6	97.6	94.1	96.7	95.5	95.4
Temperature [°C]	12.1	10.9	12.1	12.8	12.6	12.0

Table 11. Summary of median annual average climate variables during the future projected period

OTTAWA	**Rcm**	**Morph**	**QDM**	**MBCn**	**R2D2**
Rain [mm]	1073	817	820	812	943
Wind Speed [m/s]	3.6	4.0	3.9	3.9	3.9
Relative Humidity [%]	81.4	74.8	74.7	74.7	75.4
Temperature [°C]	13.5	10.8	12.0	12.0	12.0
GHI [Kj m-2]	1105	539	561	561	561
MONTREAL	**Rcm**	**Morph**	**QDM**	**MBCn**	**R2D2**
Rain [mm]	1177	960	918	902	1010
Wind Speed [m s-1]	4.3	4.2	4.3	4.3	4.3
Relative Humidity [%]	82.4	70.7	70.3	70.3	71.0
Temperature [°C]	13.9	11.9	12.8	12.8	12.8
GHI [Kj m-2]	1103	540	562	562	562
ST. JOHN'S	**Rcm**	**Morph**	**QDM**	**MBCn**	**R2D2**
Rain [mm]	1181	767	741	736	789
Wind Speed [m s-1]	8.6	6.6	6.5	6.6	6.6
Relative Humidity [%]	84.7	82.5	82.0	81.8	82.2
Temperature [°C]	11.1	9.7	10.0	10.1	10.0
GHI [Kj m-2]	1067	473	479	479	479
CALGARY	**Rcm**	**Morph**	**QDM**	**MBCn**	**R2D2**
Rain [mm]	633	404	413	402	405
Wind Speed [m s-1]	4.4	3.6	3.7	3.7	3.7
Relative Humidity [%]	80.4	63.1	63.7	63.3	63.4
Temperature [°C]	8.9	8.4	9.6	9.6	9.6
GHI [Kj m-2]	1009	536	550	550	550
VANCOUVER	**Rcm**	**Morph**	**QDM**	**MBCn**	**R2D2**
Rain [mm]	1966	1303	1416	1423	1527
Wind Speed [m s-1]	4.0	3.6	3.5	3.5	3.6
Relative Humidity [%]	87.9	79.2	78.5	78.4	78.4
Temperature [°C]	12.0	14.3	14.8	14.8	14.8
GHI [Kj m-2]	1041	531	547	547	547
KUUJJUAQ	**Rcm**	**Morph**	**QDM**	**MBCn**	**R2D2**
Rain [mm]	764	382	405	407	394
Wind Speed [m s-1]	6.6	3.8	3.9	3.9	3.9
Relative Humidity [%]	89.6	74.0	74.6	74.8	74.6
Temperature [°C]	3.1	2.5	3.3	3.2	3.3
GHI [Kj m-2]	888	381	397	397	397

Table 12. Summary of median annual average hygrothermal results during the future projected period

OTTAWA	**Rcm**	**Morph**	**QDM**	**MBCn**	**R2D2**
MC [%]	9.6	25.1	9.5	10.4	11.2
MI	0.0	5.0	0.0	0.1	1.0
Relative Humidity [%]	71.0	89.9	70.5	74.9	78.1
Temperature [°C]	18.3	12.6	14.9	14.9	14.5
MONTREAL	**Rcm**	**Morph**	**QDM**	**MBCn**	**R2D2**
MC [%]	11.7	21.7	9.2	9.5	10.6
MI	2.7	4.6	0.0	0.0	0.0
Relative Humidity [%]	78.4	86.9	69.3	70.3	75.9
Temperature [°C]	18.2	13.5	15.6	15.4	15.2
ST. JOHN'S	**Rcm**	**Morph**	**QDM**	**MBCn**	**R2D2**
MC [%]	19.0	34.6	10.9	16.3	20.4
MI	5.2	5.2	0.1	4.6	5.0
Relative Humidity [%]	93.2	95.4	77.5	89.7	94.3
Temperature [°C]	14.4	11.6	12.5	12.3	12.0
CALGARY	**Rcm**	**Morph**	**QDM**	**MBCn**	**R2D2**
MC [%]	10.7	11.5	7.6	7.2	7.2
MI	3.4	0.0	0.0	0.0	0.0
Relative Humidity [%]	75.2	63.6	58.6	55.5	54.9
Temperature [°C]	13.2	10.7	12.9	12.8	12.6
VANCOUVER	**Rcm**	**Morph**	**QDM**	**MBCn**	**R2D2**
MC [%]	27.1	24.0	22.9	19.3	19.7
MI	5.3	5.2	5.3	5.2	5.1
Relative Humidity [%]	94.9	93.3	94.4	92.1	92.6
Temperature [°C]	15.7	15.9	16.9	16.9	16.5
KUUJJUAQ	**Rcm**	**Morph**	**QDM**	**MBCn**	**R2D2**
MC [%]	22.4	12.8	10.0	9.6	9.7
MI	5.0	1.1	0.0	0.0	0.0
Relative Humidity [%]	94.9	83.5	73.7	71.4	72.0
Temperature [°C]	6.2	4.7	5.9	5.9	5.8

Among the various locations, Vancouver expectantly proved to be the wettest climate, with the most rainfall during the validation, historical, and future periods. Consequently, the amount of WDR deposited on the OSB sheathing in Vancouver is the greatest. As a result of that, the overall moisture performance of the wood-frame wall assembly simulated in Vancouver is the worst by far on account of the excessive moisture in the OSB leading to deterioration, and the large amount of mould growth with a MI of 5, covering more than 50% of the surface. These conditions are further exacerbated by climate change which leads to additional moisture loading and further deterioration of the OSB. However, mould conditions remain relatively unchanged compared to the historical conditions.

In the drier but colder climates of Ottawa and Montreal, the total amount of rainfall and thus deposited WDR is significantly less than that of Vancouver. Therefore, the performance indicated by MC and MI are less severe. During the validation period, in both cases, the MC in the OSB is within an acceptable range and does not exceed the critical threshold of 16% of the mass of the OSB sheathing. Similarly, while the mould growth on the exterior of the OSB is not negligible, the calculated mould index of 2 suggests only minimal growth which is not visually detectable yet. Additionally, due to climate change, both Ottawa and Montreal will experience increased rainfall, RH, and temperature. Consequently, the hygrothermal performance of the wall assembly will experience worsening moisture conditions, resulting in more mould growth and MC in the OSB. In an even colder climate such as that in St. John's, the RH is historically already quite high. Therefore, during the baseline validation period, MC and mould growth are significantly higher than that found in Montreal or Ottawa, where deterioration due to excessive moisture in the OSB should be expected, and mould growth covers over half of the

surface. The effects of climate change in St. John's are similar to that of other locations, where increased rainfall leads to declining moisture performance overall.

The cold and dry climate of Calgary results in ideal conditions for hygrothermal performance in terms of the MC and MI. During the baseline validation period, the relatively low temperature, RH, and rainfall results in minimal mould growth, where the MI does not even exceed 1 in most cases. Similarly, due to the low rainfall and consequently small amount of deposited WDR on the OSB, the MC of the OSB sheathing during this period will not lead to deteriorate. As with other locations, climate change will cause increased moisture loading in Calgary. Despite simulations showing increased MC and MI in the future, the changes do not reach critical levels since the baseline is so low. Kuujjuaq is the only location studied with sub-zero annual average temperatures, making it the coldest city examined in this work. The cold and dry conditions in Kuujjuaq leads to similar hygrothermal performance to that in Calgary. Therefore, during the baseline validation period, MC and mould growth is not a problem. And despite the similar impacts of climate change on the climatic conditions in Kuujjuaq to those of other cities, the moisture performance of the simulated wall assembly will not be severely affected by the increases in moisture loads in the future.

5.0 Conclusions

The objective of this work was to assess the value that different climate data generation methods have on the effects of hygrothermal performance on a wood-frame wall of relatively common construction in Canada; and to examine the potential effects of climate change on the hygrothermal performance of the wall assemblies. 6 cities were included in the analysis: Ottawa, Montreal, St. John's, Calgary, Vancouver, and Kuujjuaq, representing different climates across Canada. To achieve this goal, multiple climate data processing methods (morph, QDM, MCBn, and R2D2) were performed on hourly climate data from CanRCM4 for three periods of interest. First, a 20-year validation period spanning 1998-2017, where sufficient hourly observational climate data is available and can be compared to the bias corrected results. As well as two 30-year periods, the first representing a historical baseline from 1991-2021, and a future projected period from 2064-2094 which coincide with an increase of 3.5°C in average global temperatures. 1-D hygrothermal simulations through DELPHIN were performed to evaluate the impacts of each of the data processing techniques.

During the validation period, results of the bias corrected climate data indicate that an improvement is made compared to the raw RCM data, although the degree of success varies depending on the chosen method and climate variable. In this case, the annual total horizontal rainfall, annual average wind speed, relative humidity, temperature, solar irradiance, and WDR were examined. Generally, the RCM is seen to overestimate the amount of total annual horizontal rainfall and average solar radiation in the form of GHI, in comparison to observations. For example, in Vancouver, the median annual average total rainfall was around 1400mm, but RCM data calculated a median closer to 1800mm. Similarly, GHI is severely

overestimated at all locations, often by 500Kj/m^2 or more. Therefore, overall, the climatic variables presented by raw RCM data compares the worst against the observations; while the bias corrected data adequately correct for biases in the RCM, which result in better agreement with the observations. Similarly, morphed results typically perform as well as bias corrected data during the validation periods in terms of annual means. However, morphed data does not necessarily reduce the bias present in RCM data since changes are applied to the observational dataset, whereas bias correction methods adjust RCM data instead. These difference in data processing techniques have significant impacts on the hygrothermal assessments.

Hygrothermal performance of the various climate datasets were simulated using DELPHIN. The results included the relative humidity, temperature, moisture content and mould index on the OSB sheathing. The hygrothermal simulations resulted in some variability between the datasets, but the accuracy of the climate data was indicative of the hygrothermal performance. RCM data consistently compares the poorest against the observations in each of the studied parameters. For instance, due to the large deviations in climatic parameters in the RCM compared to observations, the hygrothermal simulation in Calgary resulted in an average mould index of 2 across the whole validation period, according to RCM climate data, whereas none of the other datasets predicted any at all. The other datasets, morph, QDM, MBCn, and R2D2 present reasonably accurate results for RH and temperature on the exterior of the OSB. However, for complex variables such as the MC and MI, which takes into consideration many different climatic conditions, there is varying degrees of success in the correction of climate data. Most notably, QDM, MBCn, and R2D2 often fail to replicate the same degree of mould growth present in the simulation with observational data. However, the morphing method is

somewhat able to reproduce the mould growth profile in the simulation. The relative success of the morphing method is strongly associated with the fact that RCM data used to calculate the morphing factors are very close to the observational period in time, and therefore, the calculated morphing factors are minimal. Consequently, applying these relatively small morphing factors to the observational data result in only slight differences which affect the mean, but the variance in time is largely identical to the original dataset, resulting in similar mould growth profiles. This shows that the actual time series of the climatic variables is another important parameter to consider.

In the absence of observed climate data, it is difficult to judge which dataset yields the most accurate simulations in absolute terms when considering the historical and future time periods. However, the relative trends can be used to examine how climate change will affect hygrothermal performance in the future. Under 3.5°C of global warming with reference to the historical 1991-2021 period, all the examined locations will experience warmer and wetter climatic conditions. According to the RCM, average rainfall will increase by at least 9% in Vancouver, while the largest gain is seen in Kuujjuaq with an estimated increment of 49%. Consequently, simulated MC of the OSB will increase due to rising amounts of deposited WDR. For historically wet climates like Vancouver the conditions will be further exacerbated, with MC increasing from 24% to 27%. As a result of increasing RH and temperature, conditions favourable for mould growth will also become more prevalent in the future, resulting in increased mould growth risks. For Ottawa and Montreal, this change in climate results in a transition from little to no observable mould growth (MI=2), to conditions where mould growth could be visually detected (MI=>3). Overall, moisture loads are expected to increase in the

future due to climate change; consequently, this will reduce the durability of these types of wood-frame walls in the studied locations.

As seen during the validation periods, QDM, MBCn, and R2D2 bias corrected datasets are applicable in reducing the bias in the raw RCM data in terms the mean. However, these methods generally do not replicate the temporal variability seen in the observational dataset, which is evident from the mould index profiles. On the other hand, simulations with morphed data are limited to historically observed weather events and do not allow for new sequences of events to occur. Consequently, imposing a historical variance on the future projected climate results in some conflicting outcomes in the hygrothermal performance of the wall assembly, despite agreement in the mean of climatic parameters calculated with bias corrected data.

One of the limitations in the proposed work arises from the time-series shuffling introduced by the multivariate bias correction methods, MBCn and R2D2, where the resulting corrected solar radiation variables are not suitable for use in hygrothermal simulations. Consequently, QDM corrected solar radiation is substituted in place of these values, because QDM leaves the diurnal cycle intact. For this reason, the effects of the multivariate bias correction methods on the hygrothermal performance of the simulated wall assembly could be muted. Another limitation arises from the fact that the orientation of the wall assembly was chosen based on the side with the most WDR during the 1998-2017 period using observational data. Therefore, in this setup, the WDR calculated with observational data will typically compare higher than other datasets. Future work should include simulations with the wall facing different orientations to better examine the impacts of the different climate data generation methods.

Lastly, tshe CanRCM4 database, from which hourly climate model data was obtained for this work, consists of 15 ensemble members where each is the product of slightly perturbed physics parameterizations. Importantly, these 15 members should be view as equally likely scenarios for future projections. However, for this work, only one member of the ensemble was chosen since this was sufficient in examining the relative differences in hygrothermal performance between the various data generation methods. But in order to more accurately study the climate change impacts, future work should incorporate all 15 members of the ensemble into the analysis to ensure the observed climate change signal is robust.

References

[1] Dukhan, T., & Sushama, L. (2021). Understanding and modelling future wind-driven rain loads on building envelopes for Canada. Building and Environment, 196, 107800. https://doi.org/10.1016/j.buildenv.2021.107800

[2] Hukka, A., & Viitanen, H. A. (1999). A mathematical model of mould growth on wooden material. Wood Science and Technology : Journal of the International Academy of Wood Science, 33(6), 475–485. https://doi.org/10.1007/s002260050131

[3] Viitanen, H., Toratti, T., Makkonen, L., Peuhkuri, R., Ojanen, T., Ruokolainen, L., & Raisanen, J. (2010). Towards modelling of decay risk of wooden materials. European Journal of Wood and Wood Products, 68(3), 303–313. https://doi.org/10.1007/s00107-010-0450-x

[4] Blocken, B., & Carmeliet, J. (2008). Guidelines for the required time resolution of meteorological input data for wind-driven rain calculations on buildings. Journal of Wind Engineering & Industrial Aerodynamics, 96(5), 621–639. https://doi.org/10.1016/j.jweia.2008.02.008

[5] Siu, C. Y., Wang, Y. Y., & Liao, Z. (2019). Impact of temperature and moisture dependent conductivity of building insulation materials on estimating heating and cooling load using typical and historical weather data. IOP Conference Series: Materials Science and Engineering, 609(7), 072017. https://doi.org/10.1088/1757-899x/609/7/072017

[6] Belcher, S. E., Hacker, J. N., & Powell, D. S. (2005). Constructing design weather data for future climates. Building Services Engineering Research and Technology, 26(1), 49–61. https://doi.org/10.1191/0143624405bt112oa

[7] Jentsch, M. F., Bahaj, A. B. S., & James, P. A. B. (2008). Climate change future proofing of buildings—generation and assessment of building simulation weather files. Energy & Buildings, 40(12), 2148–2168. https://doi.org/10.1016/j.enbuild.2008.06.005

[8] de Wilde, P., & Coley, D. (2012). The implications of a changing climate for buildings. Building and Environment, 55, 1–7. https://doi.org/10.1016/j.buildenv.2012.03.014

[9] Dear, R. D. (2006). Adapting buildings to a changing climate: But what about the occupants? Building Research & Information, 34(1), 78–81. https://doi.org/10.1080/09613210500336594

[10] Guan, L. (2009). Preparation of future weather data to study the impact of climate change on buildings. Building and Environment, 44(4), 793–800. https://doi.org/10.1016/j.buildenv.2008.05.021

[11] Nik, V. M. (2017). Application of typical and extreme weather data sets in the hygrothermal simulation of building components for future climate - a case study for a wooden frame wall. Energy & Buildings, 154, 30–45. https://doi.org/10.1016/j.enbuild.2017.08.042

[12] Palmer, T. N., & Weisheimer, A. (2011). Diagnosing the causes of bias in climate models – why is it so hard? Geophysical & Astrophysical Fluid Dynamics, 105(2-3), 351–365. https://doi.org/10.1080/03091929.2010.547194

[13] Jun, M., Knutti, R., & Nychka, D. W. (2008). Spatial analysis to quantify numerical model bias and dependence. Journal of the American Statistical Association, 103(483), 934–947. https://doi.org/10.1198/016214507000001265

[14] Lafon, T., Dadson, S., Buys, G., & Prudhomme, C. (2013). Bias correction of daily precipitation simulated by a regional climate model: a comparison of methods. International Journal of Climatology, 33(6), 1367–1381. https://doi.org/10.1002/joc.3518

[15] Luo, M., Liu, T., Meng, F., Duan, Y., Frankl, A., Bao, A., & De Maeyer, P. (2018). Comparing bias correction methods used in downscaling precipitation and temperature from regional climate models: a case study from the kaidu river basin in western china. Water, 10(8), 1046–1046. https://doi.org/10.3390/w10081046

[16] Fang, G. H., Yang, J., Chen, Y. N., & Zammit, C. (2015). Comparing bias correction methods in downscaling meteorological variables for a hydrologic impact study in an arid area in china. Hydrology and Earth System Sciences, 19(6), 2547–2559. https://doi.org/10.5194/hess-19-2547-2015

[17] Gaur, A., Lacasse, M., & Armstrong, M. (2019). Climate data to undertake hygrothermal and whole building simulations under projected climate change influences for 11 canadian cities. Data, 4(2), 72–72. https://doi.org/10.3390/data4020072

[18] Straube, J., & Burnett, E. (2001). Overview of hygrothermal (HAM) analysis methods. Moisture analysis and condensation control in building envelopes, 81-89.

[19] Hens, H. (2002). Heat, air and moisture transfer in highly insulated building envelopes (Hamtie) (p. 22). FaberMaunsell Limited.

[20] Maref, W., Kumaran, K., Lacasse, M. A., Swinton, M. C., & van Reenen, D. (2002). Laboratory measurements and benchmarking of an advanced Hygrothermal model.

Proceeding of International Heat Transfer Conference 12. https://doi.org/10.1615/ihtc12.720

[21] Kalamees, T., & Vinha, J. (2003). Hygrothermal calculations and laboratory tests on timber-framed wall structures. Building and Environment, 38(5), 689–697. https://doi.org/10.1016/S0360-1323(02)00207-X

[22] Delgado, J. M., Ramos, N. M., Barreira, E., & de Freitas, V. P. (2010). A critical review of HYGROTHERMAL models used in porous building materials. Journal of Porous Media, 13(3), 221–234. https://doi.org/10.1615/jpormedia.v13.i3.30

[23] Djebbar, R., Mukhopadhyaya, P., & Kumaran, M. K. (2002). Retrofit Strategies for a High-Rise Wall System and Analyses of their Hygrothermal Effects. In Proceedings of the 11th symposium for building physics, Dresden, Germany (pp. 738-46).

[24] Zhou, X., Derome, D., & Carmeliet, J. (2017). Hygrothermal modeling and evaluation of freeze-thaw damage risk of masonry walls retrofitted with internal insulation. Building and Environment, 125, 285–298. https://doi.org/10.1016/j.buildenv.2017.08.001

[25] Zhou, X., Carmeliet, J., & Derome, D. (2020). Assessment of risk of freeze-thaw damage in internally insulated masonry in a changing climate. Building and Environment, 175. https://doi.org/10.1016/j.buildenv.2020.106773

[26] Mukhopadhyaya, P., Kumaran, K., Tariku, F., & Van Reenen, D. (2006). Application of hygrothermal modeling tool to assess moisture response of exterior walls. Journal of architectural engineering, 12(4), 178-186.

[27] McClung, R., Ge, H., Straube, J., & Wang, J. (2014). Hygrothermal performance of cross-laminated timber wall assemblies with built-in moisture: field measurements and

simulations. Building and Environment, 71, 95–110. https://doi.org/10.1016/j.buildenv.2013.09.008

[28] Wang, L., & Ge, H. (2016). Hygrothermal performance of cross-laminated timber wall assemblies: a stochastic approach. Building and Environment, 97, 11–25. https://doi.org/10.1016/j.buildenv.2015.11.034

[29] Vololonirina, O., Coutand, M., & Perrin, B. (2014). Characterization of hygrothermal properties of wood-based products - impact of moisture content and temperature. Construction and Building Materials, 63, 223–233. https://doi.org/10.1016/j.conbuildmat.2014.04.014

[30] Sedlbauer, K. (2002). Prediction of mould growth by hygrothermal calculation. Journal of Thermal Envelope and Building Science, 25(4), 321–336. https://doi.org/10.1177/0075424202025004093

[31] Johansson, P., Svensson, T., & Ekstrand-Tobin, A. (2013). Validation of critical moisture conditions for mould growth on building materials. Building and Environment, 62, 201–209. https://doi.org/10.1016/j.buildenv.2013.01.012

[32] Gradeci, K., Kohler, J., Labonnote, N., Time, B., & 11th Nordic Symposium on Building Physics, NSB 2017 11 2017 06 11 - 2017 06 14. (2017). Mould models applicable to wood-based materials-a generic framework. Energy Procedia, 132, 177–182. https://doi.org/10.1016/j.egypro.2017.09.751

[33] Fedorik, F., & Illikainen, K. (2013). Ham and mould growth analysis of a wooden wall. International Journal of Sustainable Built Environment, 2(1), 19–26. https://doi.org/10.1016/j.ijsbe.2013.09.002

[34] Viitanen, H., & Ojanen, T. (2007). Improved model to predict mold growth in building materials. Thermal Performance of the Exterior Envelopes of Whole Buildings X–Proceedings CD, 2-7.

[35] Bindoff, N.L.; Stott, P.A.; Achuta Rao, K.M.; Allen, M.R.; Gillett, N.; Gutzler, D.; Hansingo, K.; Hegerl, G.; Hu, Y.; Jain, S.; et al. (2013). Detection and Attribution of Climate Change: From Global to Regional. Climate Change 2013: The Physical Science Basis. Contribution of Working Group I to the Fifth Assessment Report of the Intergovernmental Panel on Climate Change.

[36] Collins, M.; Knutti, R.; Arblaster, J.; Dufresne, J.-L.; Fichefet, T.; Friedlingstein, P.; Gao, X.; Gutowski,W.J.; Johns, T.; Krinner, G.; et al. (2013). Long-term Climate Change: Projections, Commitments and Irreversibility. Climate Change 2013: The Physical Science Basis. Contribution of Working Group I to the Fifth Assessment Report of the Intergovernmental Panel on Climate Change.

[37] Zhang, X., Flato, G., Kirchmeler, M., Vincent, L., Wan, H., Wang, X., Rong, R., Fyfe, J., Li, G., & Kharin, V. V. (2019). Temperature and precipitation across Canada. https://doi.org/10.4095/327811

[38] Detlef, P. van V., Jae, E., Mikiko, K., Keywan, R., Allison, T., Kathy, H., George, C. H., Tom, K., Volker, K., Jean-Francois, L., Toshihiko, M., Malte, M., Nebojsa, N., Steven, J. S., & Steven, K. R. (2011). The representative concentration pathways: an overview. Climatic Change, 109(1-2), 5–5. https://doi.org/10.1007/s10584-011-0148-z

[39] Gaterell, M. R., & McEvoy, M. E. (2005). The impact of climate change uncertainties on the performance of energy efficiency measures applied to dwellings. Energy & Buildings, 37(9), 982–995. https://doi.org/10.1016/j.enbuild.2004.12.015

[40] Jentsch, M. F., Bahaj, A. B. S., & James, P. A. B. (2008). Climate change future proofing of buildings—generation and assessment of building simulation weather files. Energy & Buildings, 40(12), 2148–2168. https://doi.org/10.1016/j.enbuild.2008.06.005

[41] Berger, T., Amann, C., Formayer, H., Korjenic, A., Pospischal, B., Neururer, C., & Smutny, R. (2014). Impacts of climate change upon cooling and heating energy demand of office buildings in vienna, austria. Energy & Buildings, 80, 517–530. https://doi.org/10.1016/j.enbuild.2014.03.084

[42] Wan, K. K. W., Li, D. H. W., Pan, W., & Lam, J. C. (2012). Impact of climate change on building energy use in different climate zones and mitigation and adaptation implications. Applied Energy, 97, 274–282. https://doi.org/10.1016/j.apenergy.2011.11.048

[43] Wang, X., Chen, D., & Ren, Z. (2010). Assessment of climate change impact on residential building heating and cooling energy requirement in australia. Building and Environment, 45(7), 1663–1682. https://doi.org/10.1016/j.buildenv.2010.01.022

[44] Zmeureanu, R., & Renaud, G. (2008). Estimation of potential impact of climate change on the heating energy use of existing houses. Energy Policy, 36(1), 303–310. https://doi.org/10.1016/j.enpol.2007.09.021

[45] Nik, V. M., & Sasic Kalagasidis, A. (2013). Impact study of the climate change on the energy performance of the building stock in stockholm considering four climate

uncertainties. Building and Environment, 60, 291–304. https://doi.org/10.1016/j.buildenv.2012.11.005

[46] Coley, D., & Kershaw, T. (2010). Changes in internal temperatures within the built environment as a response to a changing climate. Building and Environment, 45(1), 89–93. https://doi.org/10.1016/j.buildenv.2009.05.009

[47] Coley, D., Kershaw, T., & Eames, M. (2012). A comparison of structural and behavioural adaptations to future proofing buildings against higher temperatures. Building and Environment, 55, 159–166. https://doi.org/10.1016/j.buildenv.2011.12.011

[48] Ren, Z., Chen, Z., & Wang, X. (2011). Climate change adaptation pathways for australian residential buildings. Building and Environment, 46(11), 2398–2412. https://doi.org/10.1016/j.buildenv.2011.05.022

[49] Mavrogianni, A., Wilkinson, P., Davies, M., Biddulph, P., & Oikonomou, E. (2012). Building characteristics as determinants of propensity to high indoor summer temperatures in london dwellings. Building and Environment, 55, 117–130. https://doi.org/10.1016/j.buildenv.2011.12.003

[50] Lomas, K. J., & Giridharan, R. (2012). Thermal comfort standards, measured internal temperatures and thermal resilience to climate change of free-running buildings: a case-study of hospital wards. Building and Environment, 55, 57–72. https://doi.org/10.1016/j.buildenv.2011.12.006

[51] Gupta, R., & Gregg, M. (2012). Using uk climate change projections to adapt existing english homes for a warming climate. Building and Environment, 55, 20–42. https://doi.org/10.1016/j.buildenv.2012.01.014

[52] Wang, H., & Chen, Q. (2014). Impact of climate change heating and cooling energy use in buildings in the united states. Energy and Buildings, 82(C). https://doi.org/10.1016/j.enbuild.2014.07.034

[53] Grossi, C. M., Brimblecombe, P., & Harris, I. (2007). Predicting long term freeze-thaw risks on europe built heritage and archaeological sites in a changing climate. Science of the Total Environment, 377(2-3), 273–281. https://doi.org/10.1016/j.scitotenv.2007.02.014

[54] Kumar, P., & Imam, B. (2013). Footprints of air pollution and changing environment on the sustainability of built infrastructure. Science of The Total Environment, 444, 85–101. https://doi.org/10.1016/j.scitotenv.2012.11.056

[55] Talukdar, S., Banthia, N., & Grace, J. R. (2012). Carbonation in concrete infrastructure in the context of global climate change - part 1: experimental results and model development. Cement and Concrete Composites, 34(8), 924–930. https://doi.org/10.1016/j.cemconcomp.2012.04.011

[56] Nik, V. M., Sasic Kalagasidis, A., & Kjellström, E. (2012). Assessment of hygrothermal performance and mould growth risk in ventilated attics in respect to possible climate changes in sweden. Building and Environment, 55, 96–109. https://doi.org/10.1016/j.buildenv.2012.01.024

[57] Sehizadeh, A., & Ge, H. (2016). Impact of future climates on the durability of typical residential wall assemblies retrofitted to the passivehaus for the eastern canada region. Building and Environment, 97, 111–125. https://doi.org/10.1016/j.buildenv.2015.11.032

[58] Zhou, X., Derome, D., & Carmeliet, J. (2016). Robust moisture reference year methodology for hygrothermal simulations. Building and Environment, 110, 23–35. https://doi.org/10.1016/j.buildenv.2016.09.021

[59] Gaur, A., Lu, H., Lacasse, M., Ge, H., & Hill, F. (2021). Future projected changes in moisture index over canada. Building and Environment, 199. https://doi.org/10.1016/j.buildenv.2021.107923

[60] Robert Lisø, K., Olav Hygen, H., Kvande, T., & Vincent Thue, J. (2006). Decay potential in wood structures using climate data. Building Research & Information, 34(6), 546–551. https://doi.org/10.1080/09613210600736248

[61] Nik, V. M., Mundt-Petersen, S. O., Kalagasidis, A. S., & De Wilde, P. (2015). Future moisture loads for building facades in sweden: climate change and wind-driven rain. Building and Environment, 93, 362–375. https://doi.org/10.1016/j.buildenv.2015.07.012

[62] Nik, V. M., Sasic Kalagasidis, A., & Kjellström, E. (2012). Assessment of hygrothermal performance and mould growth risk in ventilated attics in respect to possible climate changes in sweden. Building and Environment, 55, 96–109. https://doi.org/10.1016/j.buildenv.2012.01.024

[63] Talukdar, S., Banthia, N., & Grace, J. R. (2012). Carbonation in concrete infrastructure in the context of global climate change - part 1: experimental results and model development. Cement and Concrete Composites, 34(8), 924–930. https://doi.org/10.1016/j.cemconcomp.2012.04.011

[64] Talukdar, S., Banthia, N., Grace, J. R., & Cohen, S. (2012). Carbonation in concrete infrastructure in the context of global climate change: part 2 - canadian urban

simulations. Cement and Concrete Composites, 34(8), 931–935. https://doi.org/10.1016/j.cemconcomp.2012.04.012

[65] Köliö, A., Pakkala, T. A., Lahdensivu, J., & Kiviste, M. (2014). Durability demands related to carbonation induced corrosion for finnish concrete buildings in changing climate. Engineering Structures, 62-63, 42–52. https://doi.org/10.1016/j.engstruct.2014.01.032

[66] Saha, M., & Eckelman, M. J. (2014). Urban scale mapping of concrete degradation from projected climate change. Urban Climate, 9, 101–114. https://doi.org/10.1016/j.uclim.2014.07.007

[67] Herrera, M., Natarajan, S., Coley, D. A., Kershaw, T., Ramallo-González, A. P., Eames, M., Fosas, D., & Wood, M. (2017). A review of current and future weather data for building simulation. Building Services Engineering Research and Technology, 38(5), 602–627. https://doi.org/10.1177/0143624417705937

[68] Eames, M., Kershaw, T., & Coley, D. (2010). On the creation of future probabilistic design weather years from UKCP09. Building Services Engineering Research and Technology, 32(2), 127–142. https://doi.org/10.1177/0143624410379934

[69] Robert, A., & Kummert, M. (2012). Designing net-zero energy buildings for the future climate, not for the past. Building and Environment, 55, 150–158. https://doi.org/10.1016/j.buildenv.2011.12.014

[70] Holmes, M. J., & Hacker, J. N. (2007). Climate change, thermal comfort and energy: meeting the design challenges of the 21st century. Energy & Buildings, 39(7), 802–814. https://doi.org/10.1016/j.enbuild.2007.02.009

[71] Tian, W., Heo, Y., de Wilde, P., Li, Z., Yan, D., Park, C. S., Feng, X., & Augenbroe, G. (2018). A review of uncertainty analysis in building energy assessment. Renewable & Sustainable Energy Reviews, 93, 285–301. https://doi.org/10.1016/j.rser.2018.05.029

[72] Kolokotroni, M., Ren, X., Davies, M., & Mavrogianni, A. (2012). London's urban heat island: impact on current and future energy consumption in office buildings. Energy & Buildings, 47, 302–311. https://doi.org/10.1016/j.enbuild.2011.12.019

[73] Cavka, B. T., & Ek, M. (2018). Future weather files to support climate resilient building design in Vancouver (Doctoral dissertation, University of British Columbia).

[74] Jentsch, M. F., James, P. A. B., Bourikas, L., & Bahaj, A. B. S. (2013). Transforming existing weather data for worldwide locations to enable energy and building performance simulation under future climates. Renewable Energy, 55, 514–524. https://doi.org/10.1016/j.renene.2012.12.049

[75] Troup, L., & Fannon, D. (2016). Morphing climate data to simulate building energy consumption. Proceedings of SimBuild, 6(1).

[76] Lu, J., Marincioni, V., Orr, S. A., & Altamirano, H. (2021). The implications of future wind-driven rain exposure on the hygrothermal performance of internally insulated solid walls in London. The Implications of Future Wind-Driven Rain Exposure on the Hygrothermal Performance of Internally Insulated Solid Walls in London. https://doi.org/10.14293/icmb210038

[77] Hall, I. J., Prairie, R. R., Anderson, H. E., & Boes, E. C. (1978). Generation of a typical meteorological year (No. SAND-78-1096C; CONF-780639-1). Sandia Labs., Albuquerque, NM (USA).

[78] Bre, F., & Fachinotti, V. D. (2016). Generation of typical meteorological years for the argentine littoral region. Energy & Buildings, 129, 432–444. https://doi.org/10.1016/j.enbuild.2016.08.006

[79] Chan, A. L. S., Chow, T. T., Fong, S. K. F., & Lin, J. Z. (2006). Generation of a typical meteorological year for hong kong. Energy Conversion and Management, 47(1), 87–96. https://doi.org/10.1016/j.enconman.2005.02.010

[80] Nascimento, M. L. M., Bauer, E., de Souza, J. S., & Zanoni, V. A. G. (2016). Wind-driven rain incidence parameters obtained by hygrothermal simulation. Journal of Building Pathology and Rehabilitation, 1(1), 1–7. https://doi.org/10.1007/s41024-016-0006-5

[81] Wang, C., Zhang, L., Lee, S.-K., Wu, L., & Mechoso, C. R. (2014). A global perspective on cmip5 climate model biases. Nature Climate Change, 4(3), 201–205. https://doi.org/10.1038/nclimate2118

[82] Ashfaq, M., Bowling, L. C., Cherkauer, K., Pal, J. S., & Diffenbaugh, N. S. (2010). Influence of climate model biases and daily-scale temperature and precipitation events on hydrological impacts assessment: a case study of the united states. Journal of Geophysical Research: Atmospheres, 115(D14). https://doi.org/10.1029/2009JD012965

[83] Xu, C.-yu. (1999). From GCMS to river flow: A review of downscaling methods and hydrologic modelling approaches. Progress in Physical Geography: Earth and Environment, 23(2), 229–249. https://doi.org/10.1177/030913339902300204

[84] Berg, P., Feldmann, H., & Panitz, H.-J. (2012). Bias correction of high resolution regional climate model data. Journal of Hydrology, 448-449, 80–92. https://doi.org/10.1016/j.jhydrol.2012.04.026

[85] Haddad, Z. S., & Rosenfeld, D. (1997). Optimality of empirical Z-R relations. Quarterly Journal of the Royal Meteorological Society, 123(541), 1283–1293. https://doi.org/10.1002/qj.49712354107

[86] Zscheischler, J., Fischer, E. M., & Lange, S. (2019). The effect of univariate bias adjustment on multivariate hazard estimates. Earth System Dynamics, 10(1), 31–43. https://doi.org/10.5194/esd-10-31-2019

[87] François, B., Vrac, M., Cannon, A. J., Robin, Y., & Allard, D. (2020). Multivariate bias corrections of climate simulations: Which benefits for which losses? Earth System Dynamics, 11(2), 537–562. https://doi.org/10.5194/esd-11-537-2020

[88] Gaur, A., Lacasse, M., & Armstrong, M. (2019). Climate data to undertake hygrothermal and whole building simulations under projected climate change influences for 11 canadian cities. Data, 4(2), 72–72. https://doi.org/10.3390/data4020072

[89] Laouadi, A., Gaur, A., Lacasse, M. A., Bartko, M., & Armstrong, M. (2020). Development of reference summer weather years for analysis of overheating risk in buildings. Journal of Building Performance Simulation, 13(3), 301–319. https://doi.org/10.1080/19401493.2020.1727954

[90] Jalaei, F., Guest, G., Gaur, A., & Zhang, J. (2020). Exploring the effects that a non-stationary climate and dynamic electricity grid mix has on whole building life cycle assessment: a multi-city comparison. Sustainable Cities and Society, 61. https://doi.org/10.1016/j.scs.2020.102294

[91] Vandemeulebroucke, I., Defo, M., Lacasse, M. A., Caluwaerts, S., & Van Den Bossche, N. (2021). Canadian initial-condition climate ensemble: hygrothermal simulation on wood-stud and retrofitted historical masonry. Building and Environment, 187. https://doi.org/10.1016/j.buildenv.2020.107318

[92] Defo, M., & Lacasse, M. (2021). Effects of climate change on the moisture performance of tallwood building envelope. Buildings, 11(2), 35–35. https://doi.org/10.3390/buildings11020035

[93] National Research Council Canada, Institute for Research in Construction. (2015). National building code of Canada.

[94] von Salzen, K., Scinocca, J. F., McFarlane, N. A., Li, J., Cole, J. N., Plummer, D., Verseghy, D., Reader, M. C., Ma, X., Lazare, M., & Solheim, L. (2013). The Canadian Fourth Generation Atmospheric Global Climate Model (CANAM4). part I: Representation of physical processes. Atmosphere-Ocean, 51(1), 104–125. https://doi.org/10.1080/07055900.2012.755610

[95] Scinocca, J. F., Kharin, V. V., Jiao, Y., Qian, M. W., Lazare, M., Solheim, L., Flato, G. M., Biner, S., Desgagne, M., & Dugas, B. (2015). Coordinated global and regional climate modeling*. Journal of Climate, 29(1), 17–35. https://doi.org/10.1175/jcli-d-15-0161.1

[96] Arora, V. K., Scinocca, J. F., Boer, G. J., Christian, J. R., Denman, K. L., Flato, G. M., Kharin, V. V., Lee, W. G., & Merryfield, W. J. (2011). Carbon emission limits required to satisfy future representative concentration pathways of greenhouse gases. Geophysical Research Letters, 38(5). https://doi.org/10.1029/2010gl046270

[97] van Vuuren, D. P., Edmonds, J., Kainuma, M., Riahi, K., Thomson, A., Hibbard, K., Hurtt, G. C., Kram, T., Krey, V., Lamarque, J.-F., Masui, T., Meinshausen, M., Nakicenovic, N., Smith, S. J., & Rose, S. K. (2011). The Representative Concentration Pathways: An overview. Climatic Change, 109(1-2), 5–31. https://doi.org/10.1007/s10584-011-0148-z

[98] Sanford, T., Frumhoff, P. C., Luers, A., & Gulledge, J. (2014). The climate policy narrative for a dangerously warming world. Nature Climate Change, 4(3), 164–166. https://doi.org/10.1038/nclimate2148

[99] Gaur, A., & Simonovic, S. P. (2015). Towards reducing climate change impact assessment process uncertainty. Environmental Processes, 2(2), 275–290. https://doi.org/10.1007/s40710-015-0070-x

[100] Saha, S., et al. (2010), NCEP Climate Forecast System Reanalysis (CFSR) Selected Hourly Time-Series Products, January 1979 to December 2010, https://doi.org/10.5065/D6513W89, Research Data Archive at the National Center for Atmospheric Research, Computational and Information Systems Laboratory, Boulder, Colo.

[101] Cannon, A. J., Sobie, S. R., & Murdock, T. Q. (2015). Bias correction of GCM precipitation by quantile mapping: How well do methods preserve changes in quantiles

and extremes? Journal of Climate, 28(17), 6938–6959. https://doi.org/10.1175/jcli-d-14-00754.1

[102] Olsson, J., Berggren, K., Olofsson, M., & Viklander, M. (2009). Applying climate model precipitation scenarios for urban hydrological assessment: A case study in Kalmar City, Sweden. Atmospheric Research, 92(3), 364–375. https://doi.org/10.1016/j.atmosres.2009.01.015

[103] Willems, P., & Vrac, M. (2011). Statistical precipitation downscaling for small-scale hydrological impact investigations of climate change. Journal of Hydrology, 402(3-4), 193–205. https://doi.org/10.1016/j.jhydrol.2011.02.030

[104] Cannon, A. J. (2017). Multivariate quantile mapping bias correction: An n-dimensional probability density function transform for climate model simulations of multiple variables. Climate Dynamics, 50(1-2), 31–49. https://doi.org/10.1007/s00382-017-3580-6

[105] Vrac, M. (2018). Multivariate bias adjustment of high-dimensional climate simulations: The rank resampling for distributions and dependences (R2d2) bias correction. Hydrology and Earth System Sciences, 22(6), 3175–3196. https://doi.org/10.5194/hess-22-3175-2018

[106] Clark, M., Gangopadhyay, S., Hay, L., Rajagopalan, B., & Wilby, R. (2004). The schaake shuffle: A method for reconstructing space–time variability in forecasted precipitation and temperature fields. Journal of Hydrometeorology, 5(1), 243–262. https://doi.org/10.1175/1525-7541(2004)005<0243:tssamf>2.0.co;2

[107] Ahmed, K. F., Wang, G., Silander, J., Wilson, A. M., Allen, J. M., Horton, R., & Anyah, R. (2013). Statistical downscaling and bias correction of climate model outputs for climate change impact assessment in the u.s. northeast. Global and Planetary Change, 100, 320–332. https://doi.org/10.1016/j.gloplacha.2012.11.003

[108] Haerter, J. O., Hagemann, S., Moseley, C., & Piani, C. (2011). Climate model bias correction and the role of Timescales. Hydrology and Earth System Sciences, 15(3), 1065–1079. https://doi.org/10.5194/hess-15-1065-2011

[109] ASHRAE. (2016). ASHRAE Standard 160-2016. Criteria for Moisture-Control Design Analysis in Buildings. Atlanta: ASHRAE.